



Setting-less Protection

Final Project Report

Power Systems Engineering Research Center

*Empowering Minds to Engineer
the Future Electric Energy System*



Setting-less Protection

Final Project Report

Project Team

Faculty

Sakis A. P. Meliopoulos, Project Leader
George J. Cokkinides
Georgia Institute of Technology

Graduate Research Assistants

Sungyun Choi
Rui Fan
Yonghee Lee
Liangyi Sun
Zhenyu Tan
Georgia Institute of Technology

PSERC Publication 13-46

September 2013

For information about this project contact:

Sakis Meliopoulos
Georgia Power Distinguished Professor
School of Electrical and Computer Engineering
Georgia Institute of Technology
Atlanta, Georgia 30332-0250
Phone: 404-894-2926
E-mail: sakis.m@gatech.edu

Power Systems Engineering Research Center

The Power Systems Engineering Research Center (PSERC) is a multi-university Center conducting research on challenges facing the electric power industry and educating the next generation of power engineers. More information about PSERC can be found at the Center's website: <http://www.pserc.org>.

For additional information, contact:

Power Systems Engineering Research Center
Arizona State University
527 Engineering Research Center
Tempe, Arizona 85287-5706
Phone: 480-965-1643
Fax: 480-965-0745

Notice Concerning Copyright Material

PSERC members are given permission to copy without fee all or part of this publication for internal use if appropriate attribution is given to this document as the source material. This report is available for downloading from the PSERC website.

© 2013 Georgia Institute of Technology. All rights reserved.

Acknowledgements

This is the final report for the Power Systems Engineering Research Center (PSERC) research project T-49G titled “Setting-less Protection”. The project has been sponsored by EPRI. We express our appreciation to EPRI, and in particular to Paul Myrda for his support and guidance for the project. We also express our appreciation for the support provided by PSERC’s industrial members, EPRI members, and by the National Science Foundation’s Industry / University Cooperative Research Center program.

The authors wish to recognize their postdoctoral researchers and graduate students at Georgia Tech who contributed to the research and creation of the reports:

- Sungyun Choi
- Rui Fan
- Yonghee Lee
- Liangyi Sun
- Zhenyu Tan

Executive Summary

The capabilities of protective relays have increased dramatically as higher end microprocessors are increasingly used in modern numerical relays, and more elaborate communication interfaces are provided. At the same time the complexity has increased primarily because numerical relays are set to mimic the traditional electromechanical counterparts. In addition, despite the progress of the last few decades, some problems or protection gaps persist. For instance, we still do not have good 100% reliable approaches for certain fault types, such as high impedance faults and faults near neutrals.

A previous report provided an overview of the state of art and present technologies in protection, identified gaps in protection, and provided an overview of emerging technologies that may have an impact on protective relaying. The goal was to challenge the research community to think "out of the box" towards new approaches that will lead to simplified but secure and reliable protection schemes that fully utilize existing and expected technology advancements. Several approaches were examined that may lead to setting-less protection schemes, such as (a) adaptive relaying, (b) component state estimation approach, (c) substation based protection, and (d) pattern recognition based approach. These approaches were evaluated with the following criteria: (a) feasibility, (b) dependability, (c) security, (d) reliability, and (e) speed of protection.

From the approaches examined, the state estimation based approach was deemed promising to meet the above criteria. The approach was pursued and demonstrated on a number of protection problems: transmission line protection, capacitor bank protection, transformer protection, reactor protection, induction motor protection, and distribution line protection. The research demonstrated that the state estimation based approach provides a secure and dependable protection scheme and it does not require coordination with other devices or protection schemes so it is "setting-less." The state estimation based approach requires complex analytics to be performed on the data acquired with the data acquisition system of the relay. The research has also demonstrated through numerical experiments that the analytics can be performed with substantial margin within the sampling period of typical data acquisition systems for relays.

The setting-less protection approach described in this report can be viewed as a generalization of differential protection, enabled with dynamic state estimation. Specifically, the proposed protection scheme is based on continuously monitoring terminal voltages and currents of the component (i.e., zone of protection) and other possible quantities, such as tap setting and temperature, appropriate for the component under protection. The monitored data are utilized in a dynamic state estimation that continuously provides the dynamic state of the component by fitting the measurement data to the model equations of the device under protection. The dynamic state is then used to determine the health of the component, i.e., whether the component is unfaulted and whether it is operating within its design limits. Whether the component should be tripped is decided on the basis of its health.

This report presents the design of the setting-less protective relay and its application to three different protection zones: transformer, reactor, and capacitor bank. For each protection zone, the setting-less protective relay is described by the model equations, and the analytics of the relay and timing results to determine the feasibility of performing the analytics in time less than the sampling rate of the measurement data. Numerical experiments are presented to validate the design.

Project Publications

1. A. P. Sakis Meliopoulos, George Cokkinides, Renke Huang, Evangelos Farantatos, Sungyun Choi, Yonghee Lee and Xuebei Yu, "Smart Grid Technologies for Autonomous Operation and Control", *IEEE Transactions on Smart Grid*, Vol. 2, No. 1, March 2011.
2. Sungyun Choi, Yonghee Lee, George Cokkinides and A. P. Sakis Meliopoulos, "Transformer Dynamic State Estimation Using Quadratic Integration", *Proceedings of the 2011 Power Systems Conference & Exposition*, Phoenix, AZ, March 20-23, 2011.
3. Sungyun Choi, Yonghee Lee, George Cokkinides, and A. P. Meliopoulos, "Dynamically Adaptive Transformer Protection Using Dynamic State Estimation", *Proceedings of the PAC World Conference 2011*, Dublin, Ireland, June 27-30, 2011.
4. A. P. Sakis Meliopoulos, George Cokkinides, Sungyun Choi, Evangelos Farantatos, Renke Huang and Yonghee Lee, "Symbolic Integration and Autonomous State Estimation: Building Blocks for an Intelligent Power Grid", *Proceedings of the 2011 ISAP*, Xersonissos, Crete, Greece, September 25-28, 2011.
5. A. P. Sakis Meliopoulos, George Cokkinides, Zhenyu Tan, Sungyun Choi, Yonghee Lee, and Paul Myrda, "Setting-less Protection: Feasibility Study", *Proceedings of the 46st Annual Hawaii International Conference on System Sciences (HICSS)*

Table of Contents

1. Introduction.....	1
2. Review of Present State of Art.....	3
2.1. History of Protection	3
2.2. Integration of Protection and Automation	4
2.3. Summary of State of Art.....	6
3. Gaps in Protection Approaches.....	7
3.1. Summary of Gaps and Challenges	8
4. Emerging Technologies	9
5. The Need for New Thinking and New Approaches.....	11
5.1. Adaptive Protection	11
5.2. Dynamic State Estimation Based Approach for Zone Protection	13
5.3. State Estimation Approach for System Protection	16
5.4. Summary of State Estimation Approaches.....	18
6. Implementation of Setting-less Protection.....	19
6.1. Protection Zone Mathematical Model	20
6.2. Object-Oriented Measurements.....	21
6.3. Object-Oriented Dynamic State Estimation	23
6.4. Bad Data Detection and Identification	24
6.5. Protection Logic / Component Health Index.....	24
6.6. Online Parameter Identification	26
6.7. Summary and Comments	26
7. Example Applications: Capacitor Bank Protection	27
7.1. Summary.....	27
7.2. Setting-less Relay Description	30
7.3. Three Phase Capacitor Bank SCAQCF Model	31
7.4. Capacitor Bank Measurements Definition	34
7.5. Creation of Measurement Models	34
7.5.1. Creation of Actual Measurement Model.....	35
7.5.2. Creation of Virtual Measurement Model	35
7.5.3. Creation of Derived Measurement Model.....	35
7.5.4. Creation of Pseudo Measurement Model	35
7.6. State Estimation Algorithm	36
7.7. Protection Logic	38
7.8. Numerical Experiments	38
7.8.1. Test Scenario 1	39
7.8.2. Test Scenario 2	41
7.8.3. Test Scenario 3	42
7.8.4. Test Scenario 4	45
7.9. Issues and Challenges Associated with State Estimation Based Three Phase Capacitor Banks Protection	47
8. Example Applications: Saturable Core Reactors.....	52
8.1. Summary.....	52
8.2. Setting-less Relay Description	55
8.3. Saturable Core Reactor SCAQCF Model.....	56

8.4	Saturable Core Reactor Measurements Definition	60
8.5	Creation of Measurement Models	60
8.5.1	Creation of Actual Measurement Model	60
8.5.2	Creation of Virtual Measurement Model	61
8.5.3	Creation of Derived Measurement Model	61
8.5.4	Creation of Pseudo Measurement Model	61
8.6	State Estimation	62
8.7	Protection Logic	64
8.8	Numerical Experiments	65
8.8.1	Test Scenario 1	65
8.8.2	Test Scenario 2	67
9.	Example Applications: Transformers	69
9.1	Summary	69
9.2	Setting-less Relay Description	71
9.3	Three Phase Transformer Model	73
9.4	Measurements Definition	77
9.5	Creation of Measurement Models	82
9.5.1	Creation of Across Measurement Model	83
9.5.2	Creation of Through Measurement Model	83
9.5.3	Creation of Virtual Measurement Model	84
9.5.4	Creation of Pseudo Measurement Model	84
9.6	State Estimation	85
9.7	Protection Logic	85
9.8	Numerical Experiments	86
9.8.1	Test Scenario 1	89
9.8.2	Test Scenario 2	91
9.8.3	Test Scenario 3	92
9.8.4	Test Scenario 4	93
9.8.5	Test Scenario 5	94
	References	100
Appendix 1	Three Phase Capacitor Banks Model Derivation	101
A1.1	Compact Model Description	101
A1.2	Quadratized Model Description	102
A1.3	SCAQCF Model Description	103
Appendix 2	Saturable Core Reactor Model Derivation	105
A2.1	Compact Model Description	105
A2.2	Quadratized Model Description	106
A2.3	SCAQCF Model Description	108
Appendix 3	Transformer Model Derivation	112
A3.1	Single-Phase Transformer Compact Model Description	112
A3.2	Single-Phase Transformer Quadratized Model Description	114
A3.3	Single-Phase Transformer SCAQCF Model Description	118
A3.4	Three-Phase Transformer SCAQCF Model Description	118
	Project Publications	122

List of Figures

Figure 2.1 State of Art for the Integration of Protection and Automation.....	5
Figure 5.1 Summary of Adaptive Relaying Attempts	12
Figure 5.2 Illustration of Setting-less Component Protection Scheme.....	14
Figure 5.3 Illustration of Setting-less Protection Logic.....	15
Figure 5.4 Overall Approach for Component Protection.....	16
Figure 5.5 Typical Configuration of Special Protection Systems.....	17
Figure 5.6 Concept of State Estimation Based Protection.....	18
Figure 6.1 Setting-Less Protection Relay Organization	19
Figure 6.2 Example Derived Measurements.....	23
Figure 6.3 Confidence Level (%) vs Parameter k	25
Figure 7.1 Three Phase Capacitor Bank Construction.....	27
Figure 7.2 Result of an Example Test System with Internal and External Faults	29
Figure 7.3 Capacitor Bank Setting-less Protection Execution Time	29
Figure 7.4 Illustration of Time Samples Utilized at Each Iteration of the Setting-less Relay Analytics.....	31
Figure 7.5 Three Phase Capacitor Banks Compact Model	32
Figure 7.6 Test System Diagram for Capacitor Bank Zone, Base Case	39
Figure 7.7 Test System Diagram for Capacitor Bank Zone, Scenario 1.....	40
Figure 7.8 Result of Scenario 1.....	40
Figure 7.9 Test System Diagram for Capacitor Bank Zone, Scenario 2.....	41
Figure 7.10 Result of Scenario 2.....	42
Figure 7.11 Test System Diagram for Capacitor Bank Zone, Scenario 3.....	43
Figure 7.12 Result of Scenario 3.....	44
Figure 7.13 Test System Diagram for Capacitor Bank Zone, Scenario 4.....	45
Figure 7.14 Result of Scenario 4.....	46
Figure 7.15 Time Relationship in Setting-less Protection	47
Figure 7.16 Capacitor Bank Setting-less Protection Operation Time.....	48
Figure 7.17 Typical Data Acquisition System Based on Merging Units.....	49
Figure 7.18 Recommended Data Acquisition Selection 1 for Capacitor Bank	50
Figure 7.19 Recommended Data Acquisition Selection 2 for Capacitor Bank	51
Figure 8.1 Single Phase Saturable Core Reactor Model.....	52

Figure 8.2 Results of Saturable Core Reactor Test System	54
Figure 8.3 Execution time.....	55
Figure 8.4 Illustration of Time Samples Utilized at Each Iteration of the Setting-less Relay Analytics.....	56
Figure 8.5 Model Parameters of Reactor	65
Figure 8.6 Test System Diagram for Single Phase Reactor.....	66
Figure 8.7 Results of Saturable Core Reactor Test System.....	66
Figure 8.8 Test System Diagram for Single Phase Reactor.....	67
Figure 8.9 Results of Saturable Core Reactor Test System.....	68
Figure 8.10 Execution time.....	68
Figure 9.1 Single-Phase Transformer Compact Model	69
Figure 9.2 Three-Phase, Delta-Wye-Connected Transformer	69
Figure 9.3 Result of an Example Test System with Internal Fault	71
Figure 9.4 Illustration of Time Samples Utilized at each iteration of the Setting-less Relay Analytics	72
Figure 9.5 Test Scheme for verifying the Proposed Protection Method.....	86
Figure 9.6 Test System for the Setting-Less Protection	87
Figure 9.7 Settings of the Three-phase Transformer under Protection.....	88
Figure 9.8 Measurement Signals of the Transformer (Normal Operating Condition)	90
Figure 9.9 Measurement Signals of the Transformer (Transformer Energization)	91
Figure 9.10 Measurement Signals of the Transformer (Transformer Overexcitation).....	92
Figure 9.11 Fault Location in the Test System (Through Fault Condition)	93
Figure 9.12 Measurement Signals of the Transformer (Through Fault Condition).....	94
Figure 9.13 Fault Location in the Test System (Internal Fault Condition).....	95
Figure 9.14 Measurement Signals of the Transformer (Internal Fault Condition).....	96
Figure 9.15 Confidence Level of the DSE (Normal Operating Condition).....	97
Figure 9.16 Confidence Level of the DSE (Transformer Energization).....	97
Figure 9.17 Confidence Level of the DSE (Transformer Overexcitation)	98
Figure 9.18 Confidence Level of the DSE (Through Fault Condition)	98
Figure 9.19 Confidence Level of the DSE (Internal Fault Condition)	99
Figure A1.1 Three Phase Capacitor Banks Compact Model	101
Figure A2.1 Single Phase Reactor Model.....	105
Figure A3.1 Single-phase Transformer Model under Protection.....	112

Figure A3.2 Delta-wye Connection of Three Single-phase Transformers	119
Figure A3.3 Delta-wye Connection Indices (Quadratic)	119

List of Tables

Table 9.1 All State Variables of the Three-Phase Transformer ($n = 5$)	74
Table 9.2 Actual Across Measurements for the Three-Phase Transformer	78
Table 9.3 Actual Through Measurements for the Three-Phase Transformer	79
Table 9.4 Virtual Measurements for the Three-Phase Transformer	79
Table 9.5 Pseudo Measurements for the Three-Phase Transformer	82
Table 9.6 Transformer Parameters (Identical at All Phases)	89
Table A3.1 Pointer Elements for Delta-Wye Connection	120

1. Introduction

The current state of art in protective relaying is quite advanced. Yet gaps exist in the sense that (a) we do not have reliable protection schemes for a number of protection problems, such as downed conductors, high impedance faults, and (b) for systems and components that do not comply to the general principle of large separation between abnormal and normal conditions the protection schemes tend to be complex with areas of compromised performance, leading to issues such as load encroachment, false tripping, etc. In this report we will assess the current state of art and will identify some of the common gaps/shortcomings in component and system protection. We will also examine the present state of protection technology, as defined with the present day high-end numerical relays that use microprocessors of equal performance as those utilized in high end personal computers. We finally would like to suggest approaches towards a more simplified and expectedly setting-less protection. The goal of the suggestions is to stimulate discussion and create a research plan towards achieving simplified but fully reliable protection schemes that cover all protection problems. The proposals, suggestions, ideas will be examined and evaluated by several criteria: (a) feasibility, (b) dependability, (c) security, (d) reliability, and (e) speed of protection. The specific approaches may be (but not limited to): adaptive relaying, component state based protection, substation state based protection, pattern recognition-based protection, etc. A brief description of the proposed approaches is as follows:

Component State Estimation Approach. A very promising approach towards setting-less protective relays is by use of dynamic state estimation. The basic approach is to use measurements from numerical relays (of device voltage, currents, and other specific quantities, for example taps for a transformer, etc.) to estimate the state of the component in real time. The dynamic state estimation enables the monitoring of the "health of the device under protection". The health of the component deteriorates only when the component experiences a fault. Preliminary results of this approach are given in [5] and background material is provided in [3], [4]. Potentially this approach can lead to true setting-less protection schemes. This approach will be carefully evaluated and protection schemes for transformers, generators, lines, reactors, capacitors, etc. will be discussed.

Substation Based Protection. This approach is an extension of the "component state estimation approach" and it is described in reference [1]. The idea here is to apply dynamic state estimation to the entire substation and then protection action will be taken on the basis of the state of the entire substation in real time. This approach requires that all IEDs in substation are reporting to the same computer/relay. These schemes are presently feasible. Issues of speed by which the substation state estimation can respond will be addressed. The feasibility, advantages and disadvantages will be examined for typical substation configurations. This approach can also lead to true setting-less protection schemes.

Finally, the problem of system (wide area) protection will be addressed. This is probably the most complex protection problem. We will investigate the concepts presented earlier

(component state estimation and substation based protection) and their extension to system protection problems. Reference [2] presents the use of GPS-synchronized measurements and substation state estimation for the purpose of developing an out of step protection scheme based on energy concepts. The approach described in reference [2] is a setting-less protection scheme for out of step protection. We will expand on this idea for other system protection problems, such as voltage swings, etc.

The approaches described above will be evaluated with the following criteria: (a) feasibility, (b) dependability, (c) security, (d) reliability, and (e) speed of protection.

2. Review of Present State of Art

Since the early days of electric power systems it was recognized that protection is essential for the operation and safeguarding of the power system assets.

2.1. History of Protection

Protective relaying was initially developed to protect individual components. As interconnections grew, system problems and system protection issues arose. In recent decades we see the development of system protection approaches. Component and system protection are distinct and they will be discussed separately.

Component Protection: Initially, electromechanical relays were introduced at the early stages of the electric power industry. Electromechanical relays are electromechanical systems that are designed to perform a logic function based on specific inputs of voltages and/or currents. This technology started with the very simple plunger type relay and evolved into highly sophisticated systems that performed complex logical operations, for example the modified mho relay is a system that monitors the impedance of the system as “seen” at a specific point in the system and will act whenever the impedance moves into a pre-specified region. In the early years of the electric power industry, the inverse time-delay overcurrent relay was developed based on the induction disk (Westinghouse) or the induction cup (GE). The overcurrent protection function is one of the main protection functions provided in practically all protections schemes. Over the years the electromechanical relays developed into sophisticated analog logic devices with great selectivity and operational reliability. The development of differential protection and distance protection were two major milestones. The introduction of the transistor in the late 40s resulted in solid state devices that can perform logic operations. In the 60s we see efforts to develop solid state relays with the same functionality as the electromechanical relays. Solid state relays were short lived as the first effort to develop digital (numerical relays) was introduced in the late sixties with the first digital relay developed in 1970 (G. Rockefeller, Eric Udren) that formulated the approach for digital relays. These efforts were refined when the microprocessor was introduced in the early 80s and led to the development of the microprocessor based relay (numerical relay). The first commercial available numerical relay appeared in the early eighties as Westinghouse and GE developed prototypes under the EPRI funding of the WESPAC project for transmission all-digital substation, and the first microprocessor relay for distribution system applications was introduced in 1984 (Schweitzer). Since then, the numerical relay increased its domination to the point that today has almost completely displaced electromechanical and solid state relays. The numerical relays today, by and large, they simply mimic the logics that developed for the electromechanical relays with much more flexible manner. Because numerical relays can pack many protection functions in one box, numerical relays are multifunctional. The increased functionality has resulted in very complex schemes that many times lead to inconsistencies and possibility of

improper protection actions.

Differential protection is one of the simplest, secure and reliable scheme. For geographically extended components, differential protection schemes involve a number of approximations to account for the fact that information from the geographically remote locations must be brought to one location and compared. A breakthrough occurred in 1992 when Macrodyne (Jay Murphy) introduced the first GPS-synchronized device that he named PMU (Phasor Measurement Unit). This technology enables true differential protection schemes of geographically extended components and presently we see the development of such systems. The evolution of fast communications has enabled this approach.

System Protection: the first system protection concept was developed for the out of step protection of generating units and it was based on impedance relays. Subsequently wide area measurements were used for system wide monitoring and protection. Special protection schemes typically use pre-computed scenarios and arming the system to identify these scenarios and respond. This approach can be classified as a "pattern recognition" approach. The introduction of GPS synchronized measurements created more possibilities for better implementation of wide area monitoring and protection. Yet, the approach remains the same and it is limited by time latencies required to transfer the data to a central location, process the data and compare them to pre-computed disturbance patterns.

2.2. Integration of Protection and Automation

The numerical relay enabled increased automation. The Figure 2.1 below shows two major approaches as evolved in the past decade. To the right of the figure, the approach of connecting numerical relays to the instrument transformers and control circuits on one side and to a station bus on the other side for easy communications and managing relay settings is shown. To the left of the figure, the introduction of the merging units and the process bus is shown. These arrangement lead to the capability to use the relays as an integral part of the SCADA system and eliminates the need for Remote Terminal Units in the usual sense. The relays or the station bus provides the functionality of the Remote Terminal Units. It also leads to the integration of protection and control.

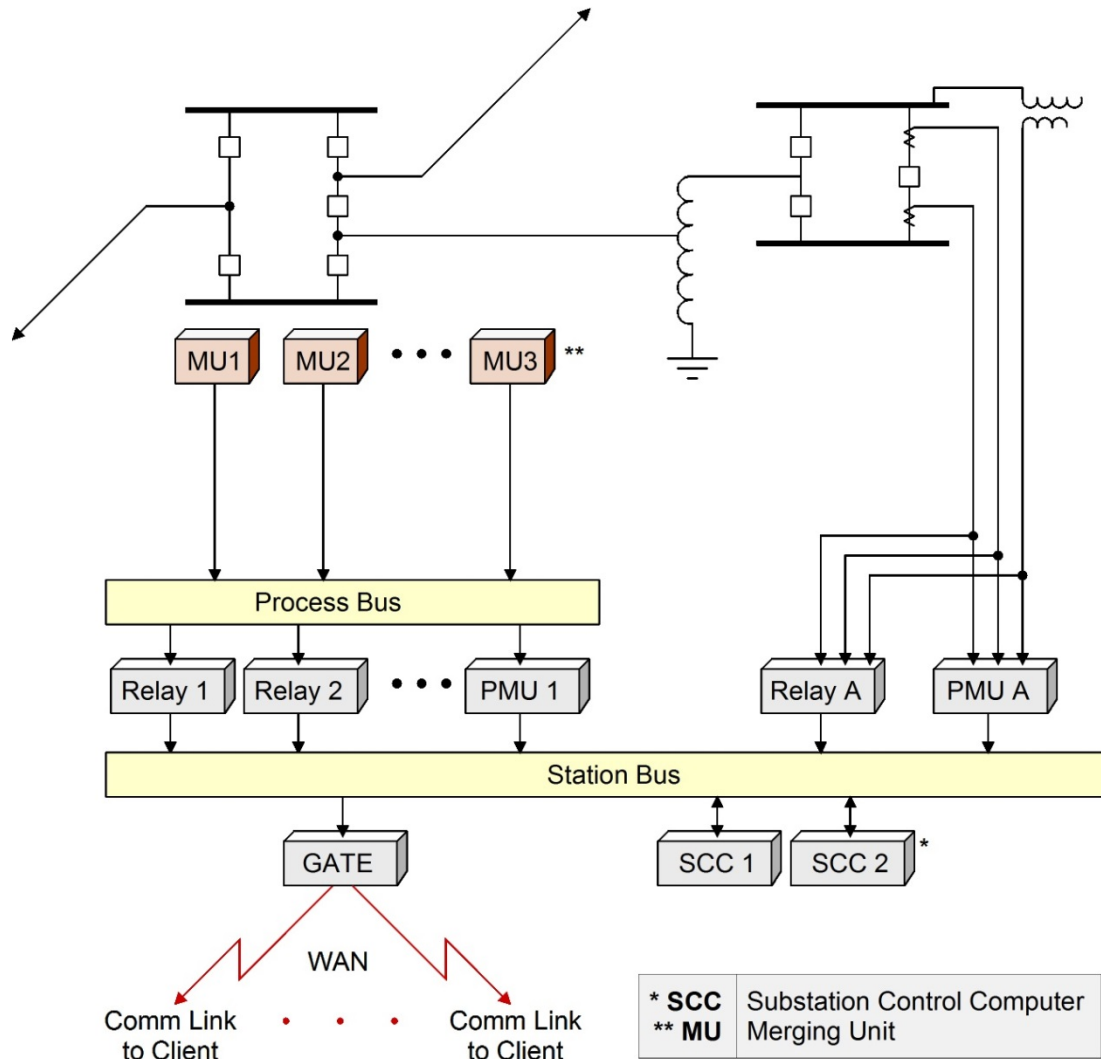


Figure 2.1 State of Art for the Integration of Protection and Automation

The above state of recent technological advances (PMU capability, merging units, process bus, station bus and interoperability) has not been accompanied with commensurate advances on the protection coordination. The settings of protective devices still utilize the same principles of many decades ago. These principles rely on distinct separations and characteristics between "fault conditions" and "normal and tolerable conditions". Even for the classical power system without renewables and a plethora of power electronic interfaced components, the separation and identification of "fault conditions" and "normal and tolerable conditions" is in many circumstances difficult, for example, short lines, weak/strong feeds, high impedance faults, etc. In the presence of renewables with power electronic interfaces, these issues multiply. The end result is that it becomes extremely difficult to develop a secure, reliable, dependable, speedy, safe and low cost protection system based on the conventional principles.

2.3. Summary of State of Art

Presently numerical relays provide multiple functionality, communications, self-diagnostics, ability to integrate other functions such as SCADA, and ability to be integrated with automated closed loop control systems. Standards are being developed to enable the integration of relays into closed loop control schemes - in particular the IEC 61850 standard provides a great tool to ensure interoperability and to coordinate intelligence among relays, such as to inform one relay to lock out or inhibit reclosing, etc. In general, protection functions require settings. There are many tools that facilitate computations required to decide the settings of the various protective functions. However, there are no analytical tools to calculate and validate optimum settings for dependable and reliable relay functions. As a result selecting protective relaying settings require human input and decisions - in general a complex procedure for typical substations.

For distribution circuits, the present state of art is based on the assumption of radial operation. It is expected in the near future that the distribution system will become active with substantial distributed generation and resources. This expectation will necessitate revisiting the common approaches to distribution protection.

Finally, despite the advanced state of art of numerical relays, certain protection problems are still evading a reliable and secure protection scheme. Some of these will be discussed next.

3. Gaps in Protection Approaches

While component and system protection has reached phenomenal sophistication, certain gaps still remain. The gaps can be classified into two categories: (a) protection problems for which a satisfactory solution does not exist, such as downed conductors, or high impedance faults, and (b) protection problems for which present protection schemes leave "compromised protection areas". The latter lead many times to false operations, such as load encroachment, sympathetic tripping, etc.

One major challenge of problems in the second category exists in systems with resources that interfaced with power electronics, such as wind farms, PV farms, distributed generation, etc. The main characteristic of these systems are that their fault current capability is limited by the power electronics creating a disparity between the grid side and the resource side. What complicates matters more is the fact that some of the power electronics have complex control functions that the protection system must recognize and distinguish between abnormal operating conditions and legitimate complex response to a disturbance. Another complexity is the fact that for better protection schemes, it is necessary to monitor the DC side of these systems as well and incorporate the conditions of the DC side into the protection schemes. With respect to this issue there is a hardware gap as present day numerical relays have been designed to monitor AC quantities only. For these systems one need numerical relays with capability to measure DC quantities.

Below we provide additional comments on specific issues and challenges.

Wind Farm protection: Wind farms are generating plants with non-conventional generation (induction machines with power electronics, for example type 3 and type 4) that present the following characteristics: (a) the fault current contributions from the power grid may be quite high but the fault current contribution from the wind generator is comparable to the load current. While present protection schemes and numerical relay capability is tweaked to develop a reasonable overall protection scheme for wind farms, the solutions are complex and lack full reliability (security, dependability and speed). Are there better ways to protect these systems? The increased complexity from mandated controls, such as zero voltage ride-through capability further makes the protection problem a challenge.

Distribution system with distributed generation: These systems present the same challenges as wind farms with the additional complexity of mixing protection systems that were designed on the basis of radial power flow to a system with bidirectional power flow. Some present standards take the easy way out by suggesting disconnection of distributed resources in case of disturbances and faults. There must be a better way if we want to increase the economic value of distributed resources.

PV Farm protection: PV farms exhibit the same protection challenges as wind farms. It is important to note that while wind farm protection and operational issues are under serious consideration and research activity, for PV farms the activity is very low and

under the radar screen. At the same time there is substantial development of utility size PV farm systems and larger activity of residential PV activity. It is important that the protection and operation of these systems be further researched and improved.

Down conductor protection: This problem has been with the industry for a long time with various attempts to solve the downed conductor protection system. While many schemes have been developed, none of the schemes can provide definitive protection against downed conductors.

Above are examples that demonstrate the need for new thinking and new approaches.

3.1. Summary of Gaps and Challenges

Despite the advanced status of numerical relays there are gaps in protection and settings may lead to compromise solutions. NERC keeps track of power system disturbances and the causes of power system disturbances. Year after year, the number one root cause of power system disturbances is listed as relaying issues. This is a definite indication that protective relaying gaps exists and the challenges is to eliminate these gaps. Some of the gaps are methodological as we do not have a technically reliable and secure way to protect against certain problems as it is discussed in Appendix A. Some of the gaps and challenges are tools and manpower related. For example we lack test beds to try new ideas, lack of tools to assess the optimality of system relaying settings, depletion of experienced protective relaying engineers. Finally there are gaps due to the introduction of new technologies and specifically wind and PV farms. These systems are characterized with different models, i.e. they do not have the same characteristics as legacy equipment and therefore new approaches for their protection are required. A related issue is the gap that is being generated by the fact that distribution systems are becoming increasingly bidirectional power flow systems with many generating resources along the distribution system.

The challenges in closing these gaps are mostly institutional. First one has to deal with the risk adverse nature of the protection and control community. There is resistance to accept different paradigms and models and to trust these models. The mindset of keeping the relay as a dedicated device with its own inputs (measurements) must change to allow multiple inputs and more information for the purpose of addressing the protection requirements in a more reliable and secure manner. Finally the challenge is to develop solutions to the existing gaps that will allow an orderly transition - not wholesale changes.

4. Emerging Technologies

Present day numerical relays use high end microprocessors for implementing multiple functions of protection. For example a transformer protection relay may include all the typical protection functions that traditionally used with electromechanical relays, i.e. differential, over-current, V/Hz function, etc. Since these functions work independently, even if they are implemented on the same relay, they suffer from the same limitations as the usual single relay/single function approach. Each function must be set separately but the settings must be coordinated with other protective devices. The coordinated settings are typically selected so that can satisfy requirements that many times are conflicting and therefore a compromise must be selected. For this reason, most of the times the settings represent a compromise and occasionally possible fault conditions may exist that may lead to an undesirable relay response.

It should be understood that numerical relays have provided many more options that have improved the above procedure. At the same time the additional options have created increased complexity and increased possibilities of human errors, while the basic nature of the problem of selecting settings has remained the same: the settings must be selected to satisfy criteria that many times are conflicting. The natural question is whether any new technologies and trends can favorably affect the protection process.

There are technologies that can enable better, integrated approach to the overall protection. Some of these technologies are (technology is in flux with many developments still to occur):

1. Merging units/separation of data acquisition and data processing/protection
2. GPS synchronized measurements (PMUs)
3. Data Concentrator (PDCs, switches, etc.)
4. Smarter sensors
5. Integrated (power system/relay) analysis programs that enable faster and more reliable assessment of settings
6. Data validation/state extraction
7. other

It is difficult to assess the full impact of these technologies on the future of protection. One thing is clear though: while there is much technology development in hardware and the capabilities of hardware, the development of new approaches to fully utilize the new capabilities is lagging. This is the classical problem of "hardware being ahead of software". This will come with realistic assessment of the new technologies and bold experimentation of new approaches and the eventual emergence of successful approaches.

One can contemplate what approaches can be enabled by emerging technologies. It is clear that the approach of individual protective functions based on a small number of measurements (for example three currents and three voltages) makes the protection

function not fully reliable since the relay tries to identify the conditions from limited information and then take control action with an algorithm that is based on limited information. This is a fundamental limitation of the present approach to protective relaying and the technology of numerical relays has not changed it. The introduction of the process bus offers the obvious possibility of bringing many measurements (as a matter of fact all the measurements) to the process bus. Now a relay can be connected to the process bus and it may have access to all the measurements available in the substation. It should be noted that even if the process bus is today a reality, the relays attached to the process bus access only a limited amount of information, i.e. three voltages and currents, in other words the design of the relay that can be connected to the process bus has not changed from the traditional design that uses analog inputs to the relay. We can project that relays connected to a process bus can be designed to connect to a larger number of channels with very little add on cost since these connections are "digital". Then it will be necessary to develop new algorithms for protective relaying logic that will depend on all available information. This will almost guarantee a dramatic improvement on the reliability of the protective scheme. The discussed scenario will require hardware changes and software development. It has the capability to eliminate one of the fundamental limitations of the usual protective relaying approach of individual relaying functions operating on limited information. The role of GPS synchronized measurements for such an approach will be critical. As measurements are collected at different locations of the substation with independent data acquisition system and then the information is brought to the process bus it will be necessary to time-align these data before they will be used by the relays. GPS synchronized measurements and standards such as C37.118 and IEC 61850 will provide standardized means for time-aligning the data. Another issue that may have to be addressed is the time latencies generated by this approach. We believe that these issues can be addressed and successfully solved.

There may be many more approaches that take full advantage of the new capabilities enabled with new technologies. The above discussion is for the purpose of stimulating discussion on how new technologies can improve protective relaying approaches.

5. The Need for New Thinking and New Approaches

There is agreement that (a) present protection schemes are complex and (b) coordination of protection schemes are based on principles introduced many decades ago. Complexity increases the possibility of human error and the coordination principles used today develop settings that many times represent a compromise among conflicting factors. The end result is that the industry is experiencing more unwanted relay responses than desired. NERC statistics on causes of disturbances list protective relaying as the top root cause.

It is also recognized that new but commercially available technology could enable new approaches to protection. We provide some thoughts towards new approaches that will automate and simplify protection. The goal of the comments below is to stimulate discussion towards developing new ideas and new approaches for simple and fully reliable protection schemes.

5.1. Adaptive Protection

The basic idea of adaptive protection is based on the recognition that as system status changes (for example a generator is tripped and the new fault levels will change), so the best settings of protective relays change. It makes sense to monitor the system conditions and when changes occur to change the settings of the protective relays accordingly. Adaptive relaying has been the focus of many attempts for the last 30 years (since the introduction of numerical relays). A summary of the attempts towards adaptive relaying is captured in Figure 5.1. The picture shows the need to monitor the status not only of the component protected by the relay but also the system so that the real time model of the system can be extracted. The real time model needed by the adaptive relaying scheme needs to provide information on breaker status (open/close), short circuit capability of system, etc. This type of real time model can be only provided with advanced state estimation techniques that are very fast. From this information, the relay settings are properly adjusted, for example the breaker failure scheme must be adjusted to reflect the present status of breaker status, etc.

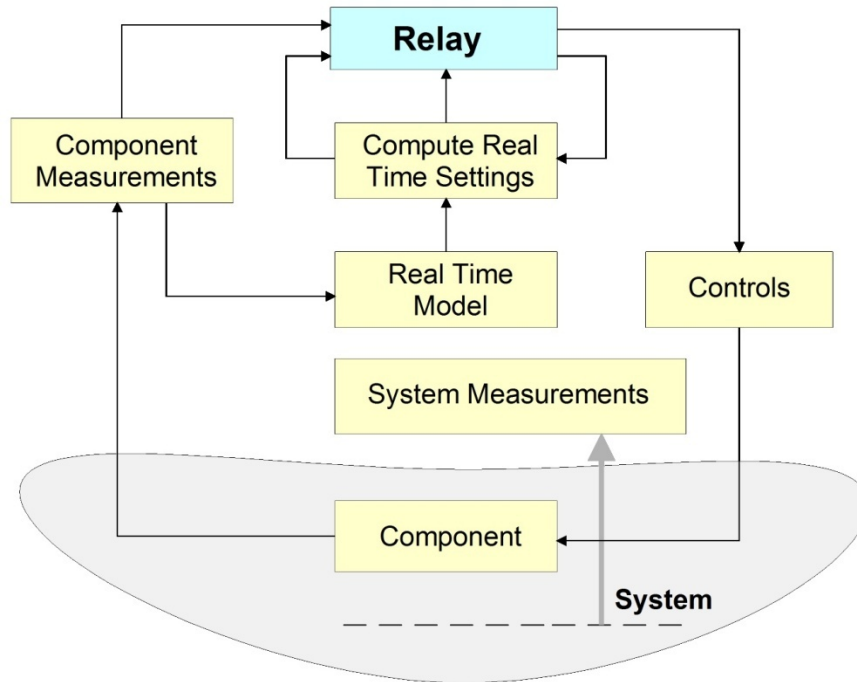


Figure 5.1 Summary of Adaptive Relaying Attempts

There are many challenges to adaptive relaying that stem from the necessity to obtain information about changing fault capabilities as generating units come on or go out of service, etc. Recent technological advances, especially GPS-synchronized measurements and fast communications can overcome some of the adaptive relaying challenges. It is also important to note that the traditional approach to adaptive relaying is to adjust the relay settings in real time. Questions that need to be raised are:

- (a) Can new technologies enable autonomous relay setting tuning and coordination in an adaptive scheme?
- (b) What is the impact of new technologies on adaptive relaying? For example new faster state estimation methods, new faster wide area monitoring technologies, etc.
- (c) The traditional approach to adaptive relaying relies on automatically adjustable settings using traditional principles for selecting settings. Is there any new ideas and approaches for a better approach to adaptive relaying that may eliminate settings altogether?

It is clear that adaptive relaying requires a complex algorithmic approach and reliable communications. Therefore it is realistic to say that the challenges for this approach are to cope with the complexity and the need for reliable communications.

5.2. Dynamic State Estimation Based Approach for Zone Protection

For secure and reliable protection of power components such as a generator, line, transformer, etc. a new approach has emerged based on component health dynamic monitoring. The proposed method uses dynamic state estimation [4-7], based on the dynamic model of the component, which accurately reflects the nonlinear characteristics of the component as well as the loading and thermal state of the component.

For more secure protection of protection zones such as transmission lines, transformers, capacitor banks, motors, generators, generator/transformer unit, etc., this paper proposes a new method. The method has been inspired from the fact that differential protection is one of the most secure protection schemes that we have and it does not require coordination with other protection function. Differential protection simply monitors the validity of Kirchoff's current law in a device, i.e. the weighted sum of the currents going into a device must be equal to zero. This concept can be generalized into monitoring the validity of all other physical laws that the device must satisfy, such as Kirchoff's voltage law, Faraday's law, etc. This monitoring can be done in a systematic way by the use of dynamic state estimation. Specifically, all the physical laws that a component must obey are expressed in the dynamic model of the component. Dynamic state estimation is used to continuously monitor the dynamic model of the component (zone) under protection. If any of the physical laws for the component under protection is violated, the dynamic state estimation will capture this condition. Thus, it is proposed to use dynamic state estimator to extract the dynamic model of the component under protection [2-5] and to determine whether the physical laws for the component are satisfied. The dynamic model of the component accurately reflects the condition of the component and the decision to trip or not to trip the component is based on the condition of the component only irrespectively of the condition (faults, etc.) of other system components. Figure 1 illustrates this concept. The proposed method requires a monitoring system of the component under protection that continuously measures terminal data (such as the terminal voltage magnitude and angle, the frequency, and the rate of frequency change - this task is identical to present day numerical relays), other variables such as temperature, speed, etc., as appropriate, and component status data (such as the tap setting, breaker status, etc.). The dynamic state estimation processes these measurements and extracts the real time dynamic model of the component and its operating conditions.

After estimating the operating conditions, the well-known chi-square test [6] calculates the probability that the measurement data are consistent with the component model, i.e. the physical laws that govern the operation of the component (see Figure 5.2). In other words, this probability, which indicates the confidence level of the goodness of fit of the component model to the measurements, can be used to assess the health of the component. The high confidence level indicates a good fit between the measurements and the model, which indicates that the operating condition of the component is normal. However, if the component has internal faults, the confidence level would be almost zero (i.e., the very poor fit between the measurement and the component model).

In general, the proposed method can identify any internal abnormality of the component within a cycle and trip the component immediately. Furthermore, it does not degrade the security because a relay does not trip in the event of normal behavior of the component, for example, in case of transformer protection, inrush currents or over excitation currents, since in these cases, as long as the inrush currents are consistent with the transient behavior of the transformer as dictated by the dynamic model, the method will produce a high confidence level that the transients are consistent with the model of the component. Note also that the method does not require any settings or any coordination with other relays.

It is important to note that the proposed scheme will perform best when: (a) the measurements are as accurate as possible - dependent on the type of instrument transformer used, i.e. VT, CT, etc. and the instrumentation channel, i.e. control cable, etc. and (b) the accuracy of the dynamic model of the component under protection. These issues, while important, are beyond the scope of this paper. These issues will be addressed in a subsequent paper.

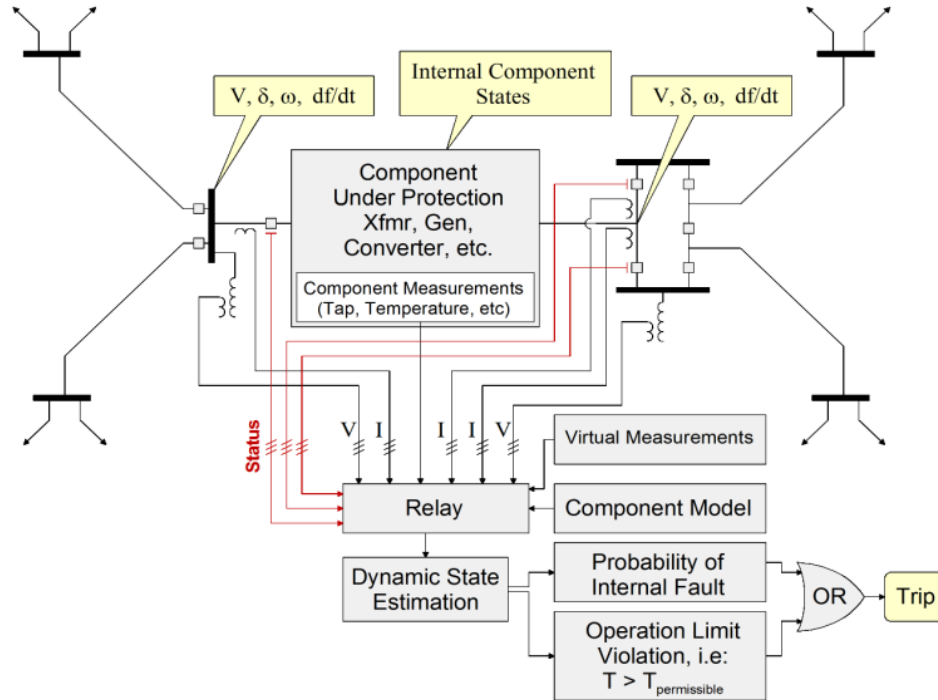


Figure 5.2 Illustration of Setting-less Component Protection Scheme

The approach is briefly illustrated in Figure 5.3. The method requires a monitoring system of the component under protection that continuously measures terminal data (such as the terminal voltage magnitude and angle, the frequency, and the rate of frequency change) and component status data (such as tap setting (if transformer) and temperature). The dynamic state estimation processes these measurement data with the dynamic model of the component yielding the operating conditions of the component.

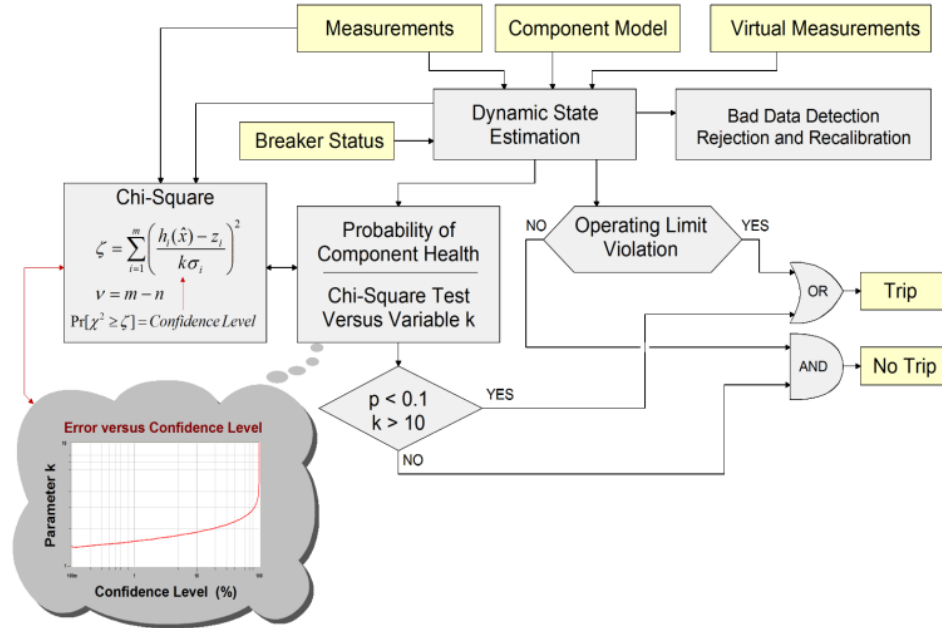


Figure 5.3 Illustration of Setting-less Protection Logic

This approach faces some challenges which can be overcome with present technology. A partial list of the challenges is given below:

1. Ability to perform the dynamic state estimation in real time
2. Initialization issues
3. Communications in case of a geographically extended component (i.e. lines)
4. New modeling approaches for components - connects well with the topic of modeling
5. Requirement for GPS synchronized measurements in case of multiple independent data acquisition systems.
6. other

The modeling issue is fundamental in this approach. For success the model must be high fidelity so that the component state estimator will reliably determine the operating status (health) of the component. For example consider a transformer during energization. The transformer will experience high in-rush current that represent a tolerable operating condition and therefore no relay action should occur. The component state estimator should be able to "track" the in-rush current and determine that they represent a tolerable operating condition. This requires a transformer model that accurately models saturation and in-rush current in the transformer. We can foresee the possibility that a high fidelity model used for protective relaying can be used as the main depository of the model which can provide the appropriate model for other applications. For example for EMS applications, a positive sequence model can be computed from the high fidelity model and send to the EMS data base. The advantage of this approach will be that the EMS model will come from a field validated model (the utilization of the model by the relay in real time provide the validation of the model). Figure 5.4 shows the overall approach.

Since protection is ubiquitous, it makes economic sense to use relays for distributed model data base that provides the capability of perpetual model validation.

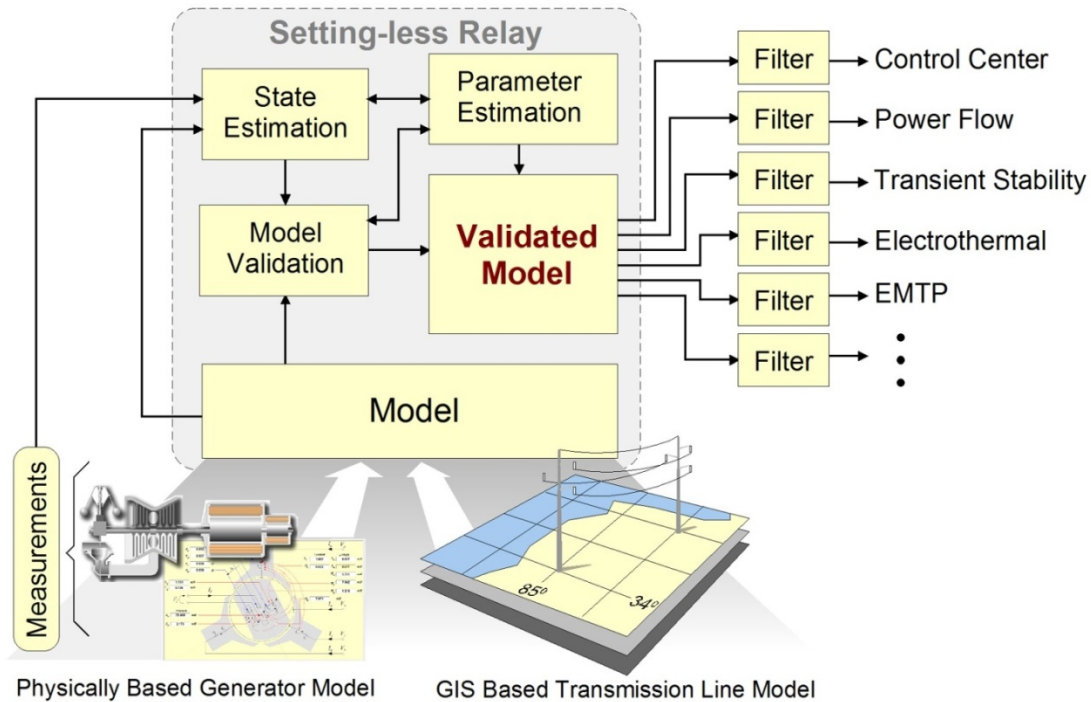


Figure 5.4 Overall Approach for Component Protection

5.3 State Estimation Approach for System Protection

By far the most complex protection problem exists at the system level. System level protection issues may involve events that develop in a very short time, such as pole slipping in a generator, or events that develop in relatively long times, such as voltage stability/collapse. The events can be numerous. Can new technology provide better and simpler solutions to system problems? What will be the principles and the underlined approaches?

The present day approach to out of step protection leads to excessive wear and tear of equipment as in general the out of step condition is recognized only after it has occurred resulting in delays in tripping the unstable unit and excessive exposure to high currents and abnormal conditions. Is there an approach that can be predictive and simple (not requiring settings for determining the condition?). A predictive approach is described in [2]. Can this approach be successfully implemented using present and future technology?

The present day special protection systems are based on "pattern recognition" approaches. The creation of the patterns requires extensive simulations of the system. They also require wide area measurements which in turn generate time latencies and complicate the analytics and the protection logic. Is there a better approach that will not

need the pre-computation of patterns? The key for an advanced approach will be improvements in wide area measurements and fast communication of the system status to a central location. For discussion reference, Figure 5.5 shows the typical configuration of special protection systems.

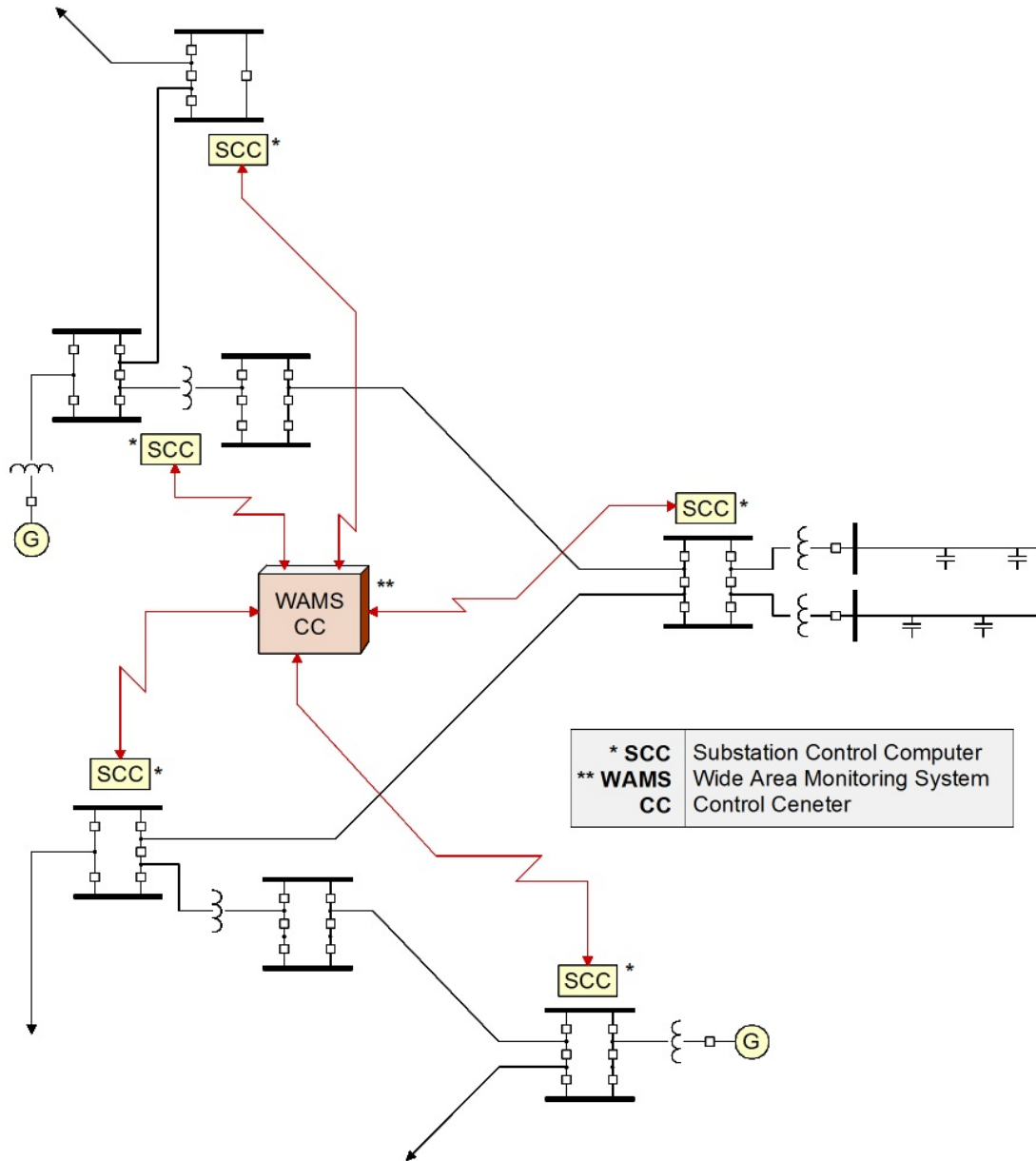


Figure 5.5 Typical Configurations of Special Protection Systems

A fundamental issue is the collection of the actual operating conditions (dynamics) of the system at the central location where the system protection "relay" will reside. One can analyze the constituent parts of the general configuration and determine what will be needed for a new reliable system protection scheme. One idea for discussion may be the use of local dynamic state estimators (distributed dynamic state estimators) at the

substation level and transmitting the substation dynamic states to the location of the system "relay" via fast communications. This approach will provide the dynamic system state to the system relay in the minimum possible time latency. System protection algorithms must be developed that will take advantage of this approach. Potentially, this approach can be direct and reliable in the sense that the protective relaying algorithm will be based on the dynamic state of the system.

5.4 Summary of State Estimation Approaches

The technology is ready today to use dynamic state estimation for protection. Of course challenges exist and it will take research activities to achieve the goal of taking protection decision on the basis of reliable and secure data from the dynamic state estimator. The advantage of state estimation approaches to protection is that it enables true setting-less protection schemes. The protection logic acts on the basis of the operating condition and health of a zone (component) or the system. The protection logic simply compares the condition to the operating limits of the component or the system. We believe it is feasible to develop and demonstrate setting-less zone protection (it is a low hanging fruit!!!). It also has the side benefit of providing a distributed model data base with perpetual validation.

The state estimation based protection approach represents a new paradigm that moves away from the traditional approach of mimicking the operation of electromechanical relays to the concept of monitoring the health and operating characteristics of components and systems as it is conceptually shown in Figure 5.6.

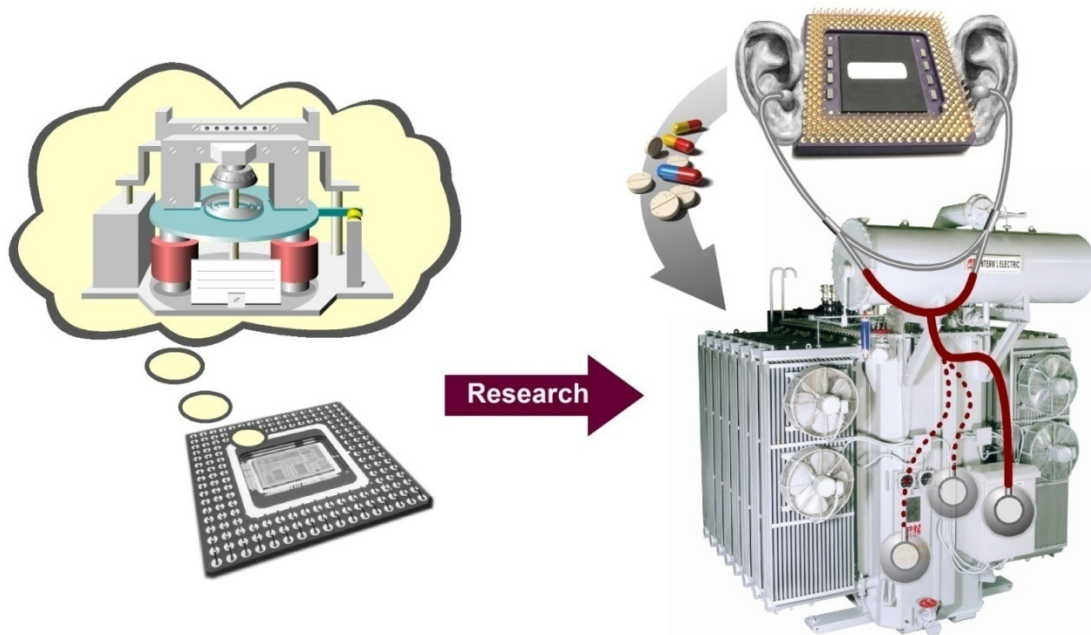


Figure 5.6 Concept of State Estimation Based Protection

6. Implementation of Setting-less Protection

The implementation of the setting-less protection has been approached from an object orientation point of view. For this purpose the constituent parts of the approach have been evaluated and have been abstracted into a number of objects. Specifically, the setting-less approach requires the following objects:

1. the mathematical model of the protection zone
2. the physical measurements that may consist of analog and digital data
3. the mathematical model of the physical measurements
4. the mathematical model of the virtual measurements
5. the mathematical model of the derived measurements
6. the mathematical model of the pseudo measurements
7. the dynamic state estimation algorithms
8. the bad data detection and identification algorithm
9. the protection logic and trip signals
10. online parameter identification method

The last task has not been addressed in the report but it is an integral part of the overall approach as in many cases it will be necessary to fine tune the model of the protection zone via online parameter identification methods.

An overview of the design of the setting-less protection relay is shown in Figure 6.1.

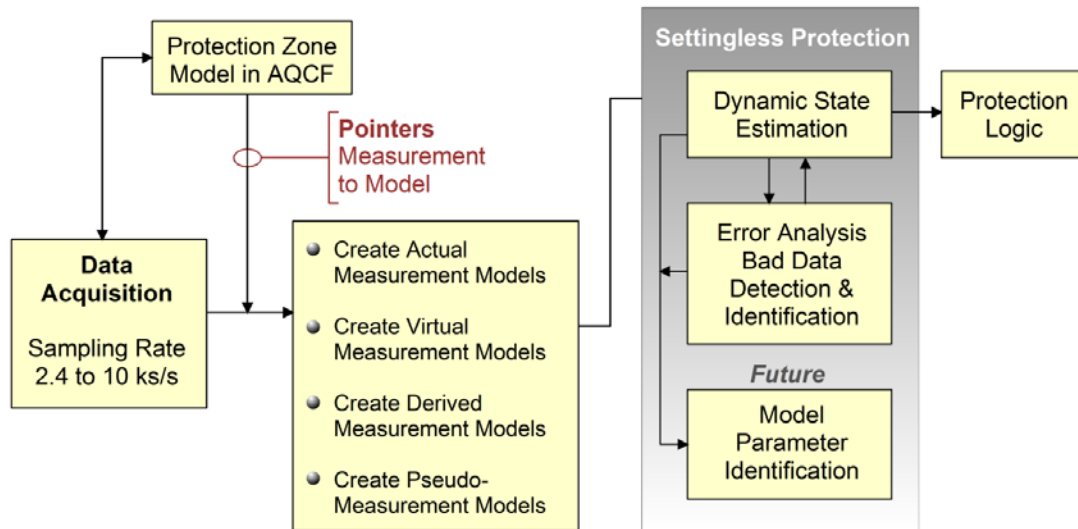


Figure 6.1 Setting-Less Protection Relay Organization

6.1 Protection Zone Mathematical Model

The protection zone mathematical model is required in a standard form. A standard has been defined in the form of the Algebraic Quadratic Companion Form (AQCF) and in a specified syntax to be defined later. The AQCF for a specific protection zone is derived with three computational procedures. Specifically, the dynamic model of a protection zone consists of a set of algebraic and differential equations. We refer to this model as the compact model of the protection zone. Subsequently this model is quadratized, i.e. in case there are nonlinearities of order greater than 2, additional state variables are introduced so that at the end the mathematical model consists of a set of linear and quadratic equations. We refer to this model as the quadratized model. Finally, the quadratized model is integrated using the quadratic integration method which converts the quadratized model of the protection zone into a set of algebraic (quadratic) function. This model is cast into a generalized Norton form. We refer to this model as the Algebraic Quadratic Companion Form. Examples of protection zone models in this form are provided in the six reports that accompany this main report.

The standard Algebraic Quadratic Companion Form is obtained with two procedures: (a) model quadratization, and (b) quadratic integration. The model quadratization reduces the model nonlinearities so that the dynamic model will consist of a set of linear and quadratic equations. The quadratic integration is a numerical integration method that is applied to the quadratic model assuming that the functions vary quadratically over the integration time step. The end result is an algebraic companion form that is a set of linear and quadratic algebraic equations that are cast in the following standards form:

$$\begin{bmatrix} i(t) \\ 0 \\ i(t_m) \\ 0 \end{bmatrix} = Y_{eq} \begin{bmatrix} v(t) \\ y(t) \\ v(t_m) \\ y(t_m) \end{bmatrix} + \begin{bmatrix} v(t) \\ y(t) \\ v(t_m) \\ y(t_m) \end{bmatrix}^T \cdot F_{eq,1} \cdot \begin{bmatrix} v(t) \\ y(t) \\ v(t_m) \\ y(t_m) \end{bmatrix} - b_{eq}, \quad (1)$$

where $i(t)$ is the through variable (current) vector, t is present time, t_m is the midpoint between the present and previous time, $v(t)$ is the across variable (voltage) vector, y is the internal state variables vector, Y_{eq} admittance matrix, $F_{eq,i}$ nonlinear matrices, and

$$b_{eq} = \sum_i A_i \cdot \begin{bmatrix} v(t-i \cdot h) \\ y(t-i \cdot h) \end{bmatrix} + \sum_i B_i \cdot \begin{bmatrix} i(t-i \cdot h) \\ 0 \end{bmatrix} + C. \quad (2)$$

The derivation of the standard Algebraic Quadratic Companion Form for specific protection zones is provided in the appropriate reports that describe the application of the setting-less protection schemes for specific protection zones.

This standardization allows the object oriented handling of measurements in state estimation; in addition it converts the dynamic state estimation into a state estimation that has the form of a static state estimation.

6.2 Object-Oriented Measurements

Any measurement, i.e. current, voltage, temperature, etc. can be viewed as an object that consists of the measured value and a corresponding function that expresses the measurement as a function of the state of the component. This function can be directly obtained (autonomously) from the Algebraic Quadratic Companion Form of the component. Because the algebraic companion form is quadratic at most, the measurement model will be also quadratic at most. Thus, the object-oriented measurement model can be expressed as the following standard equation:

$$\begin{aligned} z_k(t) = & \sum_i a_{i,t}^k \cdot x_i(t) + \sum_i a_{i,m}^k \cdot x_i(t_m) \\ & + \sum_{i,j} b_{i,j,t}^k \cdot x_i(t) \cdot x_j(t) \\ & + \sum_{i,j} b_{i,j,m}^k \cdot x_i(t_m) \cdot x_j(t_m) \\ & + c_k(t) + \eta_k, \end{aligned} \quad (3)$$

where z is the measured value, t the present time, t_m the midpoint between the present and previous time, x the state variables, a the coefficients of linear terms, b the coefficients of nonlinear terms, c the constant term, and η the measurement error.

The measurements can be identified as: (a) actual measurements, (b) virtual measurements, (c) derived measurements and (d) pseudo measurements. The types of measurements will be discussed next.

Actual Measurements: In general the actual measurements can be classified as across and through measurements. Across measurements are measurements of voltages or other physical quantities at the terminals of a protection zone such as speed on the shaft of a generator/model. These quantities are typically states in the model of the component. For this reason, the across measurements has a simple model as follows:

$$z_j(t) = x_j(t) + \eta_j. \quad (4)$$

Through measurements are typically currents at the terminals of a device or other quantities at the terminals of a device such as torque on the shaft of a generator/motor. The quantity of a through measurement is typically a function of the state of the device. For this reason, the through measurement model is extracted from the algebraic companion form, i.e. the measurement model is simply one equation of the ACF model, as follows:

$$z_j(t) = Y_{eq}^{(k)} \begin{bmatrix} v(t) \\ y(t) \\ v(t_m) \\ y(t_m) \end{bmatrix} + \begin{bmatrix} v(t) \\ y(t) \\ v(t_m) \\ y(t_m) \end{bmatrix}^T \cdot F_{eq,k} \cdot \begin{bmatrix} v(t) \\ y(t) \\ v(t_m) \\ y(t_m) \end{bmatrix} - b_{eq}^{(k)}, \quad (5)$$

where the superscript k means the k^{th} row of the matrix or the vector.

Virtual Measurements: The virtual measurements represent a physical law that must be satisfied. For example we know that at a node the sum of the currents must be zero by Kirchoff's current law. In this case we can define a measurement (sum of the currents); note that the value of the measurement (zero) is known with certainty. This is a virtual measurement.

The model can provide virtual measurements in the form of equations that must be satisfied. Consider for example the m^{th} AQCF model equation below:

$$0 = Y_{eq}^{(m)} \begin{bmatrix} v(t) \\ y(t) \\ v(t_m) \\ y(t_m) \end{bmatrix} + \begin{bmatrix} v(t) \\ y(t) \\ v(t_m) \\ y(t_m) \end{bmatrix}^T \cdot F_{eq,m} \cdot \begin{bmatrix} v(t) \\ y(t) \\ v(t_m) \\ y(t_m) \end{bmatrix} - b_{eq}^{(m)} \quad (6)$$

This equation is simply a relationship among the states the component that must be satisfied. Therefore we can state that the zero value is a measurement that we know with certainty. We refer to this as a virtual measurement.

Derived Measurements: A derived measurement is a measurement that can be defined for a physical quantity by utilizing physical laws. An example derived measurement is shown in Figure 6.2. The figure illustrates a series compensated power line with actual measurements on the line side only. Then derived measurements are defined for each capacitor section. Note that the derived measurements enable the observation of the voltage across the capacitor sections.

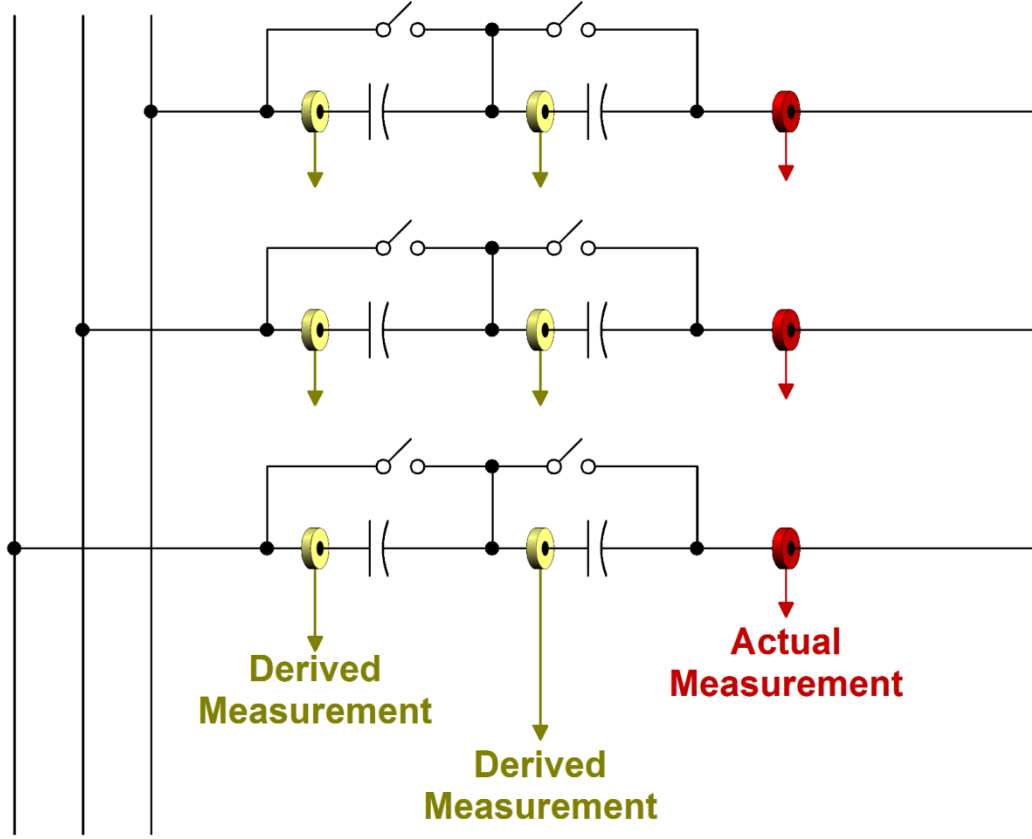


Figure 6.2 Example Derived Measurements

Pseudo Measurements: Pseudo measurements are hypothetical measurements for which we may have an idea of their expected values but we do not have an actual measurement. For example a pseudo measurement can be the voltage at the neutral; we know that this voltage will be very small under normal operating conditions. In this case we can define a measurement of value zero but with a very high uncertainty.

Summary: Eventually, all the measurement objects form the following measurement set:

$$z = h(x, t) + \eta = c + a^T x(t) + b^T x(t_m) + \begin{bmatrix} x^T(t) & x^T(t_m) \end{bmatrix} F \begin{bmatrix} x(t) \\ x(t_m) \end{bmatrix} + \eta, \quad (7)$$

where z is the measurement vector, x the state vector, h the known function of the model, a , b are constant vectors, F are constant matrices, and η the vector of measurement errors.

6.3 Object-Oriented Dynamic State Estimation

The proposed dynamic state estimation algorithm is the weighted least squares (WLS). The objective function is formulated as follows:

$$\text{Minimize } J(x,t) = [z - h(x,t)]^T W [z - h(x,t)], \quad (8)$$

where W is the diagonal matrix whose non-zero entries are the inverse of the variance of the measurement errors. The solution is obtained by the iterative method:

$$\hat{x}^{j+1} = \hat{x}^j + (H^T W H)^{-1} H^T W (z - h(\hat{x}^j, t)), \quad (9)$$

where \hat{x} is the best estimate of states and H the Jacobian matrix of $h(x,t)$.

It is important to note that the dynamic state estimation requires only the mathematical model of all measurements. It should be also noted that for any component, the number of actual measurements and virtual, derived, and pseudo measurements exceed the number of states and they are independent. This makes the system observable and with substantial redundancy.

6.4 Bad Data Detection and Identification

It is possible that the streaming measurements may include bad data. In this case the algorithm must detect the bad data and identify the data. For the case of setting-less protection, it is important to recognize that in case of a component internal fault, all data may appear as bad data. It is important to determine whether any detected bad data are coming from instrumentation and meter errors or from altered component model due to internal faults. This topic is still under investigation as to what the best approach would be.

6.5 Protection Logic / Component Health Index

The solution of the dynamic state estimation provides the best estimate of the dynamic state of the component. The well-known chi-square test provides the probability that the measurements are consistent with the dynamic model of the component. Thus the chi-square test quantifies the goodness of fit between the model and measurements (i.e., confidence level). The goodness of fit is expressed as the probability that the measurement errors are distributed within their expected range (chi-square distribution). The chi-square test requires two parameters: the degree of freedom (ν) and the chi-square critical value (ζ). In order to quantify the probability with one single variable, we introduce the variable k in the definition of the chi-square critical value:

$$\nu = m - n, \quad \zeta = \sum_{i=1}^m \left(\frac{h_i(\hat{x}) - z_i}{k \sigma_i} \right)^2, \quad (10)$$

where m is the number of measurements, n the number of states, and \hat{x} the best estimate of states. Note that since m is always greater than n , the degrees of freedom are always positive. Note also that if k is equal to 1.0 then the standard deviation of the measurement error corresponds to the meter error specifications. If k equals 2.0 then the standard

deviation will be twice as much as the meter specifications, and so on. Using this definition, the results of the chi square test can be expressed as a function of the variable k . Specifically, the goodness of fit (confidence level) can be obtained as follows:

$$\Pr[\chi^2 \geq \zeta(k)] = 1.0 - \Pr[\chi^2 \leq \zeta(k)] = 1.0 - \Pr(\zeta(k), \nu). \quad (11)$$

A sample report of the confidence level function (horizontal axis) versus the chi-square critical value, k , (vertical axis) is depicted in Figure 6.3.

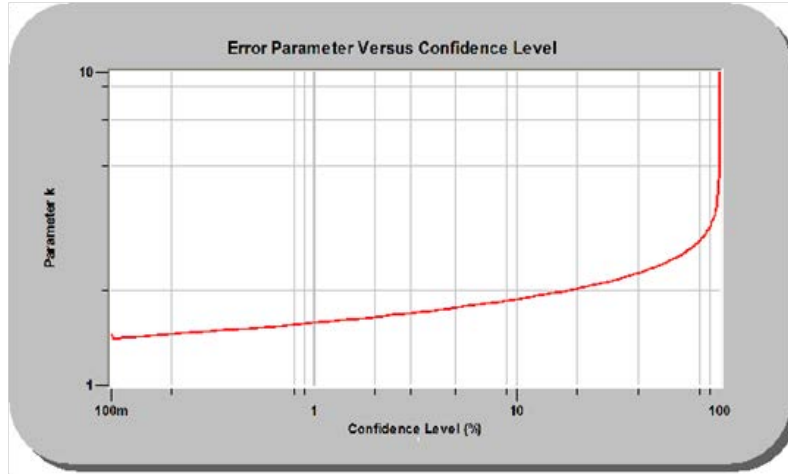


Figure 6.3 Confidence Level (%) vs Parameter k

The proposed method uses the confidence level as the health index of a component. A high confidence level indicates good fit between the measurement and the model, and thus we can conclude that the physical laws of the component are satisfied and the component has no internal fault. A low confidence level, however, implies inconsistency between the measurement and the model; therefore, we can conclude that an abnormality (internal fault) has occurred in the component and has altered the model. The discrepancy is an indication of how different the faulty model of the component is as compared to the model of the component in its healthy status.

It is important to point out that the component protection relay must not trip circuit breakers except when the component itself is faulty (internal fault). For example, in case of a transformer, inrush currents or overexcitation currents, should be considered normal and the protection system should not trip the component. The proposed protection scheme can adaptively differentiate these phenomena from internal faults. Similarly, the relay should not trip for start-up currents in a motor, etc.

6.6 Online Parameter Identification

The dynamic state estimation can be extended to include as states parameters of components. In this case, the parameters of the components can be identified from measurements. This represents a fine tuning of the component model.

This option should not be continuously applied. Instead, it should be exercised only when there is doubt about the correctness of the component parameters. The issue will be addressed in greater detail in the filed applications of the setting-less protective relay.

6.7 Summary and Comments

The previous subsections have presented the approach for setting-less protection. The method is based on dynamic state estimation. The dynamic state estimation requires a detail model of the component under protection (protection zone) and a data acquisition system that acquires data with sufficient speed, such as 2,000 samples per second or higher. The accuracy of the data acquisition system is important, the more accurate it is the better the selectivity of the relay.

The proposed protection approach has been applied to several types of components (i.e. transformers, transmission lines, capacitor banks, etc.). We present examples in the next section.

7. Example Applications: Capacitor Bank Protection

This section presents example applications of setting-less protection for capacitor banks. The setting-less protection algorithm could be built in a relay and the constituent parts of the relay are described. The application has been evaluated by a number of numerical experiments.

7.1 Summary

A capacitor bank typically consists of strings of capacitor cans connected in series and in parallel to form the capacitor bank of the proper ratings. Figure 7.1 shows an example capacitor bank. It is important to point out that the instrumentation of capacitor banks typically includes the terminal voltages and currents as well as other measurements such as neutral voltage and current, current in parallel strings of capacitor cans, etc. All the available measurements should be included in the analytics of the protection function for the capacitor bank. We briefly describe the constituent parts of the setting-less protection for the capacitor bank and then present an example result, typical timing data and discussion of issues associated with capacitor bank protection.

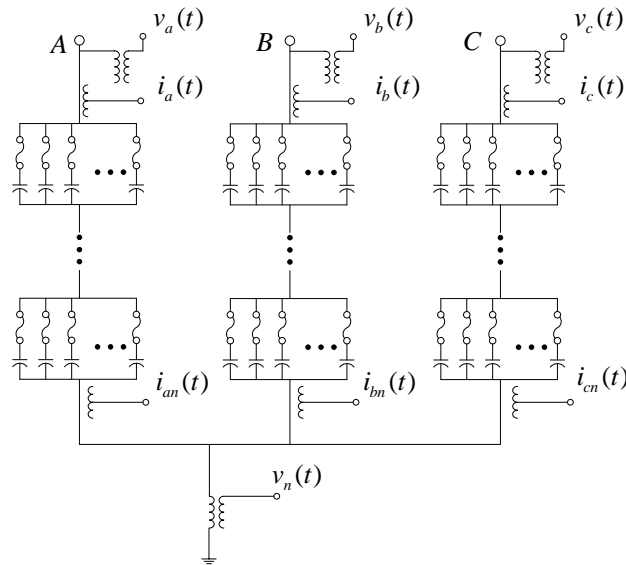


Figure 7.1 Three Phase Capacitor Bank Construction

Mathematical Model: The mathematical model of the capacitor bank is expressed in the SCAQCF (State and Control Algebraic Quadratic Companion Form). The exact model and form is provided in the Appendix 1.

System State: The system state is defined in the SCAQCF model. Note that the states are classified as external state and internal states. The **external states** are the three terminal voltages at time t (phase A-G, phase B-G, and phase C-G) and three terminal voltages at time t_m (phase A-G, phase B-G, and phase C-G). The **internal states** are the neutral

voltage, the voltages at internal points of the capacitor bank and the current through the current limiting inductors.

Measurements: They consist of the actual, virtual, derived and pseudo measurement. The minimum **actual measurements** for the capacitor bank are the phase voltages and currents at the terminals of the capacitor bank. Many capacitor banks may have additional measurements, such as current and voltage at the neutral of the bank, electric current through each parallel string of capacitor cans, etc. From the setting-less protection point of view, the more measurements the better the performance of the algorithm will be.

The virtual measurements represent the zero value on the left hand side of the equations: two measurements with value equal zero at time t ; two measurements with value equal zero at time $t_m = t - h/2$. For these measurements the measurement error is assume to have a standard deviation equal to 0.001 pu (as a matter of fact these measurements have zero error but the algorithm does not permit zero as it will generate singularity in the state estimation algorithm).

The **derived measurements** are electric current measurements at individual capacitor cans.

The **pseudo measurements** for the capacitor bank are typically the voltage at the neutral of the capacitor bank in case there is no actual measurement of the neural voltage.

Numerical experiments were performed with a three phase capacitor bank. For this example the capacitor bank model is expressed in terms of 10 states. The number of measurements is 24: 20 actual measurements, 4 virtual measurements, and 0 pseudo measurements. The redundancy is 140% $((24-10)/10)$.

Using the above model the following events were considered: (a) external line-to-line faults, (b) external single line-to-ground faults, (c) internal faults. For each event, the system was simulated and a COMTRADE file was generated with the time waveforms of the actual measurements. Subsequently the COMTRADE file was “played” back through the setting-less protection for the capacitor bank. The results were recorded into another COMTRADE file. The output file includes the following data: (a) the actual measurements, (b) the estimated states of the capacitor bank, (c) the estimated values of the actual measurements, (d) the normalized measurement residuals, i.e. difference between the actual measurements and the estimated values of the actual measurements divided by the meter accuracy (meter standard deviation of measurement error) and (e) the relay decision (trip/no-trip). Specifically, Figure 7.2 illustrates the measured voltages, the estimated voltage, the normalized residuals of the voltage measurements and the trip/no-trip decision. Note that this event includes an internal fault at time 1.25 sec that clears at 1.45 sec, an external system change at time 2.0 sec and two external faults, one at time 2.25 sec and another at time 2.45 sec. Note the relay tripped for the internal fault only.

Execution Time: For this event, the execution time of the state estimation at each set of data was measured and reported in Figure 7.3. Note that average execution time for each state estimation process is around 400 μ s. This value is to be compared with the sampling rate of the data acquisition system of the relay. The sampling rate is 4000 s/s. This means that the state estimation is called 4000/2 times per second. This means that the data for the state estimation are coming in one set per 0.0005 seconds. Therefore the state estimation is performed in less time that the period between two successive sets of data. The objective is to perform the analytics of the setting-less protection in less than 50% of the time between two successive sets of data. Since the code has not been optimized and the computer hardware has much room to improve, this objective can be easily achieved.

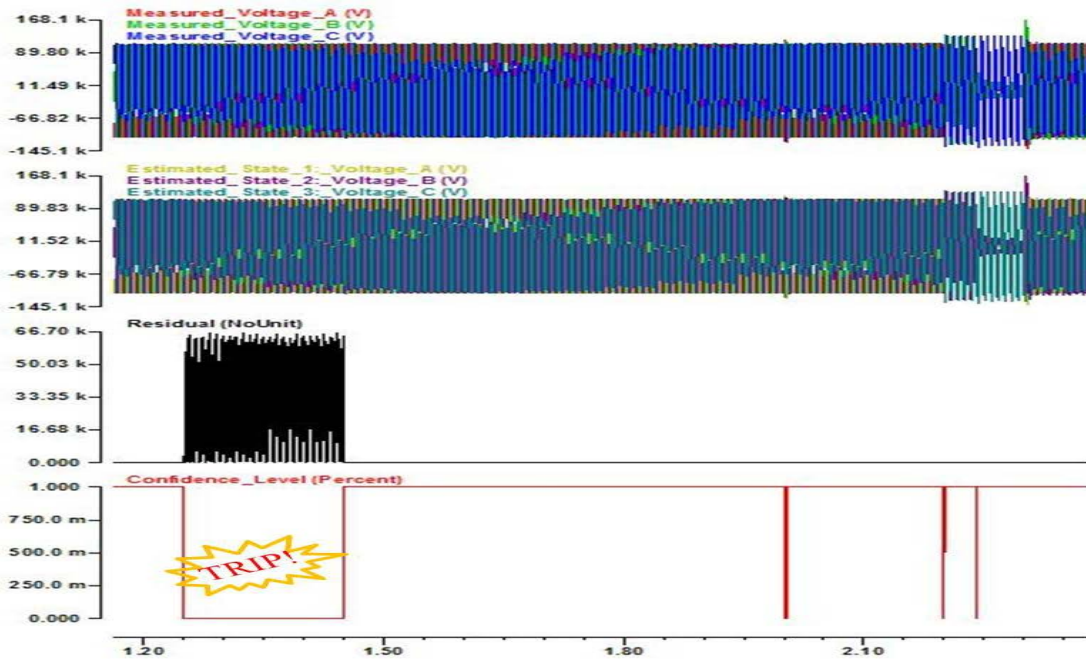


Figure 7.2 Result of an Example Test System with Internal and External Faults

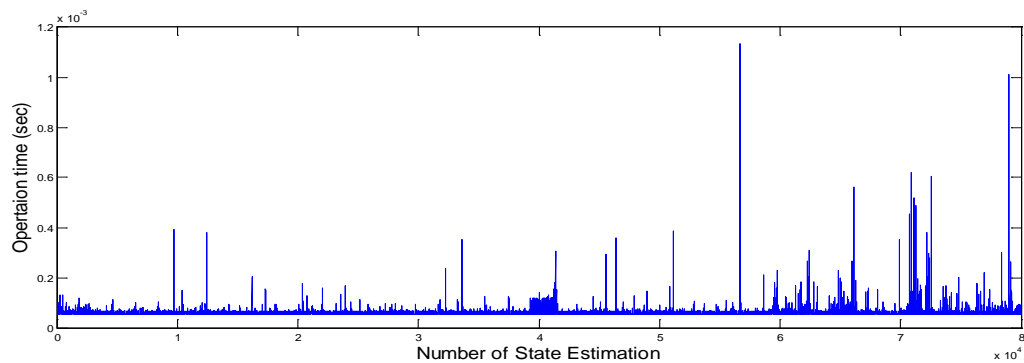


Figure 7.3 Capacitor Bank Setting-less Protection Execution Time

The numerical experiments with the above mentioned events have demonstrated the feasibility of setting-less protection and the ability to perform the analytics of the setting-less protection within the time interval of two consecutive sets of data. This is the first try of the approach. Many possible improvement have been identified: (a) the analytics can be performed in faster times by optimizing the code - a dramatic speedup can be achieved by using sparsity techniques, (b) derived measurements can be used to achieve full observability of the capacitor bank, i.e. estimating the voltage at each one of the capacitor cans, (c) it is possible to identify individual failed cans instead of simply issuing a trip/no-trip command. These issues and improvements will be the subject of continuing investigation.

This section describes the implementation approach for the setting-less protective relay for three phase capacitor banks (state estimation based approach). The models and the algorithmic procedures of the analytics are also described. Numerical experiments with an example system are presented that illustrate the operation of the setting-less protection for capacitor banks. The execution times of the analytics of the setting-less protection are also presented for the numerical experiments. Even if the computer code is not optimized the execution times are lower than the sampling period of the data indicating the feasibility of the approach. Finally, the various configurations and hardware requirements for the setting-less protective relay are discussed.

7.2 Setting-less Relay Description

This section describes the overall implementation of the setting-less protective relay. The architecture of this relay is shown in Figure 6.1. Note that the relay requires the model of the zone to be protected and the actual (physical) measurements from the data acquisition system. The model must be provided in the SCAQCF syntax which is defined in this document. Then the remaining analytics are automatically constructed and executed. These are: the pointers that provide the interrelationship of the actual measurements to the zone model, the creation of the measurement models for the actual, virtual, derived and pseudo measurements, the dynamic state estimation, the bad data detection and identification and the protection logic.

Note that the data acquisition system is continuously streaming measurement into the relay with a specific rate. Typical rates are 2,000 to 5,000 samples per second. As it will be seen later, the model of the component to be protected is derived in the SCAQCF by using the quadratic integration. The SCAQCF model is expressed in terms of the values of the various variables at two consecutive time instances (two consecutive samples) and past history samples. This means that the analytics of the setting-less relay operate on samples of two consecutive time instances. This is illustrated in Figure 7.4. The samples (measurements) at the two consecutive time instances t and $(t-t_s)$ are used. Note that t_s defines the sampling period. For the typical sampling rates referenced above the minimum sampling period will be 200 microseconds (5,000 samples per second). This means that the analytics of the setting-less relay must be performed within the time

interval of 400 microseconds (before the next set of data arrive). Obviously, there should be a margin. For this reason the goal for the setting-less relay is to perform the analytics in time less than 200 microseconds. Numerical experiments have been performed and the performance is documented in this report.

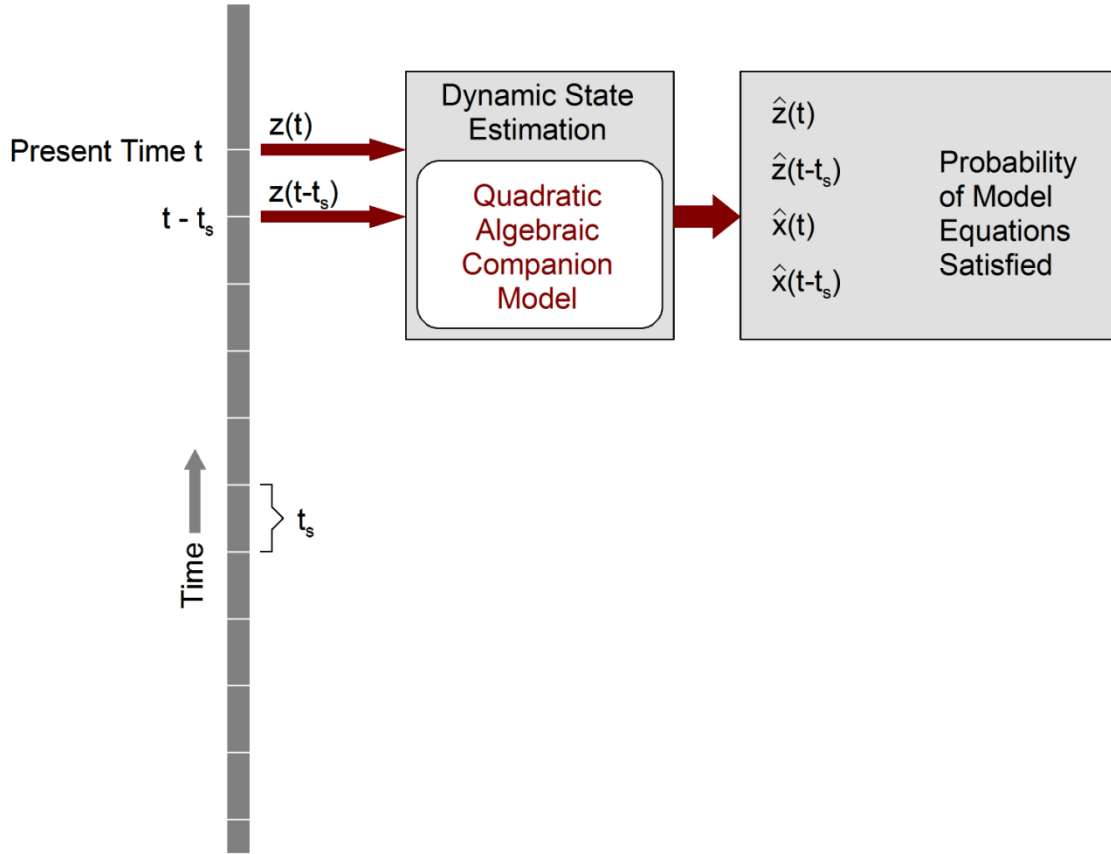


Figure 7.4 Illustration of Time Samples Utilized at Each Iteration of the Setting-less Relay Analytics

7.3 Three Phase Capacitor Bank SCAQCF Model

The three phase capacitor banks SCAQCF model is presented in this session.

The circuit model of the three phase capacitor bank is shown in Figure 7.5.

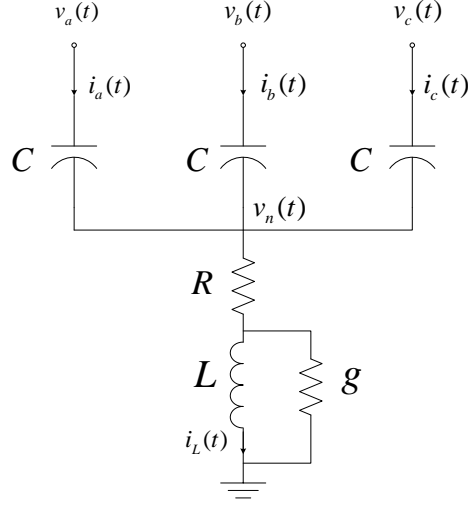


Figure 7.5 Three Phase Capacitor Banks Compact Model

The state and control algebraic quadratic companion form model of the three phase capacitor bank model is given below. The derivation of this model is provided in Appendix 1. Note that there is no control variable in this model.

At time t ,

$$\begin{aligned}
 i_a(t) &= -4 \cdot i_a(t_m) + \frac{6}{h} \cdot C \cdot (v_a(t) - v_n(t)) - (i_a(t-h) + \frac{6}{h} \cdot C \cdot (v_a(t-h) - v_n(t-h))) \\
 i_b(t) &= -4 \cdot i_b(t_m) + \frac{6}{h} \cdot C \cdot (v_b(t) - v_n(t)) - (i_b(t-h) + \frac{6}{h} \cdot C \cdot (v_b(t-h) - v_n(t-h))) \\
 i_c(t) &= -4 \cdot i_c(t_m) + \frac{6}{h} \cdot C \cdot (v_c(t) - v_n(t)) - (i_c(t-h) + \frac{6}{h} \cdot C \cdot (v_c(t-h) - v_n(t-h))) \\
 0 &= \frac{h}{6} \cdot G \cdot v_n(t) + \frac{2h}{3} \cdot G \cdot v_n(t_m) - (G \cdot L \cdot i_L(t) + C \cdot (v_a(t) + v_b(t) + v_c(t) - 3 \cdot v_n(t))) \\
 &\quad + (\frac{h}{6} \cdot G \cdot v_n(t-h) + G \cdot L \cdot i_L(t-h) + C \cdot (v_a(t-h) + v_b(t-h) + v_c(t-h) - 3 \cdot v_n(t-h))) \\
 0 &= \frac{h}{6} \cdot i_L(t) + \frac{2h}{3} \cdot i_L(t_m) - (C \cdot (v_a(t) + v_b(t) + v_c(t) - 3 \cdot v_n(t)) - g \cdot L \cdot i_L(t)) \\
 &\quad + (\frac{h}{6} \cdot i_L(t-h) + C \cdot (v_a(t-h) + v_b(t-h) + v_c(t-h) - 3 \cdot v_n(t-h)) - g \cdot L \cdot i_L(t-h))
 \end{aligned}$$

At time t_m ,

$$i_a(t_m) = \frac{1}{8} \cdot i_a(t) + \frac{3}{h} \cdot C \cdot (v_a(t_m) - v_n(t_m)) - \frac{3}{h} \cdot (\frac{5h}{24} \cdot i_a(t-h) + C \cdot (v_a(t-h) - v_n(t-h)))$$

$$\begin{aligned}
i_b(t_m) &= \frac{1}{8} \cdot i_b(t) + \frac{3}{h} \cdot C \cdot (v_b(t_m) - v_n(t_m)) - \frac{3}{h} \cdot \left(\frac{5h}{24} \cdot i_b(t-h) + C \cdot (v_b(t-h) - v_n(t-h)) \right) \\
i_c(t_m) &= \frac{1}{8} \cdot i_c(t) + \frac{3}{h} \cdot C \cdot (v_c(t_m) - v_n(t_m)) - \frac{3}{h} \cdot \left(\frac{5h}{24} \cdot i_c(t-h) + C \cdot (v_c(t-h) - v_n(t-h)) \right) \\
0 &= -\frac{h}{24} \cdot G \cdot v_n(t) + \frac{h}{3} \cdot G \cdot v_n(t_m) - (G \cdot L \cdot i_L(t_m) + C \cdot (v_a(t_m) + v_b(t_m) + v_c(t_m) - 3 \cdot v_n(t_m))) \\
&\quad + \left(\frac{5h}{24} \cdot G \cdot v_n(t-h) + G \cdot L \cdot i_L(t-h) + C \cdot (v_a(t-h) + v_b(t-h) + v_c(t-h) - 3 \cdot v_n(t-h)) \right) \\
0 &= -\frac{h}{24} \cdot i_L(t) + \frac{h}{3} \cdot i_L(t_m) - (C \cdot (v_a(t_m) + v_b(t_m) + v_c(t_m) - 3 \cdot v_n(t_m)) - g \cdot L \cdot i_L(t_m)) \\
&\quad + \left(\frac{5h}{24} \cdot i_L(t-h) + C \cdot (v_a(t-h) + v_b(t-h) + v_c(t-h) - 3 \cdot v_n(t-h)) - g \cdot L \cdot i_L(t-h) \right)
\end{aligned}$$

Based on the above equations, it is very easy to write all equations into the following SCAQCF standard syntax:

$$\begin{bmatrix} i(t) \\ 0 \\ i(t_m) \\ 0 \end{bmatrix} = Y_{eq} \begin{bmatrix} v(t) \\ y(t) \\ v(t_m) \\ y(t_m) \end{bmatrix} + \begin{bmatrix} \begin{bmatrix} v(t) \\ y(t) \\ v(t_m) \\ y(t_m) \end{bmatrix}^T \\ \vdots \end{bmatrix} \cdot F_{eq,1} \cdot \begin{bmatrix} v(t) \\ y(t) \\ v(t_m) \\ y(t_m) \end{bmatrix} - b_{eq}$$

For three phase capacitor banks, there are 10 states (5 for time step t and 5 for intermediate time step t_m).

For time step t , the states are listed below.

The states are defined as follows:

External states:

0. $v_a(t)$: terminal voltage at phase A (kV);
1. $v_b(t)$: terminal voltage at phase B (kV);
2. $v_c(t)$: terminal voltage at phase C (kV);

Internal states:

0. $v_n(t)$: terminal voltage at neutral point (kV)
1. $i_L(t)$: current through the inductance (kA)

For time step t_m , the states are the same.

7.4 Capacitor Bank Measurements Definition

Measurements consist of the actual, virtual, derived and pseudo measurement. The minimum **actual measurements** for the capacitor bank are the phase voltages and currents at the terminals of the capacitor bank. Many capacitor banks may have additional measurements, such as current and voltage at the neutral of the bank, electric current through each parallel string of capacitor cans, etc. For the setting-less protection point of view, the more measurements the better the performance of the algorithm will be.

Here in this report, just the most basic measurements are used:

Actual measurements: six currents at time t (phase A, phase B, and phase C; cap bank terminals and near neutral point); four voltages at time t (phase A-G, phase B-G, phase C-G, and Neutral-G); six currents at time $t_m=t-h/2$ (phase A, phase B, and phase C; cap bank terminals and near neutral point); four voltages at time $t_m=t-h/2$ (phase A-G, phase B-G, and phase C-G, and Neutral-G); For these measurements assume a measurement error with standard deviation equal to 0.01 pu.

Virtual measurements: these measurements represent the zero value on the left hand side of the equations 4, 5, 9 and 10: two measurements with value equal zero at time t (equations 4 and 5); two measurements with value equal zero at time $t_m=t-h/2$ (equations 9 and 10). For these measurements assume a measurement error with standard deviation equal to 0.001 pu (as a matter of fact these measurements have zero error but you cannot use zero as this will generate singularity in the state estimation algorithm).

Derived Measurements: are electric current measurements at individual capacitor cans. They are used to achieve full observability of the capacitor banks. For the most basic case we will not consider derived measurements

Pseudo measurements: in this case we will not consider pseudo measurements

In summary, for the three phase capacitor bank, there are 20 actual measurements, 4 virtual measurements, and zero derived and pseudo measurements, a total of 24 (12 for time step t and 12 for intermediate time step t_m). There would be 10 states, which provides a redundancy of 140% $((24-10)/10)$.

$$\text{In summary, the measurements are } z = h(x) = \begin{bmatrix} i(x) \\ v(x) \\ 0 \end{bmatrix}$$

7.5 Creation of Measurement Models

This section describes the creation of the mathematical models of the measurements.

7.5.1 Creation of Actual Measurement Model

If the measurement is an actual through measurement, it is related to a specific row of the SCAQCF model.

The model of this kind of measurement is as follows:

$$I^k(t) = \sum_i Y_{eq,i}^k \cdot x_i - \sum_i b_{eq,i}^k + \eta_k$$

where k is the corresponding pointer for the terminal number.

If the measurement is an actual across measurement, it is not related to a specific row of the SCAQCF model but it is related directly to the state of the capacitor bank. The model of this kind of measurement is as follows:

$$V^m = x_i \pm x_j + \eta$$

where x_i, x_j , are all the states related to this measurement.

7.5.2 Creation of Virtual Measurement Model

The virtual measurements are not real measurements so they cannot be measured. It is related to a specific row of the SCAQCF model.

The model of this kind of measurement is as follows:

$$0 = \sum_i Y_{eq,i}^k \cdot x_i - \sum_i b_{eq,i}^k + \eta_k$$

where k stands for kth row of this measurement.

7.5.3 Creation of Derived Measurement Model

There are no derived measurements in this capacitor banks case so no derived measurement model is needed.

7.5.4 Creation of Pseudo Measurement Model

There are no pseudo measurements in this capacitor banks case so no pseudo measurement model is needed.

7.6 State Estimation Algorithm

The dynamic state estimation is described as follows: First the model of the three phase capacitor bank under protection is cast into a standard algebraic quadratic companion form which is shown above. The measurements are classified into (a) actual measurements, (b) virtual measurements and (c) derived measurements, (d) pseudo measurements. All the measurements are listed in 7.4.

A physical measurement, a virtual measurement or a pseudo-measurement at time t has the following generalized SCAQCF form:

$$\mathbf{y}(\mathbf{x}, \mathbf{u}) = Y_{m,x} \mathbf{x} + \left\{ \begin{array}{c} \vdots \\ \mathbf{x}^T F_{m,x}^i \mathbf{x} \\ \vdots \end{array} \right\} + Y_{m,u} \mathbf{u} + \left\{ \begin{array}{c} \vdots \\ \mathbf{u}^T F_{m,u}^i \mathbf{u} \\ \vdots \end{array} \right\} + \left\{ \begin{array}{c} \vdots \\ \mathbf{x}^T F_{m,xu}^i \mathbf{u} \\ \vdots \end{array} \right\} + C_m$$

where:

$\mathbf{y}(\mathbf{x}, \mathbf{u})$: measurement variables of the component model at both time t and time t_m ,

$\mathbf{y} = [\mathbf{y}(t), \mathbf{y}(t_m)]$

\mathbf{x} : external and internal state variables of the component model, $\mathbf{x} = [\mathbf{x}(t), \mathbf{x}(t_m)]$

\mathbf{u} : control variables of the component model, i.e. transformer tap, etc. $\mathbf{u} = [\mathbf{u}(t), \mathbf{u}(t_m)]$

$Y_{m,x}$: matrix defining the linear part for state variables,

$F_{m,x}$: matrices defining the quadratic part for state variables,

$Y_{m,u}$: matrix defining the linear part for control variables,

$F_{m,u}$: matrices defining the quadratic part for control variables,

$F_{m,xu}$: matrices defining the quadratic part for the product of state and control variables,

C_m : constant vector of the measurement model (past history).

The weighted least squares approach will be used for the state estimator. The algorithm is defined as follows:

$$\sigma_{n_k} = \sqrt{\text{Var}(n_k)}$$

$$\text{Minimize } J = \sum_{i=1}^m \left(\frac{h_i(x) - z_i}{\sigma_i} \right)^2 = \sum_{i=1}^m s_i^2 = \eta^T W \eta$$

where: $s_i = \frac{\eta}{\sigma_i}$, $W = \text{diag} \left\{ \frac{1}{\sigma_1^2}, \frac{1}{\sigma_2^2}, \dots, \frac{1}{\sigma_m^2} \right\}$

The solution is given with the following iterative algorithm:

$$x^{v+1} = x^v - (H^T W H)^{-1} H^T W (h(x^v) - z)$$

where H is the Jacobean matrix: $H = \frac{\partial h(x)}{\partial x}$, computed at $x = x^\nu$

At each time step of the estimation algorithm, the contributions of each measurement to the information matrix $H^T W H$ and the vector $H^T W (h(x^\nu) - z)$ must be computed. For example assuming that the i-th measurement has the following generic form (for simplicity only one linear and one quadratic term is included):

$$z_i = c_i + a_{i1} \cdot x_{i1} + a_{i2} \cdot x_{i2} \cdot x_{i3} + \eta_i$$

Then the Jacobean matrix's i-th row will be:

$$[0 \quad \cdots \quad a_{i1} \quad \cdots \quad a_{i2} \cdot x_{i2} \quad \cdots \quad a_{i2} \cdot x_{i3} \quad \cdots \quad 0]$$

The contribution of this row to the information matrix $H^T W H$ is the following:

$$\begin{bmatrix} 0 & \cdots & 0 & \cdots & 0 & \cdots & 0 & \cdots & 0 \\ \vdots & & \vdots & & \vdots & & \vdots & & \vdots \\ 0 & \cdots & w_i a_{i1} a_{i1} & \cdots & w_i a_{i1} a_{i2} x_{i2} & \cdots & w_i a_{i1} a_{i2} \cdot x_{i3} & \cdots & 0 \\ \vdots & & \vdots & & \vdots & & \vdots & & \vdots \\ 0 & \cdots & w_i a_{i1} a_{i2} \cdot x_{i2} & \cdots & w_i (a_{i2} \cdot x_{i2})^2 & \cdots & w_i a_{i2}^2 \cdot x_{i2} x_{i3} & \cdots & 0 \\ \vdots & & \vdots & & \vdots & & \vdots & & \vdots \\ 0 & \cdots & w_i a_{i1} a_{i2} \cdot x_{i3} & \cdots & w_i a_{i2}^2 \cdot x_{i2} x_{i3} & \cdots & w_i (a_{i2} \cdot x_{i3})^2 & \cdots & 0 \\ \vdots & & \vdots & & \vdots & & \vdots & & \vdots \\ 0 & \cdots & 0 & \cdots & 0 & \cdots & 0 & \cdots & 0 \end{bmatrix}$$

The contribution of the measurement to the vector $H^T W (h(x^\nu) - z)$ is the following:

$$\begin{bmatrix} 0 \\ \vdots \\ w_i a_{i1} b_i \\ \vdots \\ w_i a_{i2} \cdot x_{i2} b_i \\ \vdots \\ w_i a_{i2} \cdot x_{i3} b_i \\ \vdots \\ 0 \end{bmatrix}, \quad \text{where} \quad b_i = c_i + a_{i1} \cdot x_{i1} + a_{i2} \cdot x_{i2} \cdot x_{i3} - z_i$$

The above general formulae lead to a very simple algorithm for forming the information matrix H^TWH and $H^TW(h(x^v) - z)$ the vector and updating the state x .

7.7 Protection Logic

The entire protection logic is based on the measurements obtained from the data acquisition system and the results of dynamic state estimation.

Once the microprocessor gets the measurements from the three phase of capacitor bank, the dynamic state estimation is run according to the capacitor bank AQCF model. Then the Chi-square of all the measurements is calculated to check whether all the actual measurement values are consisted with the model of the capacitor bank.

$$\text{Chi-square: } \chi^2(t) = \|r(t)\|_2$$

Based on the Chi-square, the confidence level (or probability) that the measurements and the model of the capacitor back fit together within the accuracy of the meters is computed with:

$$Pr[\chi^2 \geq \xi_1] = 1 - Pr[\chi^2 \leq \xi_1] = 1 - Pr(\xi_1, v), \quad v \text{ is the degree of freedom}$$

If the confidence level drop to low values for several cycles, then it means the measurements do not fit the model, thus there is somewhere internal to the capacitor bank a fault or an alteration that changes the model. This indicates an abnormality (internal fault, capacitor can failure, etc.). In this case the relay would activate the breaker and trip the capacitor banks immediately. Meanwhile, during the state estimation process, the operating limits of the capacitor bank are being monitored (for example excessive harmonic currents, etc.) so that the three phase capacitor banks will be tripped once it violates the operating limit.

7.8 Numerical Experiments

The above described setting-less relay for three phase capacitor banks has been tested with simulated data. Specifically a test system is used to create a number of scenarios. For each scenario the system is simulated and all the measurements of the system are stored in a COMTRADE file. Our setting-less protection algorithm is applied on each scenario and the results are stored in a new COMTRADE file combined with the old one. From the results, we can see our setting-less protection can differentiate the capacitor banks external and internal faults and take the trip or no trip action correctly.

The test system including capacitor banks under protection and an integrated system around it is shown in Figure 7.6:

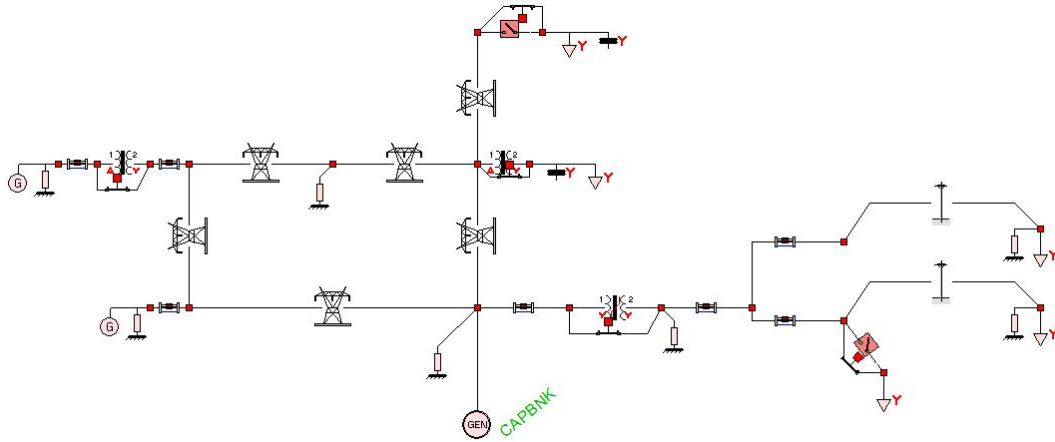


Figure 7.6 Test System Diagram for Capacitor Bank Zone, Base Case

7.8.1 Test Scenario 1

In this section, an external line-to-line fault is simulated. Figure 7.7 shows how the test system is created. The red dash block shows the location where Phase A and Phase C are shorted.

Figure 7.8 is the test result of the external line-to-line fault. In the figure, the measured voltages (states), the estimated states, the residual and the confidence level are shown. It can be seen that when there is no fault, the estimated states from state estimation is exactly same as the measured states, which indicates that the entire state estimation process is correct. When the external line-to-line fault happens at 1.75s, the residual becomes large and the confidence level drops to zero very quickly. But the confidence level goes back to one immediately which indicates the fault is an external fault and the states still match the cap bank model. It means that there is no fault inside the capacitor bank and no trip needs to be acted.

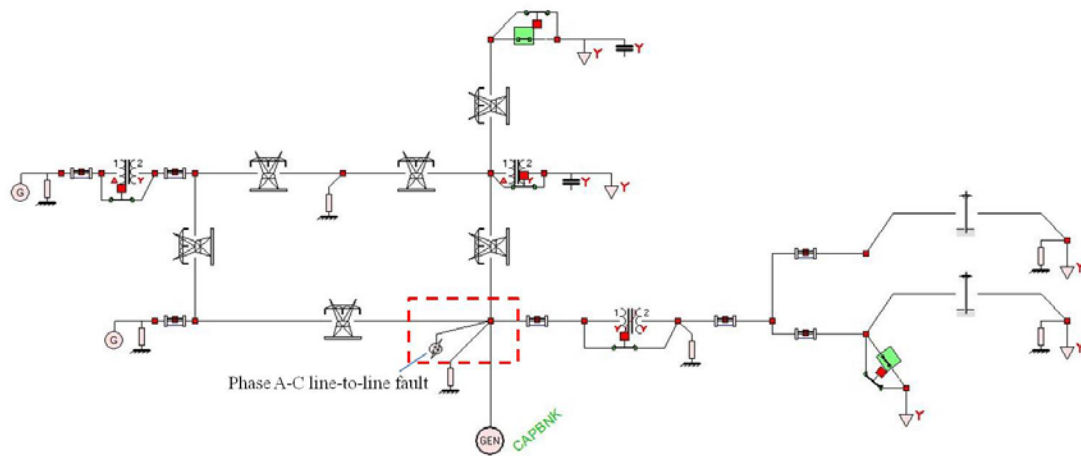


Figure 7.7 Test System Diagram for Capacitor Bank Zone, Scenario 1

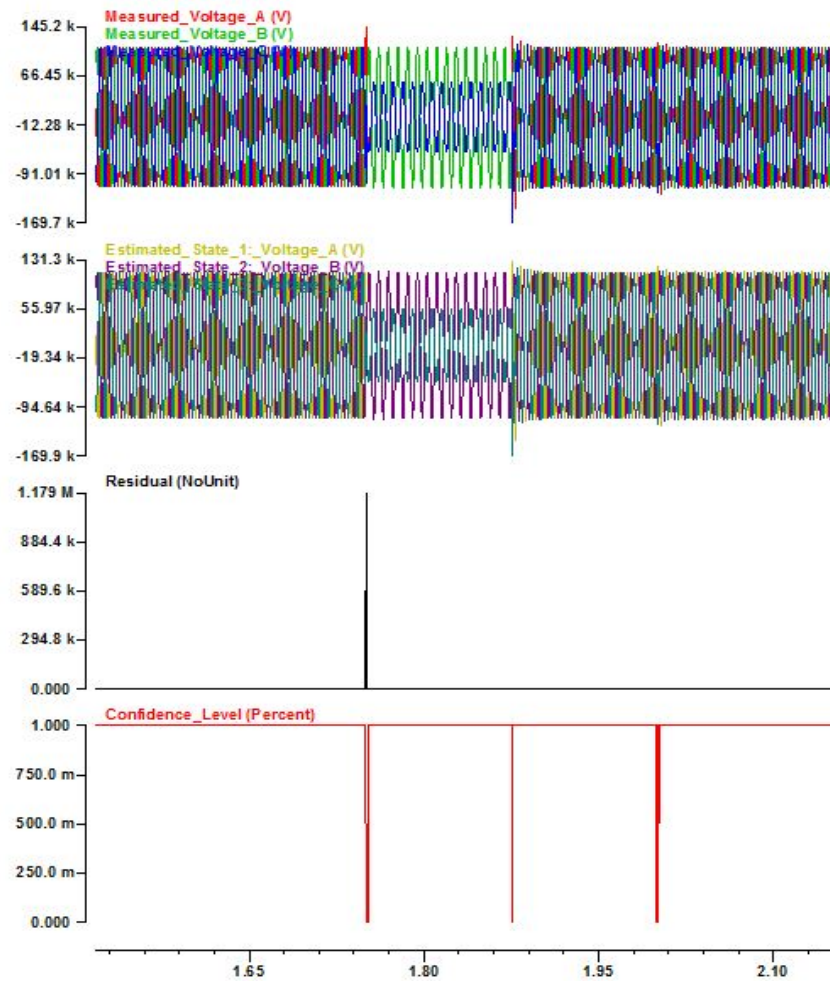


Figure 7.8 Result of Scenario 1

7.8.2 Test Scenario 2

In this section, an external single line-to-ground fault is simulated. Figure 7.9 shows how the test system is created. The red dash block shows the location where Phase B and ground are shorted, while the green dash block shows where Phase C is shorted to ground.

Figure 7.10 shows the test result of the external single line-to-ground fault. In the figure, the measured states, the estimated states, the residual and the confidence level are shown. It can be seen that the external single line-to-ground fault happens at 2.2s and another external line-to-ground fault happens at 2.24s. Because of the fault, the residual becomes large and the confidence level drops to zero very quickly. But the confidence level goes back to one immediately which indicates all the faults are external faults and the states still match the model. It means that there is no fault inside the capacitor bank and no trip needs to be acted.

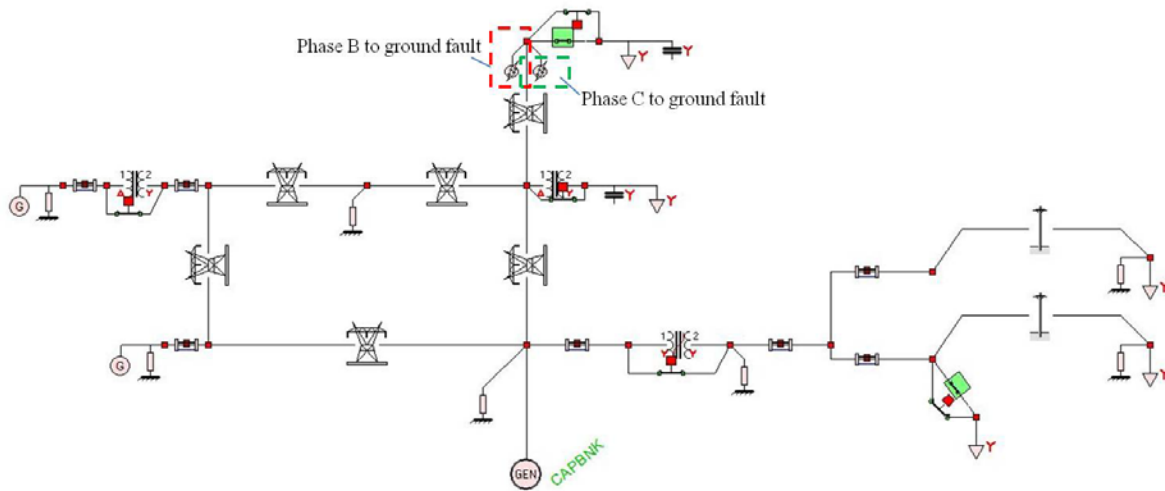


Figure 7.9 Test System Diagram for Capacitor Bank Zone, Scenario 2

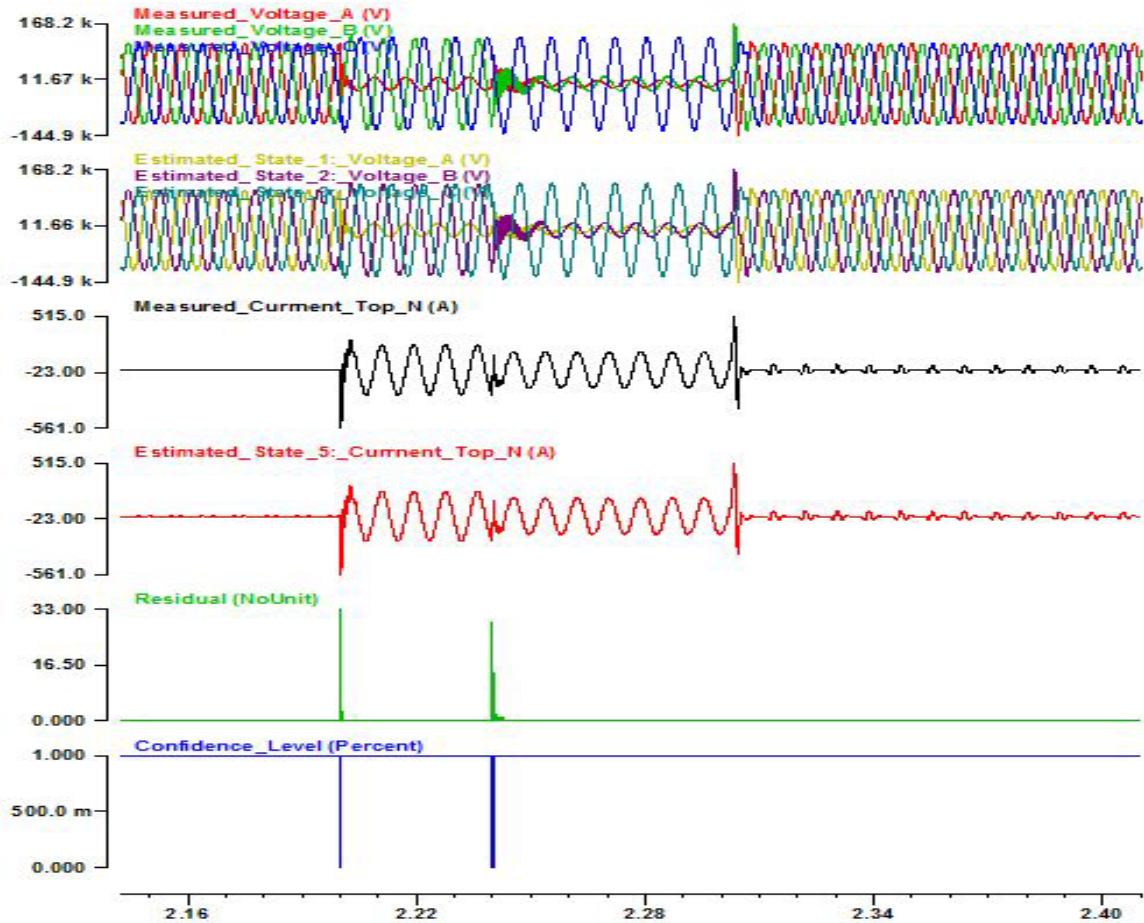


Figure 7.10 Result of Scenario 2

7.8.3 Test Scenario 3

In this section, an internal fault is simulated. Figure 7.11 shows how the test system is created. The red dash block shows where fault happens.

Figure 7.12 shows the test results of the above system. In the figure, the measured states, the estimated states, the residual and the confidence level are shown. It can be seen that the internal fault happens at 1.5s and clears at 1.9s. Because of the fault, the residual becomes large and the confidence level drops to zero very quickly. Different from scenario 0 and 1, the confidence level remains to be zero until the fault gets cleared, which means the fault is an internal fault and our protection devices should trip this capacitor bank.

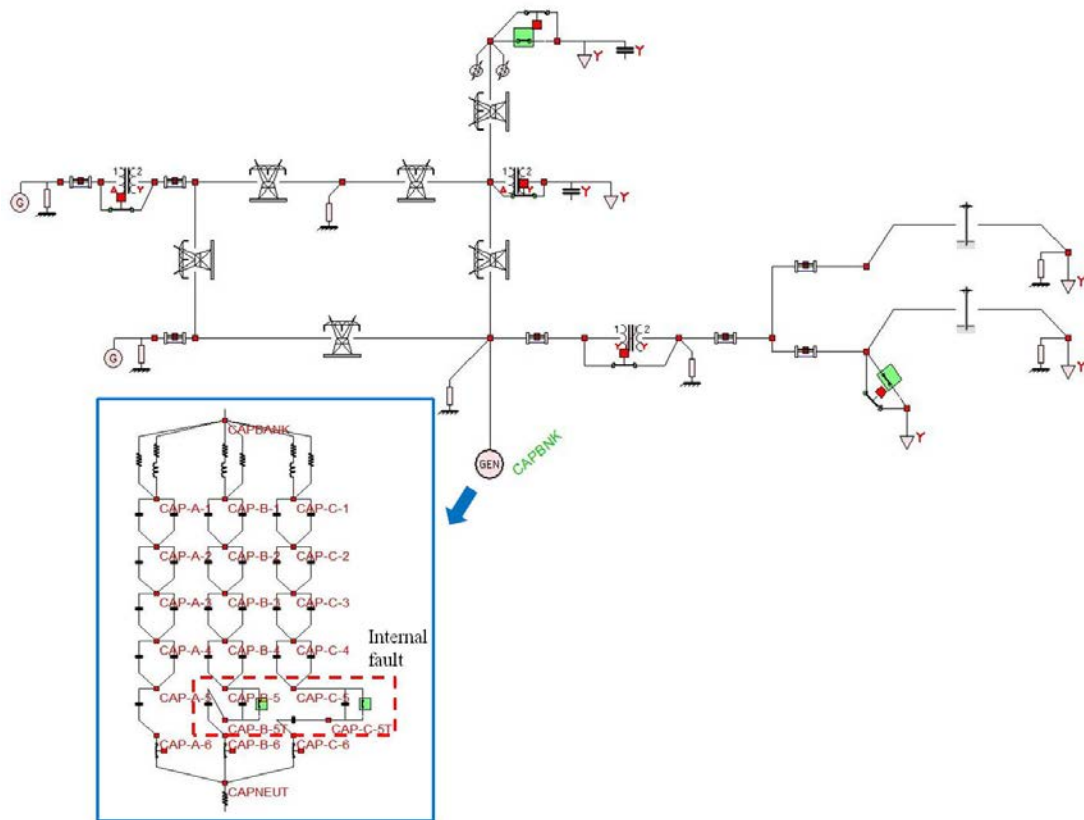


Figure 7.11 Test System Diagram for Capacitor Bank Zone, Scenario 3

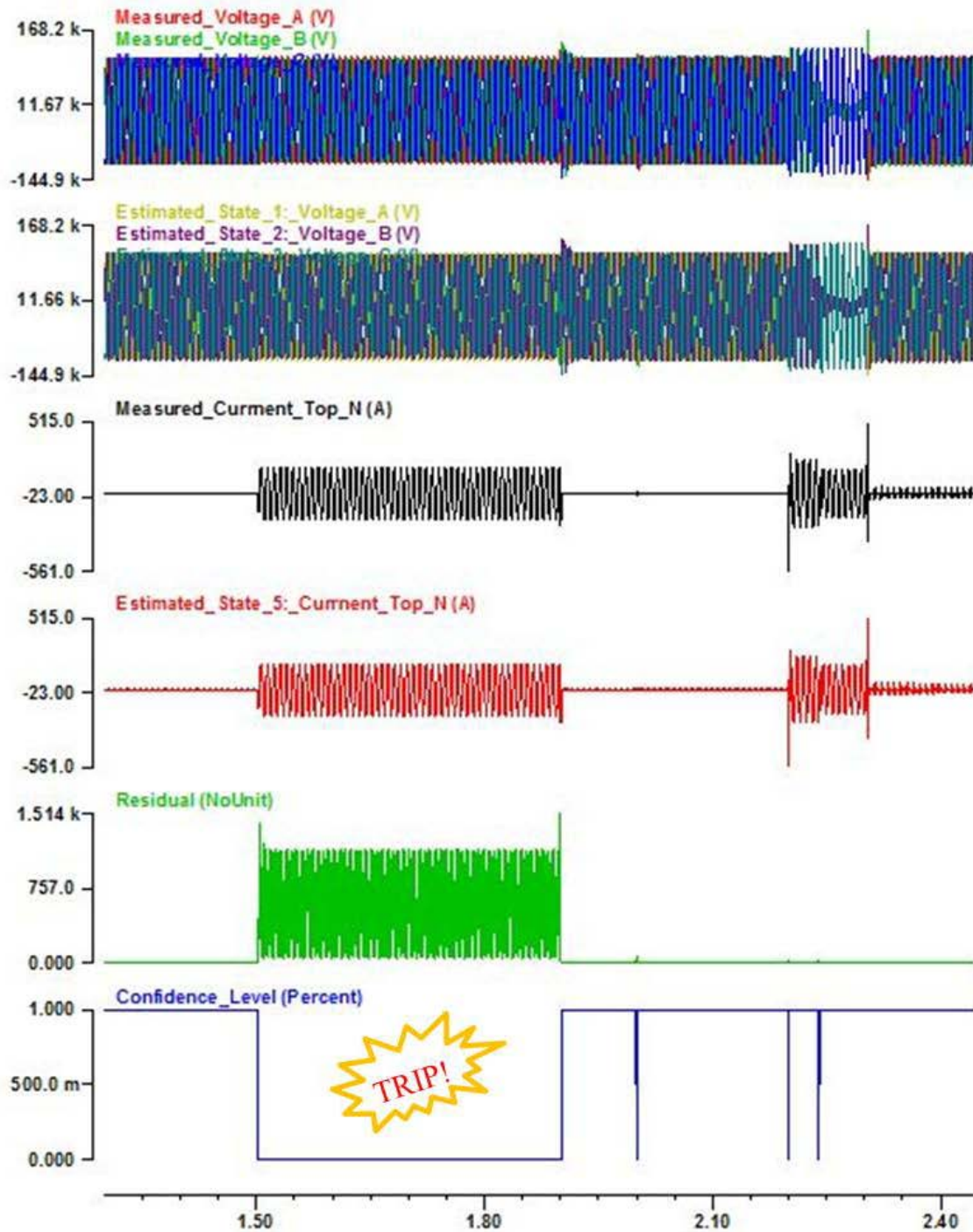


Figure 7.12 Result of Scenario 3

7.8.4 Test Scenario 4

In this section, an internal fault is simulated. Figure 7.13 shows how the test system is created. The red dash block shows where fault happens.

Figure 7.14 shows the test result of the above system. In the figure, the measured states, the estimated states, the residual and the confidence level are shown. It can be seen that the internal fault happens at 1.25s and clears at 1.45s. Because of the fault, the residual becomes large and the confidence level drops to zero very quickly. Different from scenario 0 and 1, the confidence level remains to be zero until the fault gets cleared, which means the fault is an internal fault and our protection devices should trip this capacitor bank.

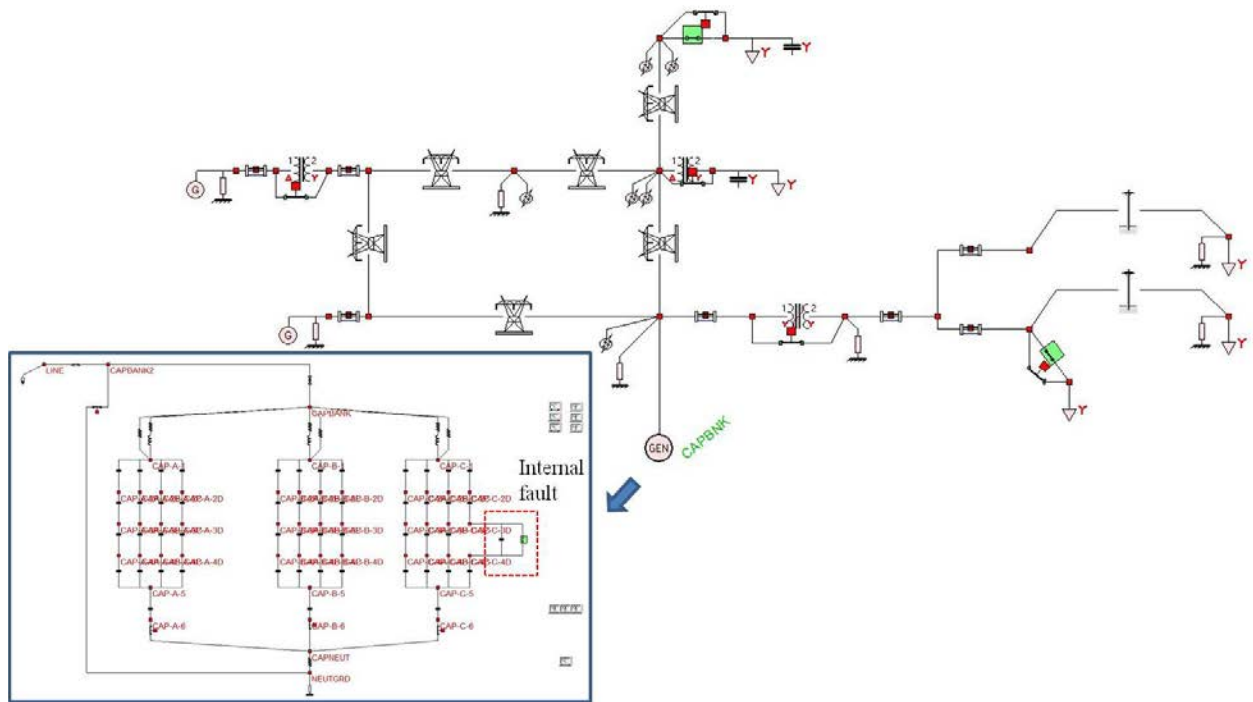


Figure 7.13 Test System Diagram for Capacitor Bank Zone, Scenario 4

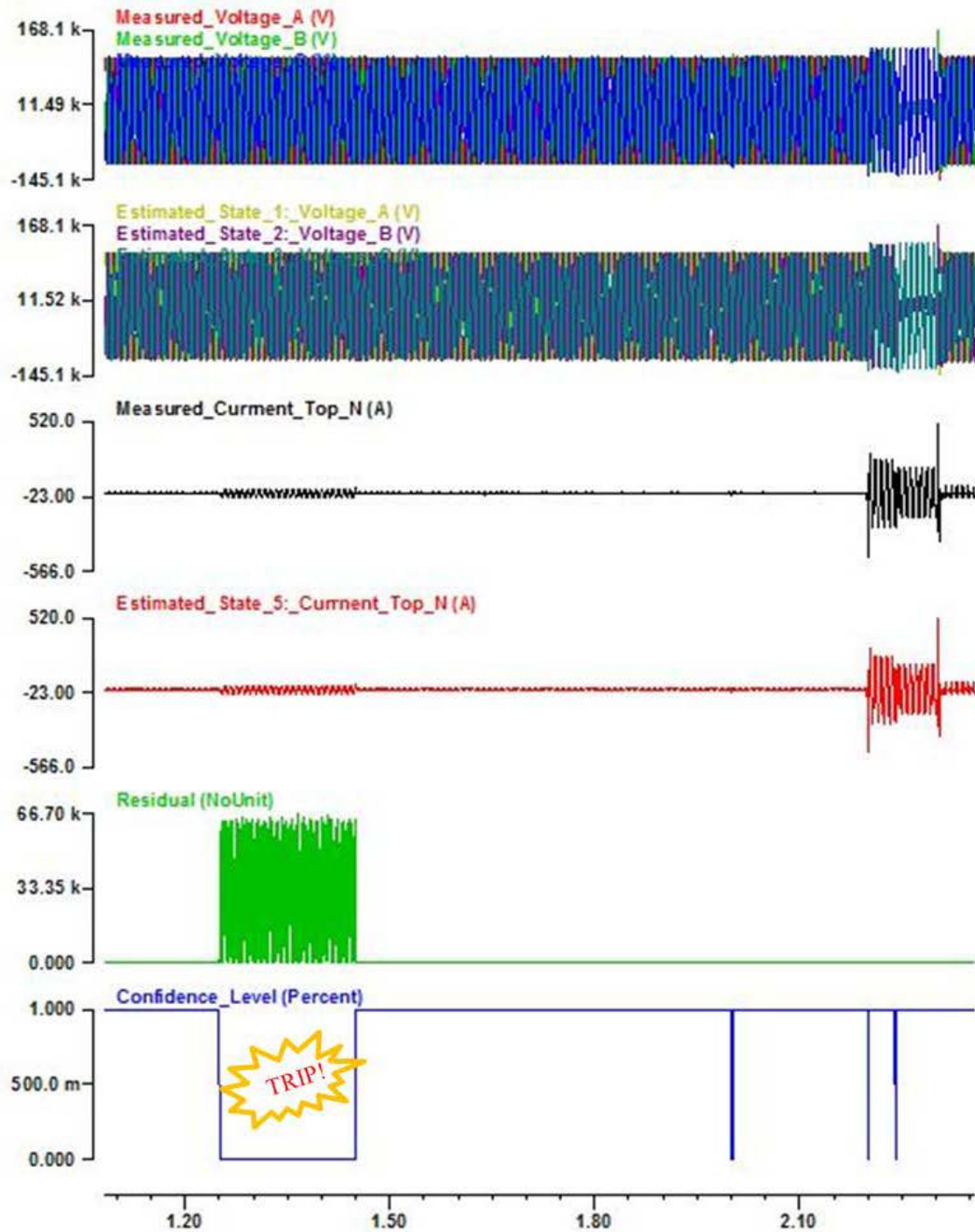


Figure 7.14 Result of Scenario 4

7.9 Issues and Challenges Associated with State Estimation Based Three Phase Capacitor Banks Protection

This section describes the main challenges for the state estimation based three phase capacitor banks setting-less protection. Most of these challenges and issues also exist in other protection schemes. Good methods to conquer them could bring more reliable protection to capacitor banks.

Time Limits: The analytics of the setting-less protection represent a substantial computational task that must be performed within the time interval of two consecutive sampled data sets. In the three phase capacitor banks protection case, based on the current technology, the relay may acquire more than 5000 samples (measurements) per second. Since the measurements at two time steps are used for one state estimation, more than 2500 state estimation calculations must be performed per second. This means each state estimation operation time should be less than $400\mu\text{s}$.

Figure 7.15 illustrates the time relationship and requirements for the protection scheme. Note that for a sampling rate of 5000 sample/s a new set of state estimation data will be available each 400 microseconds.

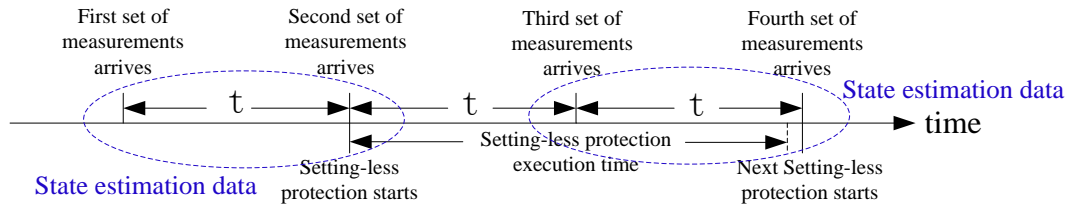


Figure 7.15 Time Relationship in Setting-less Protection

During the numerical experiments, the execution time for performing all the analytics for one set of estimation data was measured. Figure 7.16 illustrates an example of execution times for capacitor bank setting-less protection. From the figure, we can tell that the average operation time for each state estimation process is around $340\mu\text{s}$, which can satisfy the real time protection requirements. Moreover, the code has not been optimized and more advanced computer hardware could be used to provide much shorter operation time.

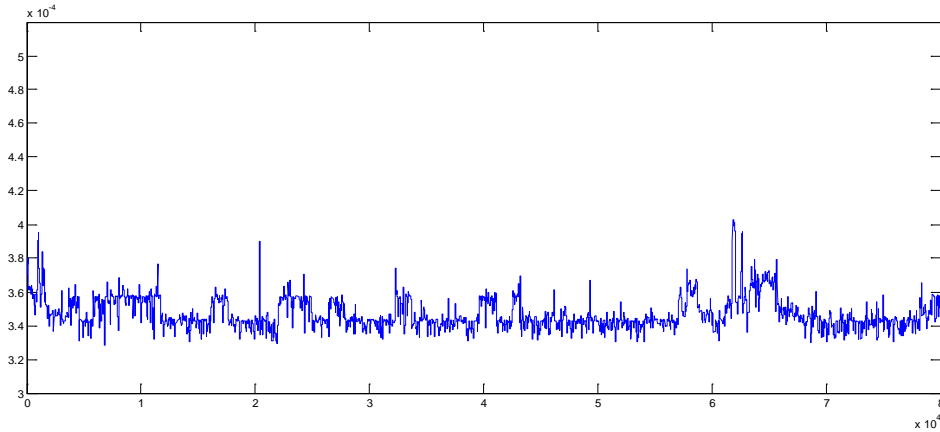


Figure 7.16 Capacitor Bank Setting-less Protection Operation Time

The proposed approach works best when: (a) the data acquisition system is as accurate as possible, (b) the data are GPS synchronized in case they are coming from more than one data acquisition systems, and (c) in case of telemetered data as is the case for transmission lines, communications are as fast as possible and they support the required throughput which depends on the sampling rate. A discussion of these issues follows.

Data Acquisition Accuracy: The setting-less protection works better as the accuracy of the data acquisition system increases. The data are utilized in a dynamic state estimation. This process requires data in the time domain, sampled at frequencies that can provide enough resolution of the transients. A modern data acquisition system that can provide this data in a form usable by a numerical relay or PC acting as a setting-less protective relay is the merging unit connected to a process bus. We propose to use this technology for the implementation of the setting-less protection.

A typical data acquisition system based on merging units and process bus is shown in Figure 7.17. For simplicity the figure shows only one voltage instrumentation channel and one current instrumentation channel. The illustrated data acquisition system has the capability to perform GPS synchronized measurements. Specifically the process bus can send the GPS signal (in a number of different ways) to the merging unit. The merging unit then uses this signal to synchronize the measurements. The latency imposed by the fiber optic cable and associated processing is typically small because of the short distances. For higher accuracy, the latency can be computed and compensated for the purpose to increasing the timing accuracy.

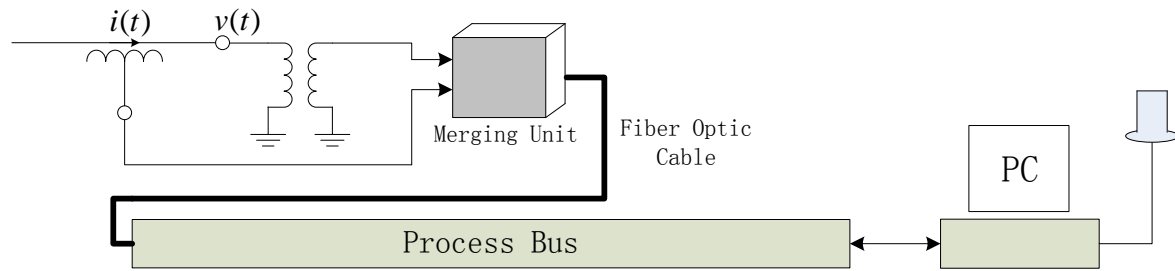


Figure 7.17 Typical Data Acquisition System Based on Merging Units

The accuracy of the data acquisition system of Figure 7.17 depends only on the accuracy of each instrument transformer because the separation distance between the merging unit and the instrument transformer is very short. In other words the data acquisition channel consists of the instrument transformer, a short connection between the merging unit and the instrument transformer and the input impedance of the merging unit. The component that introduces error in this case is practically only the instrument transformer. The most accurate instrument transformers are wound type potential transformers for voltage and magnetic core current transformers for current. The instrument transformers should be the highest accuracy class. It is important to note these instrument transformers are very accurate during steady state conditions but during transients introduce substantial transient errors. As long as the transient errors are short in duration, the performance of the setting-less protection will not be affected.

GPS Synchronized Measurements: The dynamic state estimation works best when all the data are GPS synchronized or they are coming from one single data acquisition system. In most cases, the measurement data may come from multiple data acquisition systems, i.e. multiple merging units, telemetered data (in case of transmission lines), etc. If the data are not GPS synchronized the analytics of the dynamic state estimation become very complex and the computational burden increases. For this reason, we assume that the setting-less protection will require GPS synchronized data. Merging units are capable of providing GPS synchronized measurements by receiving the GPS signal via GOOSE messaging.

Communications: Communications are required in case of telemetered data, as is the case of transmission line protection where the measurements from one terminal are telemetered to the other terminal. The communication link should provide speedy transmission so that latencies are minimized and should be able to provide the necessary throughput so that the data will be continuously streaming into the setting-less protective relay.

Above conditions are the recommended selections for the proposed approach. For the capacitor banks protection this translates into the following selections:

Recommended Selection 1: Merging units, highest accuracy PTs and CTs. This selection is shown in Figure 7.18. The merging units accept the actual analog measurements from electro-magnetic PTs/CTs and transfer them into digital signals. Meanwhile, the GPS IRIG-B or 1 pps signal can gradually adjust the sampling interval of all intelligent sampling modules through the merging unit to realize the synchronous sampling automatically. The merging units and the personal computer are connected through optical fibers based on IEC 61850 protocol. In this case the personal computer acts as the setting-less protective relay.

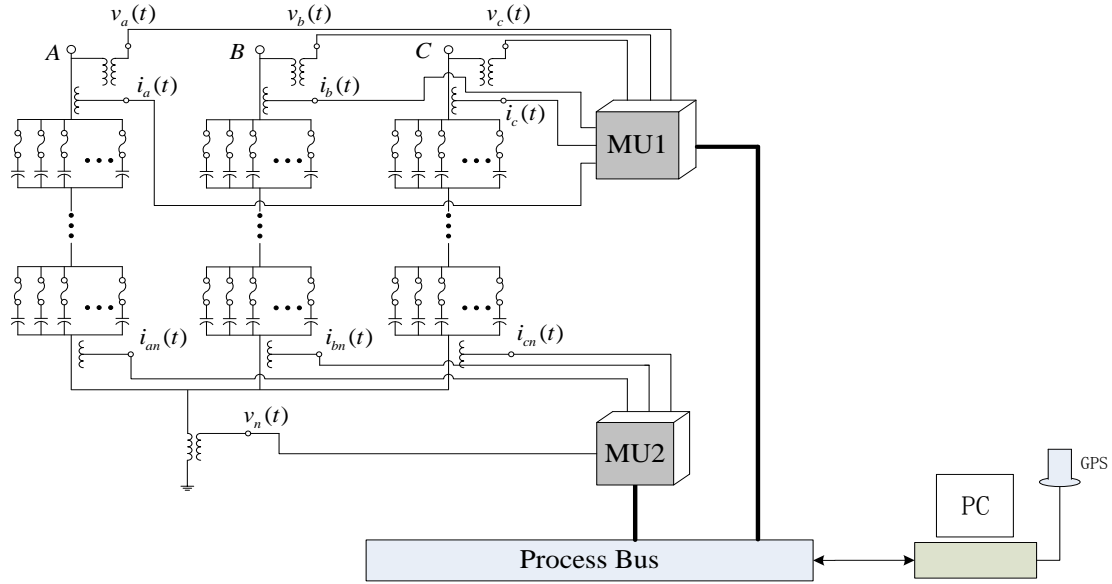


Figure 7.18 Recommended Data Acquisition Selection 1 for Capacitor Bank

Recommended Selection 2: The setting-less relay is used and it provides another alternative for the implementation of the proposed method. As a matter of fact a large number of relays exist in the current power system and every relay is equipped with a microprocessor. The setting-less protection algorithm can be programmed in the relay and the present protection algorithm can be removed so that the microprocessor can provide a faster computational time. As a result, the introduction of the setting-less relay results in simpler function and faster running speed that will be very advantageous for the proposed method. Also this new relay provides more flexible choices for the protection location. The use of the setting-less relay will result to the recommended selection 2 which is shown in Figure 7.19.

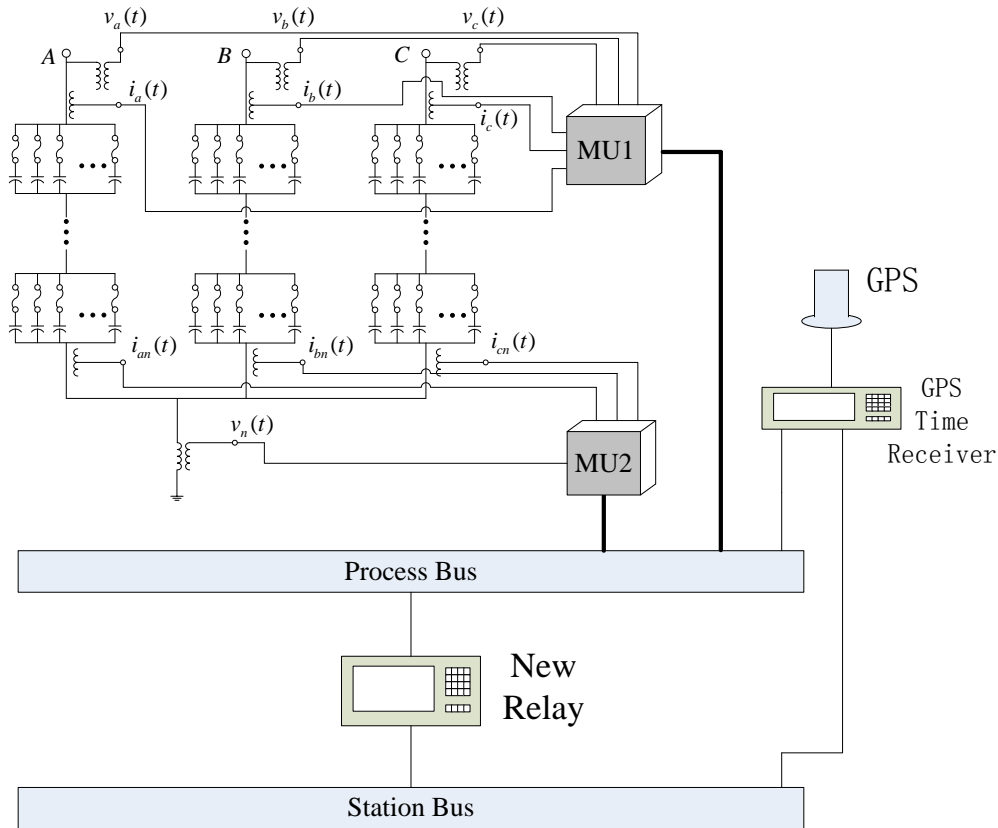


Figure 7.19 Recommended Data Acquisition Selection 2 for Capacitor Bank

In many instances, the existing instrumentation may be different. We will discuss here the most challenges or issues we may face:

No GPS clock or loss of GPS: In many cases, merging units are not available for the specific bus and relays will be there instead. Or even if the GPS clock is available for the bus, there are still some possibilities that the GPS communication is lost. In this case the measurements do not have a global synchronized time stamp. In order to solve this problem, an angle could be added to the state estimation process as one additional state so that the phase difference caused by the different time stamps that used in the two merging units could be calculated. As a result, even if the measurements are not GPS clock synchronized, the state estimation based setting-less protection approach still could be applied for the capacitor bank and it also could be used to coordinate and share information with the other devices in the system where PMUs are available.

Communication latency or loss between merging units and process bus: When the communication between merging units and process bus is lost or delayed, the protection approach cannot run properly and timely. In order to solve this kind of situation, usually a backup communication system, including merging units and fiber optic cables, will be installed so that the redundant communication system could provide the data which is needed for the protection schemes.

8. Example Applications: Saturable Core Reactors

This section describes the implementation approach for the setting-less protective relay for single phase saturable core reactors (state estimation based approach). The models and the algorithmic procedures of the analytics are also described. The application has been evaluated by numerical experiments.

8.1 Summary

Saturable core reactors are used for compensation of long transmission lines, current limiting applications as well as in filters to limit harmonics. The circuit model of a single phase reactor is shown in Figure 8.1. Note that in Figure 8.1, g_L is the conductance that presents the core loss, g_c is the conductance of the “stabilizer”. Current transformer and potential transformer are used to measure the current and voltage. The merging units are GPS synchronized. The measurements are utilized in a dynamic state estimation. Any violation of the physical laws would imply an internal fault in the reactors. The protection logic would trip the reactor when either the physical laws are violated or the operating condition exceeds operating limits.

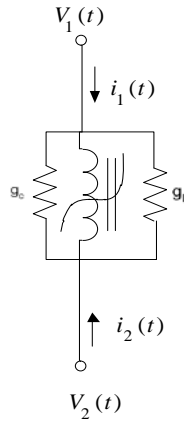


Figure 8.1 Single Phase Saturable Core Reactor Model

Mathematical Model: The mathematical model of the saturable core reactor is expressed in the SCAQCF (State and Control Algebraic Quadratic Companion Form).

System State: The system state is defined in the SCAQCF model. Note that the states are classified as external states and internal states. The external states are two terminal voltages at time t (V_1 , V_2) and two terminal voltages at time t_m (V_1 , V_2). The internal states are magnetic flux in the cores.

Measurements: They consist of the actual, virtual, derived and pseudo measurement.

Actual Measurements: two currents at time t (I_1, I_2); two voltages at time t (V_1, V_2); two currents at time $t_m=t-h/2$ (I_1, I_2); two voltages at time $t_m=t-h/2$ (V_1, V_2).

Virtual Measurements: In this case, there are 6 virtual measurements at time t ; 6 measurements with value equal to zero at time $t_m=t-h/2$.

Derived Measurements and Pseudo Measurements: None.

In summary, for the single phase saturable core reactor, there are 8 actual measurements, 12 virtual measurements, zero derived and pseudo measurements, a total of 20. There would be 16 states, which provide a redundancy of 25% $((20-16)/(16))$.

The above mentioned report provides details and simulated events. Here an example case of an external single phase line-to-ground fault as well as an internal fault is provided. Figure 8.2 shows the voltage and current of this test system as well as the confidence level. From the figure, it is easy to see the confidence level drops to zero very quickly because of the fault. But the confidence level goes back to 100% immediately, which indicates all the faults are external faults and the states still match the model. Therefore, the fault doesn't exist inside the saturator reactors and no trip needs to be acted. However, when there is an internal fault, the confidence stays zero, indicating the fault is in the reactor and protection is needed.

Execution Time: Due to the nonlinearity of reactors, the Jacobean matrix changes at state estimation, increasing the computation time for “setting-less” protection. The average computation time is about 100 μs . This value is to be compared with the sampling rate of the data acquisition system of the relay. The sampling rate is 4000 times per second. This means that the state estimation is 4000/2 times per second. This means that the data for the state estimation are coming in one set per 500 μs . Since the code has not been optimized and the computer hardware has much room to improve, the execution speed can be further improved. The execution time is show in Figure 8.3.

d:\comtrade\fileresults - Jul 10, 2013, 10:30:00.000000 - 20000.0 samples/sec - 19999 Samples

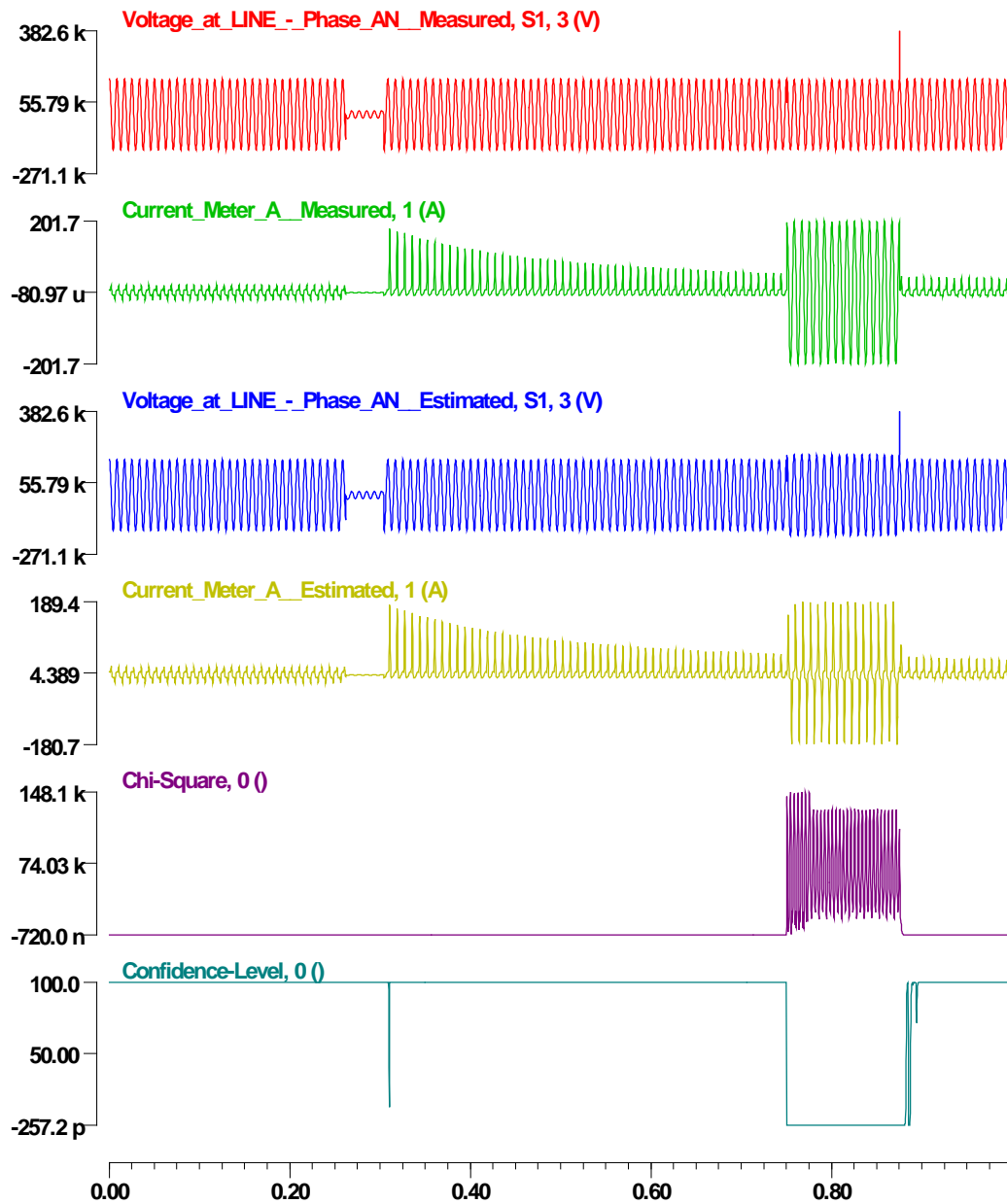


Figure 8.2 Results of Saturable Core Reactor Test System

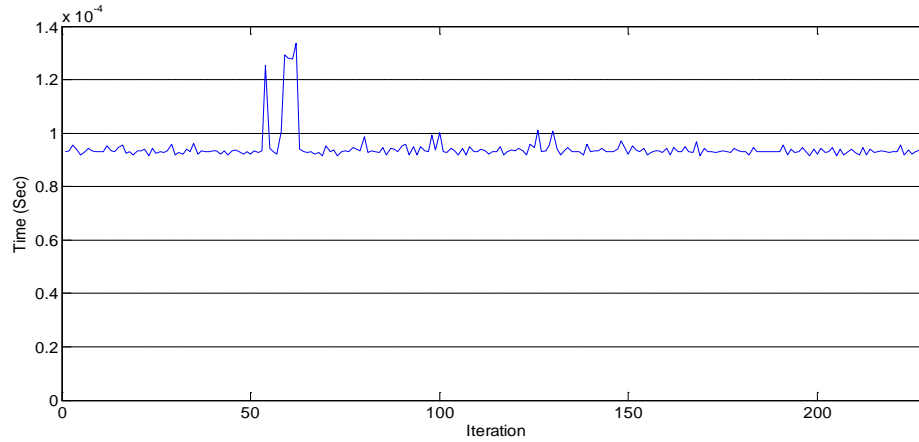


Figure 8.3 Execution time

8.2 Setting-less Relay Description

This section describes the overall implementation of the setting-less protective relay. The architecture of this relay is shown in Figure 6.1. Note that the relay requires the model of the zone to be protected and the actual (physical) measurements from the data acquisition system. The model must be provided in the SCAQCF syntax which is defined in this document. Then the remaining analytics are automatically constructed and executed. These are: the pointers that provide the interrelationship of the actual measurements to the zone model, the creation of the measurement models for the actual, virtual, derived and pseudo measurements, the dynamic state estimation, the bad data detection and identification and the protection logic.

Note that the data acquisition system is continuously streaming measurement into the relay with a specific rate. Typical rates are 2,000 to 5,000 samples per second. As it will be seen later, the model of the component to be protected is derived in the SCAQCF by using the quadratic integration. The SCAQCF model is expressed in terms of the values of the various variables at two consecutive time instances (two consecutive samples) and past history samples. This means that the analytics of the setting-less relay operate on samples of two consecutive time instances. This is illustrated in Figure 8.4. The samples (measurements) at the two consecutive time instances t and $(t-t_s)$ are used. Note that t_s defines the sampling period. For the typical sampling rates referenced above the minimum sampling period will be 200 microseconds (5,000 samples per second). This means that the analytics of the setting-less relay must be performed within the time interval of 400 microseconds (before the next set of data arrive). Obviously, there should be a margin. For this reason the goal for the setting-less relay is to perform the analytics in time less than 200 microseconds. Numerical experiments have been performed and the performance is documented in this report.

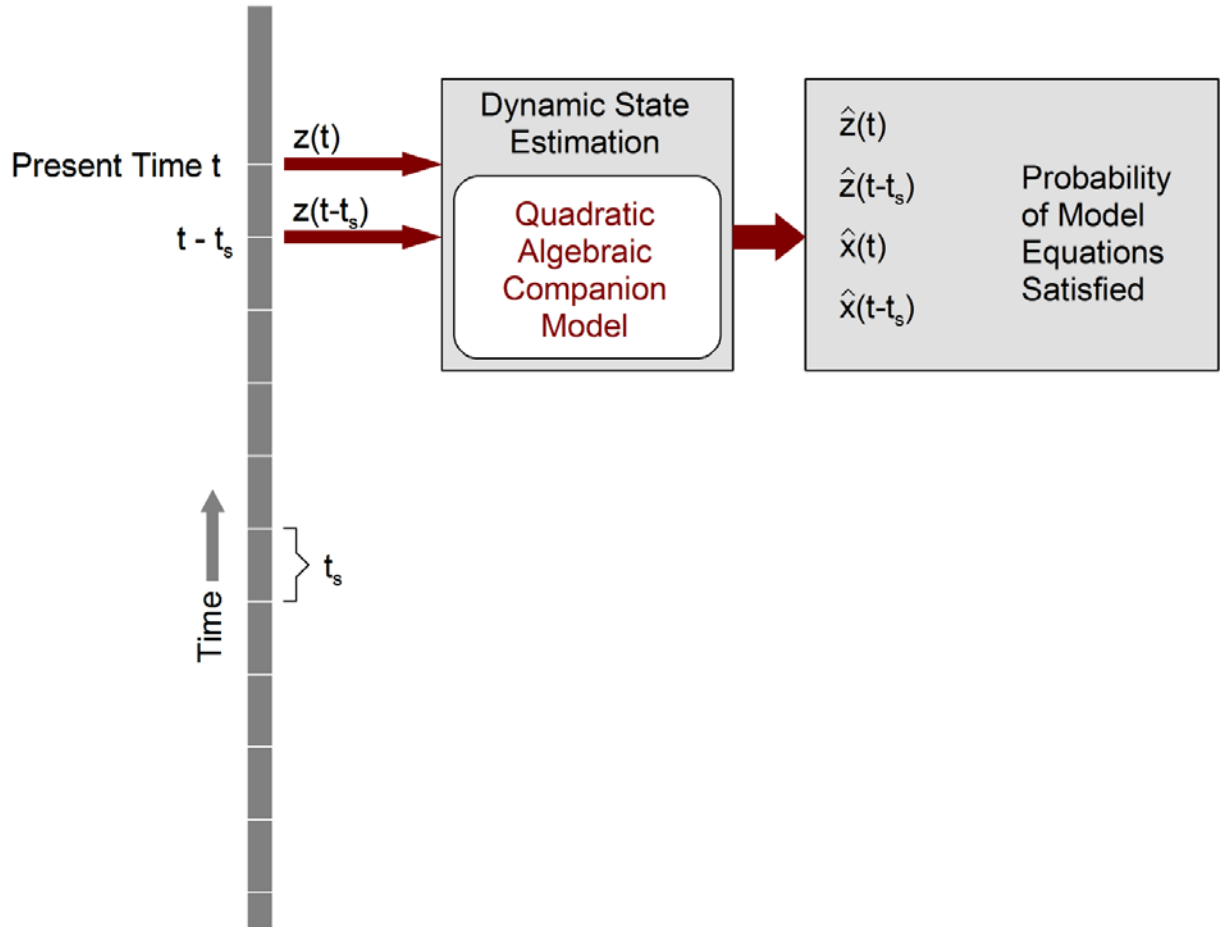


Figure 8.4 Illustration of Time Samples Utilized at Each Iteration of the Setting-less Relay Analytics

8.3 Saturable Core Reactor SCAQCF Model

The circuit model of the single phase reactor is shown in Figure 8.1. Note that in this figure, g_L is the conductance that models the core losses. In this section, “numerical stabilizers” have been included to eliminate possible numerical problems caused by the numerical integration rule. In Figure 8.1, g_c is the conductance of the “stabilizer”. The SCAQCF model of the single phase saturable core reactor model is given below. The derivation of this model is provided in Appendix 2.

$$\begin{bmatrix} i(t) \\ 0 \\ i(t_m) \\ 0 \end{bmatrix} = Y_{eq} \cdot \begin{bmatrix} v(t) \\ y(t) \\ v(t_m) \\ y(t_m) \end{bmatrix} + \begin{bmatrix} [v^T(t) \quad y^T(t) \quad v^T(t_m) \quad y^T(t_m)] \cdot F_{eq1(16 \times 16)} \cdot \begin{bmatrix} v(t) \\ y(t) \\ v(t_m) \\ y(t_m) \end{bmatrix} \\ \vdots \\ [v^T(t) \quad y^T(t) \quad v^T(t_m) \quad y^T(t_m)] \cdot F_{eq16(16 \times 16)} \cdot \begin{bmatrix} v(t) \\ y(t) \\ v(t_m) \\ y(t_m) \end{bmatrix} \end{bmatrix} \\ + B \cdot \begin{bmatrix} v(t-h) \\ y(t-h) \end{bmatrix}$$

where:

$$i(t) = \begin{bmatrix} i_1(t) \\ i_2(t) \end{bmatrix}, v(t) = \begin{bmatrix} v_1(t) \\ v_2(t) \end{bmatrix}, v(t-h) = \begin{bmatrix} v_1(t-h) \\ v_2(t-h) \end{bmatrix}, y(t) = \begin{bmatrix} \lambda_1(t) \\ y_1(t) \\ y_2(t) \\ y_3(t) \\ y_4(t) \\ y_5(t) \end{bmatrix}$$

$$y(t-h) = [\lambda_1(t-h)],$$

$$Y_{eq} = \begin{bmatrix} g_L & -g_L & 0 & 0 & 0 & 0 & 0 & \frac{i_0}{|\lambda_0|^{11}} & 0 & 0 & 0 & 0 & 0 & 0 & 0 \\ -g_L & g_L & 0 & 0 & 0 & 0 & 0 & -\frac{i_0}{|\lambda_0|^{11}} & 0 & 0 & 0 & 0 & 0 & 0 & 0 \\ -\frac{h}{6} & \frac{h}{6} & 1 & 0 & 0 & 0 & 0 & 0 & -\frac{2h}{3} & \frac{2h}{3} & 0 & 0 & 0 & 0 & 0 \\ 0 & 0 & 0 & 1 & 0 & 0 & 0 & 0 & 0 & 0 & 0 & 0 & 0 & 0 & 0 \\ 0 & 0 & 0 & 0 & 1 & 0 & 0 & 0 & 0 & 0 & 0 & 0 & 0 & 0 & 0 \\ 0 & 0 & 0 & 0 & 0 & 1 & 0 & 0 & 0 & 0 & 0 & 0 & 0 & 0 & 0 \\ 0 & 0 & 0 & 0 & 0 & 0 & 1 & 0 & 0 & 0 & 0 & 0 & 0 & 0 & 0 \\ 0 & 0 & 0 & 0 & 0 & 0 & 0 & 1 & 0 & 0 & 0 & 0 & 0 & 0 & 0 \\ 0 & 0 & 0 & 0 & 0 & 0 & 0 & 0 & g_L & -g_L & 0 & 0 & 0 & 0 & \frac{i_0}{|\lambda_0|^{11}} \\ 0 & 0 & 0 & 0 & 0 & 0 & 0 & 0 & -g_L & g_L & 0 & 0 & 0 & 0 & -\frac{i_0}{|\lambda_0|^{11}} \\ \frac{h}{24} & -\frac{h}{24} & 0 & 0 & 0 & 0 & 0 & 0 & -\frac{h}{3} & \frac{h}{3} & 1 & 0 & 0 & 0 & 0 \\ 0 & 0 & 0 & 0 & 0 & 0 & 0 & 0 & 0 & 0 & 0 & 1 & 0 & 0 & 0 \\ 0 & 0 & 0 & 0 & 0 & 0 & 0 & 0 & 0 & 0 & 0 & 0 & 1 & 0 & 0 \\ 0 & 0 & 0 & 0 & 0 & 0 & 0 & 0 & 0 & 0 & 0 & 0 & 0 & 1 & 0 \\ 0 & 0 & 0 & 0 & 0 & 0 & 0 & 0 & 0 & 0 & 0 & 0 & 0 & 0 & 1 \end{bmatrix}$$

$$B_{16 \times 3} = \begin{bmatrix} 0_{2 \times 3} \\ B_{1(1 \times 3)} \\ 0_{7 \times 3} \\ B_{2(1 \times 3)} \\ 0_{5 \times 3} \end{bmatrix}$$

$$B_1 = \begin{bmatrix} -\frac{h}{6} & \frac{h}{6} & -1 \end{bmatrix}$$

$$B_2 = \begin{bmatrix} -\frac{5h}{24} & \frac{5h}{24} & -1 \end{bmatrix}$$

$$\begin{aligned}
F_{eq1} &= \dots = F_{eq3} = 0_{16 \times 16} \\
F_{eq4}: f_{eq[3 \times 3]} &= -1, & \text{other elements are 0} \\
F_{eq5}: f_{eq[4 \times 4]} &= -1, & \text{other elements are 0} \\
F_{eq6}: f_{eq[5 \times 5]} &= -1, & \text{other elements are 0} \\
F_{eq7}: f_{eq[6 \times 4]} &= -1, & \text{other elements are 0} \\
F_{eq8}: f_{eq[7 \times 3]} &= -1, & \text{other elements are 0}
\end{aligned}$$

$$\begin{aligned}
F_{eq9} &= \dots = F_{eq11} = 0_{16 \times 16} \\
F_{eq12}: f_{eq[11 \times 11]} &= -1, & \text{other elements are 0} \\
F_{eq13}: f_{eq[12 \times 12]} &= -1, & \text{other elements are 0} \\
F_{eq14}: f_{eq[13 \times 13]} &= -1, & \text{other elements are 0} \\
F_{eq15}: f_{eq[14 \times 12]} &= -1, & \text{other elements are 0} \\
F_{eq16}: f_{eq[15 \times 11]} &= -1, & \text{other elements are 0}
\end{aligned}$$

Assumption (just for now): the exponent **n** is odd. (It will be removed in the future).
For the single phase reactor, there are 12 states (6 for time step **t** and 6 for intermediate time step **t_m**).

For time step **t**, the states are listed below.

External states:

0. $v_1(t)$: terminal voltage at Terminal 1 (kV);
1. $v_2(t)$: terminal voltage at Terminal 2 (kV);

Internal states:

0. $\lambda_1(t)$: Reactor Flux (kWb)
- 1-5. $y_1(t) \dots y_5(t)$: introduced flux states for inductance

For time step **t_m**, the states are listed below.

External states:

0. $v_1(t_m)$: terminal voltage at Terminal 1 (kV);
1. $v_2(t_m)$: terminal voltage at Terminal 2 (kV);

Internal states:

0. $\lambda_1(t_m)$: Reactor Flux (kWb)
- 1-5. $y_1(t_m) \dots y_5(t_m)$: introduced flux states for inductance

8.4 Saturable Core Reactor Measurements Definition

The measurements can be actual measurements, virtual measurements, derived measurements and pseudo measurements. For the saturable core reactor model these measurements are described next.

Actual Measurements: This type of measurement is a physical measurement that can be obtained by typical measurement equipment. The actual measurements are: two current measurements at time t ; two voltage at time t ; two current measurements at time $t_m=t-h/2$; two voltages at time $t_m=t-h/2$. For these measurements assume a measurement error with standard deviation equal to 0.01 pu.

Virtual Measurements: This type of measurement is not a physical measurement. Virtual measurements are physical laws that a device must obey. These physical laws are expressed with specific equations. These equations must be exactly satisfied and therefore the virtual measurements are exact measurements (noiseless). The number of virtual measurements equals to the number of the equations whose left side value is zero (equations 3~8 and 11~16). In this case, there are 6 virtual measurements at time t ; 6 measurements with value equal zero at time $t_m=t-h/2$ and zero error. Since the state estimation cannot accept zero standard deviation of the error, a small value is assumed, i.e. 0.001 pu.

Derived and Pseudo Measurements: none in this case.

In summary, for the single phase saturable core reactor, there are 8 actual measurements, 12 virtual measurements, and zero derived and pseudo measurements, a total of 20. There would be 16 states, which provide a redundancy of 25% $((20-16)/(16))$.

8.5 Creation of Measurement Models

This section describes the creation of the mathematical models of the measurements.

8.5.1 Creation of Actual Measurement Model

If the measurement is an actual through measurement, it is related to a specific row of the SCAQCF model. The reactor currents I_1 and I_2 (at time t and t_m) are the actual through measurements.

The model of this kind of measurement is as follows:

$$i_k^m = \sum_i Y_{eq,i}^k \cdot x_i + \sum_{i,j} F_{eq,i,j}^k \cdot x_i \cdot x_j - b_{eq}^k + \eta_k$$

where $Y_{eq,i}^k$ are the elements of the k^{th} row of the Y_{eq} matrix of the corresponding device.

$F_{eq,i,j}^k$ are the elements of the F_{eq} structure that correspond to the k^{th} equation of the of the device model.

b_{eq}^k is the k^{th} element of the b_{eq} (past history) vector of the corresponding device.

If the measurement is an actual across measurement, it is not related to a specific row of the SCAQCF model.

The model of this kind of measurement is as follows:

$$V^m = x_i \pm x_j + \eta$$

where x_i, x_j , are all the states related to this measurement..

8.5.2 Creation of Virtual Measurement Model

The virtual measurements are not real measurements so they cannot be measured. It is related to a specific row of the SCAQCF model. The model of this kind of measurement is as follows:

$$0 = \sum_i Y_{eq,i}^k \cdot x_i + \sum_{i,j} F_{eq,i,j}^k \cdot x_i \cdot x_j - b_{eq}^k + \eta_k$$

where k stands for k^{th} row of this measurement.

8.5.3 Creation of Derived Measurement Model

There are no derived measurements in this saturable core reactors case so that no derived measurement model is needed.

8.5.4 Creation of Pseudo Measurement Model

There are no pseudo measurements in this saturable core reactors case so no derived measurement model is needed.

8.6 State Estimation

The dynamic state estimator is described as follows: First the model of the single phase reactor under protection is cast into a standard algebraic companion form which is shown above. The measurements are classified into (a) actual measurements, (b) virtual measurements and (c) pseudo measurements.

A physical measurement, a virtual measurement or a pseudo-measurement at time t has the following generalized SCAQCF form:

$$\mathbf{y}(\mathbf{x}, \mathbf{u}) = Y_{m,x} \mathbf{x} + \left\{ \begin{array}{c} \vdots \\ \mathbf{x}^T F_{m,x}^i \mathbf{x} \\ \vdots \end{array} \right\} + Y_{m,u} \mathbf{u} + \left\{ \begin{array}{c} \vdots \\ \mathbf{u}^T F_{m,u}^i \mathbf{u} \\ \vdots \end{array} \right\} + \left\{ \begin{array}{c} \vdots \\ \mathbf{x}^T F_{m,xu}^i \mathbf{u} \\ \vdots \end{array} \right\} + C_m$$

where:

$\mathbf{y}(\mathbf{x}, \mathbf{u})$: measurement variables of the component model at both time t and time t_m ,

$\mathbf{y} = [\mathbf{y}(t), \mathbf{y}(t_m)]$

\mathbf{x} : external and internal state variables of the component model, $\mathbf{x} = [\mathbf{x}(t), \mathbf{x}(t_m)]$

\mathbf{u} : control variables of the component model, i.e. transformer tap, etc. $\mathbf{u} = [\mathbf{u}(t), \mathbf{u}(t_m)]$

$Y_{m,x}$: matrix defining the linear part for state variables,

$F_{m,x}$: matrices defining the quadratic part for state variables,

$Y_{m,u}$: matrix defining the linear part for control variables,

$F_{m,u}$: matrices defining the quadratic part for control variables,

$F_{m,xu}$: matrices defining the quadratic part for the product of state and control variables,

C_m : constant vector of the measurement model (past history).

The weighted least squares approach will be used for the state estimator. The algorithm is defined as follows:

$$\text{Minimize } J = \sum_{i=1}^m \left(\frac{h_i(x) - z_i}{\sigma_i} \right)^2 = \sum_{i=1}^m s_i^2 = \eta^T W \eta$$

where: $s_i = \frac{\eta}{\sigma_i}$, $W = \text{diag} \left\{ \frac{1}{\sigma_1^2}, \frac{1}{\sigma_2^2}, \dots, \frac{1}{\sigma_1^2} \right\}$

The solution is given with the following iterative algorithm:

$$x^{\nu+1} = x^{\nu} - (H^T W H)^{-1} H^T W (h(x^{\nu}) - z)$$

where H is the Jacobean matrix: $H = \frac{\partial h(x)}{\partial x}$, computed at $x = x^{\nu}$

At each time step of the estimation algorithm, the contributions of each measurement to the information matrix H^TWH and the vector $H^TW(h(x^\nu) - z)$ must be computed. For example assuming that the i -th measurement has the following generic form (for simplicity only one linear and one quadratic term is included):

$$z_i = c_i + a_{i1} \cdot x_{i1} + a_{i2} \cdot x_{i2} \cdot x_{i3} + \eta_i$$

Then the Jacobean matrix's i -th row will be:

$$[0 \quad \cdots \quad a_{i1} \quad \cdots \quad a_{i2} \cdot x_{i2} \quad \cdots \quad a_{i2} \cdot x_{i3} \quad \cdots \quad 0]$$

The contribution of this row to the information matrix H^TWH is the following:

$$\begin{bmatrix} 0 & \cdots & 0 & \cdots & 0 & \cdots & 0 & \cdots & 0 \\ \vdots & & \vdots & & \vdots & & \vdots & & \vdots \\ 0 & \cdots & w_i a_{i1} a_{i1} & \cdots & w_i a_{i1} a_{i2} x_{i2} & \cdots & w_i a_{i1} a_{i2} \cdot x_{i3} & \cdots & 0 \\ \vdots & & \vdots & & \vdots & & \vdots & & \vdots \\ 0 & \cdots & w_i a_{i1} a_{i2} \cdot x_{i2} & \cdots & w_i (a_{i2} \cdot x_{i2})^2 & \cdots & w_i a_{i2}^2 \cdot x_{i2} x_{i3} & \cdots & 0 \\ \vdots & & \vdots & & \vdots & & \vdots & & \vdots \\ 0 & \cdots & w_i a_{i1} a_{i2} \cdot x_{i3} & \cdots & w_i a_{i2}^2 \cdot x_{i2} x_{i3} & \cdots & w_i (a_{i2} \cdot x_{i3})^2 & \cdots & 0 \\ \vdots & & \vdots & & \vdots & & \vdots & & \vdots \\ 0 & \cdots & 0 & \cdots & 0 & \cdots & 0 & \cdots & 0 \end{bmatrix}$$

The contribution of the measurement to the vector $H^TW(h(x^\nu) - z)$ is the following:

$$\begin{bmatrix} 0 \\ \vdots \\ w_i a_{i1} b_i \\ \vdots \\ w_i a_{i2} \cdot x_{i2} b_i \\ \vdots \\ w_i a_{i2} \cdot x_{i3} b_i \\ \vdots \\ 0 \end{bmatrix}, \quad \text{where} \quad b_i = c_i + a_{i1} \cdot x_{i1} + a_{i2} \cdot x_{i2} \cdot x_{i3} - z_i$$

The above general formulae lead to a very simple algorithm for forming the information matrix H^TWH and $H^TW(h(x^\nu) - z)$ the vector and updating the state x .

8.7 Protection Logic

The solution of the dynamic state estimation provides the best estimate of the dynamic state of the component. The well-known chi-square test provides the probability that the measurements are consistent with the dynamic model of the component. Thus the chi-square test quantifies the goodness of fit between the model and measurements (i.e., confidence level). The goodness of fit is expressed as the probability that the measurement errors are distributed within their expected range (chi-square distribution). The chi-square test requires two parameters: the degree of freedom (ν) and the chi-square critical value (ζ). In order to quantify the probability with one single variable, we introduce the variable k in the definition of the chi-square variable:

$$\nu = m - n, \quad \zeta = \sum_{i=1}^m \left(\frac{h_i(\hat{x}) - z_i}{k\sigma_i} \right)^2,$$

where m is the number of measurements, n the number of states, and \hat{x} the best estimate of states. Note that since m is always greater than n , the degrees of freedom are always positive. Note also that if k is equal to 1.0 then the standard deviation of the measurement error corresponds to the meter error specifications. If k equals 2.0 then the standard deviation will be twice as much as the meter specifications, and so on. Using this definition, the results of the chi square test can be expressed as a function of the variable k . Specifically, the goodness of fit (confidence level) can be obtained as follows:

$$\Pr[\chi^2 \geq \zeta(k)] = 1.0 - \Pr[\chi^2 \leq \zeta(k)] = 1.0 - \Pr(\zeta(k), \nu).$$

The proposed method uses the confidence level as the health index of a component. A high confidence level indicates good fit between the measurement and the model, and thus we can conclude that the physical laws of the component are satisfied and the component has no internal fault. A low confidence level, however, implies inconsistency between the measurement and the model; therefore, we can conclude that an abnormality (internal fault) has occurred in the component.

It is important to point out that the component protection relay must not trip circuit breakers except when the component itself is faulty (internal fault). For example, in case of a saturable core reactor, inrush currents or over excitation currents should be considered normal and the protection system should not trip the component. The proposed protection scheme can adaptively differentiate these phenomena from internal faults.

8.8 Numerical Experiments

A test system has been used for numerical experiments that include a single phase reactor under protection and an integrated system around it. The model parameters of the reactor are shown in Figure 8.5.

Copy Print Help

Nonlinear Saturable Inductor Cancel Accept

Saturable Core Reactor

Rated Voltage (kV) 66.4

Rated Current (kA) 0.1

Flux Constant L_o (pu) 1.0 0.176131 kVb

Exponent (n) 11

Current Constant l_o (pu) 0.005 0.000500 kA

Nominal Core Loss (pu) 0.0 0.000000 Mhos

$$i(t) = l_o * \left(\frac{L(t)}{L_o} \right)^n * \text{sgn}(L(t))$$

Circuit Number 1

First Node Name LINE_A Second Node Name NEUTRAL_N

Program WinQS-1 - Form 103 M172

Figure 8.5 Model Parameters of Reactor

8.8.1 Test Scenario 1

This scenario involves two external fault at the connection terminal as well as an internal fault at saturable core reactors. Figure 8.6 shows the example test system. The voltage and current of this test system, the Chi-square & confidence level is shown in Figures 8.7.

In Figure 8.7 it can be seen that when there is no fault, the confidence level maintains at value one. The confidence level drops down very quickly when the external single phase-to-ground fault clears. But the confidence level goes back to one immediately which indicates the fault is an external fault and the states still match the single phase saturable core reactors model. It means that there is no fault inside the saturable core reactors and no trip needs to be acted. However, when the internal fault happens the confidence level drops down very quickly again. The confidence level stays at one, indicating it is an internal fault and trip needs to be acted.

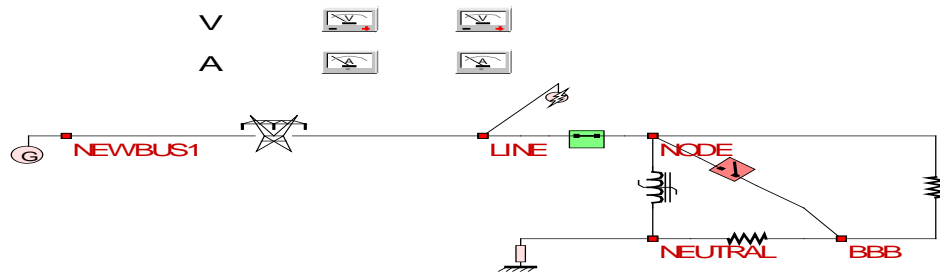


Figure 8.6 Test System Diagram for Single Phase Reactor

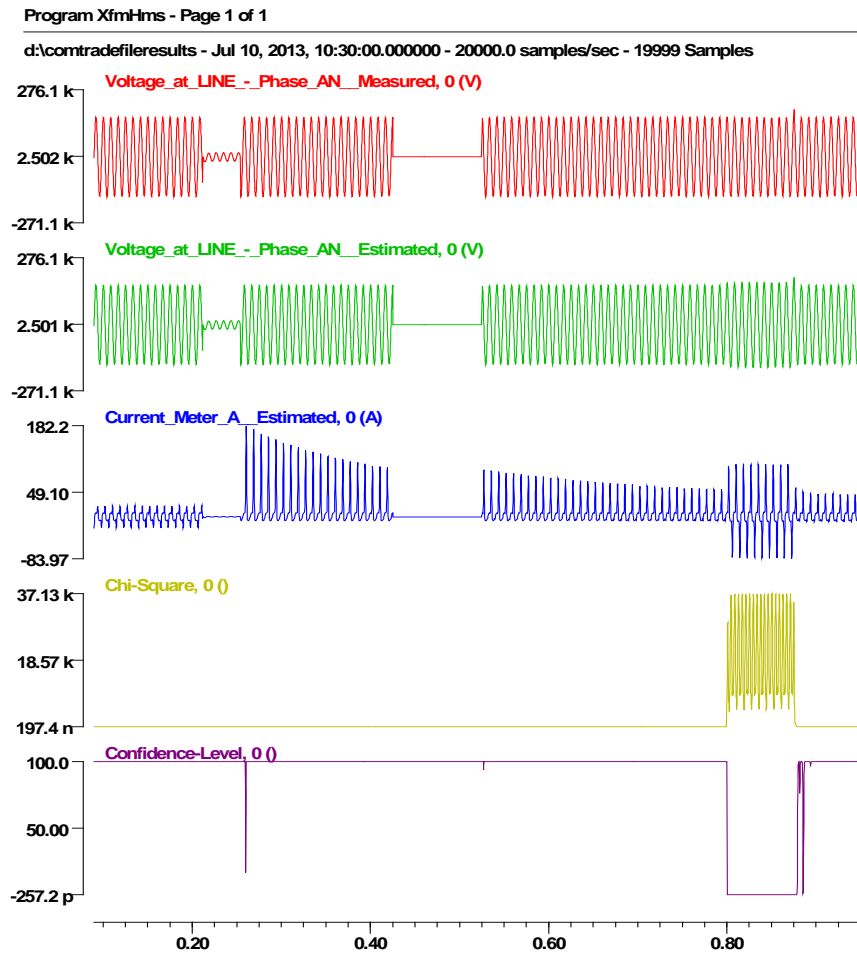


Figure 8.7 Results of Saturable Core Reactor Test System

8.8.2 Test Scenario 2

This scenario involves an external single phase-to-ground fault at the connection terminal as well as an internal fault at saturable core reactors. Figure 8.8 shows the example test system. The voltage and current of this test system, the Chi-square & confidence level is shown in Figures 8.9.

In Figure 8.9 it can be seen that when there is no fault, the confidence level maintains at value one. The confidence level drops down very quickly when the external single phase-to-ground fault clears. But the confidence level goes back to one immediately which indicates the fault is an external fault and the states still match the single phase saturable core reactors model. It means that there is no fault inside the saturable core reactors and no trip needs to be acted. However, when the internal fault happens the confidence level drops down very quickly again. The confidence level stays at one, indicating it is an internal fault and trip needs to be acted. The average computation time is about 100 us. Since the code has not been optimized and the computer hardware has much room to improve, this objective can be easily achieved. The execution time is show in Figure 8.10.

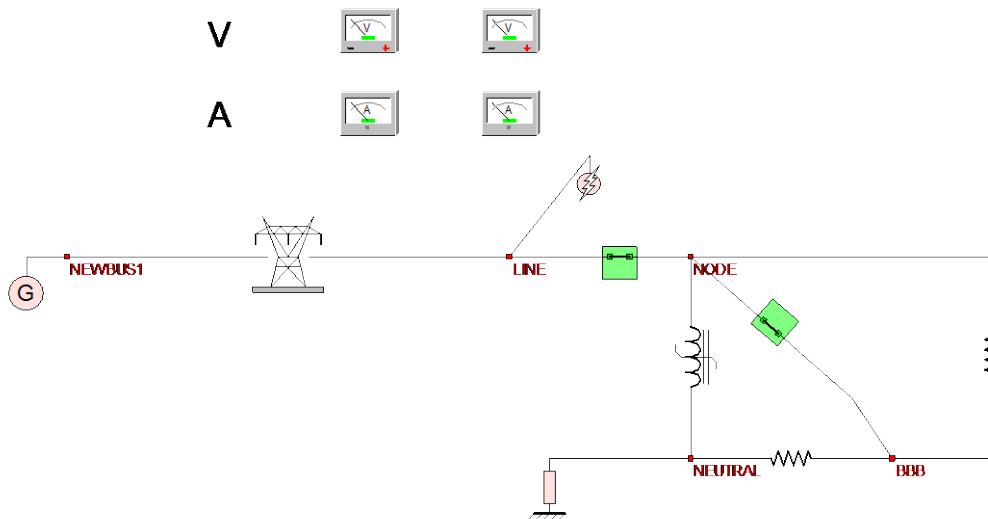


Figure 8.8 Test System Diagram for Single Phase Reactor

d:\contrade\fileresults - Jul 10, 2013, 10:30:00.000000 - 20000.0 samples/sec - 19999 Samples

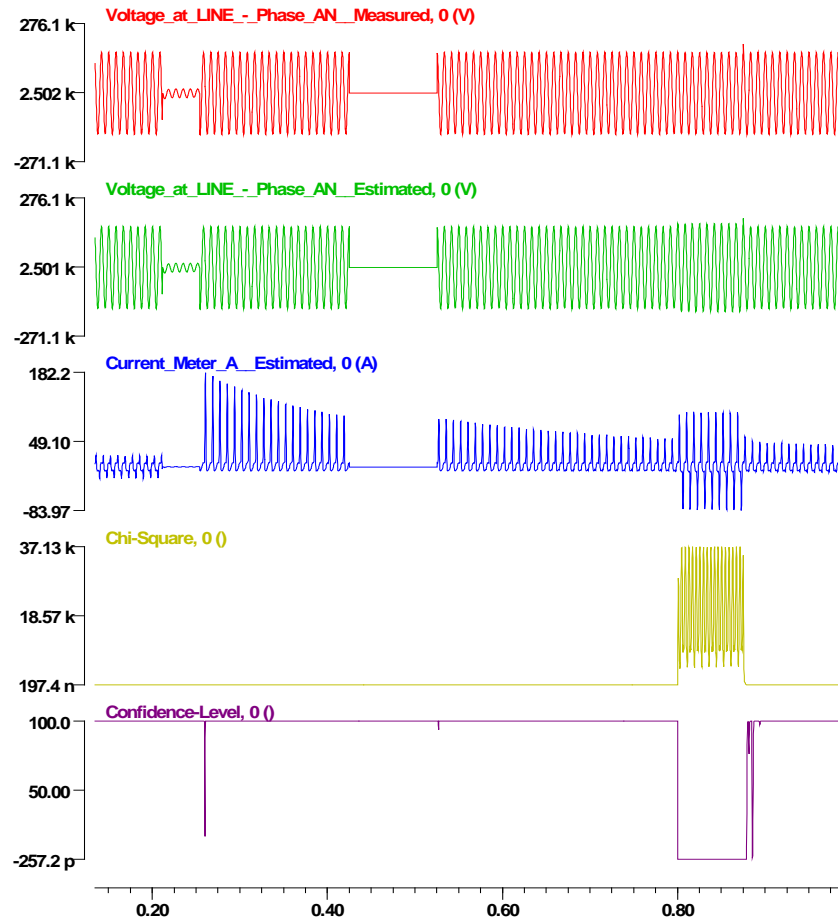


Figure 8.9 Results of Saturable Core Reactor Test System

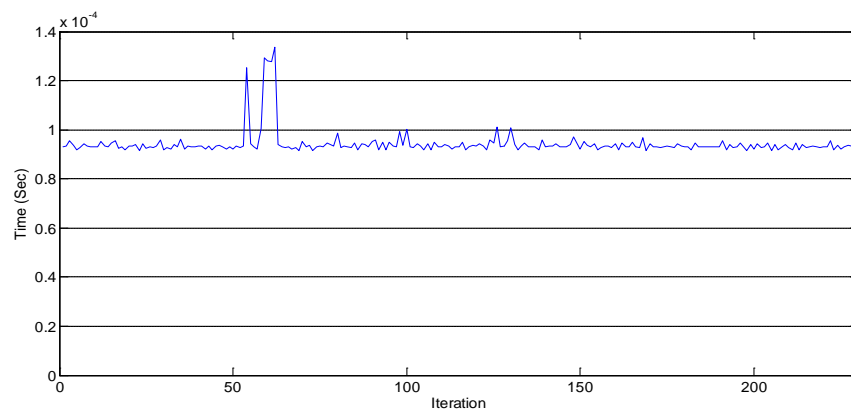


Figure 8.10 Execution time

9. Example Applications: Transformers

This section describes the implementation approach for the setting-less protective relay for three phase transformer. The models and the algorithmic procedures of the analytics are also described. The application has been evaluated by numerical experiments.

9.1 Summary

The transformer model in the SCAQCF has been developed by first developing the single phase indicated in Figure 9.1. The figure shows a single-phase two-winding, variable-tap, saturable-core transformer model. Three single phase transformer models are integrated to obtain a three-phase transformer model, as it is illustrated in Figure 9.2. Current transformer and potential transformer are used to measure the current and voltage. The merging units are GPS synchronized. The measurements are utilized in a dynamic state estimation. Any violation of the physical laws would imply an internal fault in the reactors. The protection logic would trip the reactor when either the physical laws are violated or the operating condition exceeds operating limits.

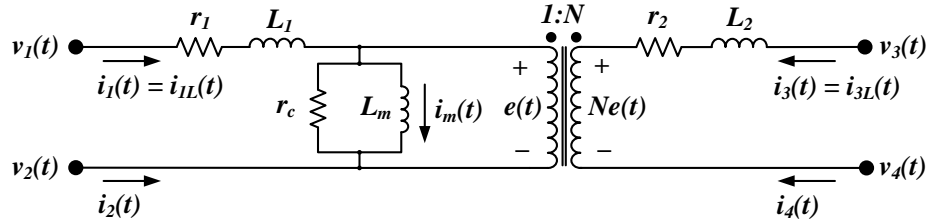


Figure 9.1 Single-Phase Transformer Compact Model

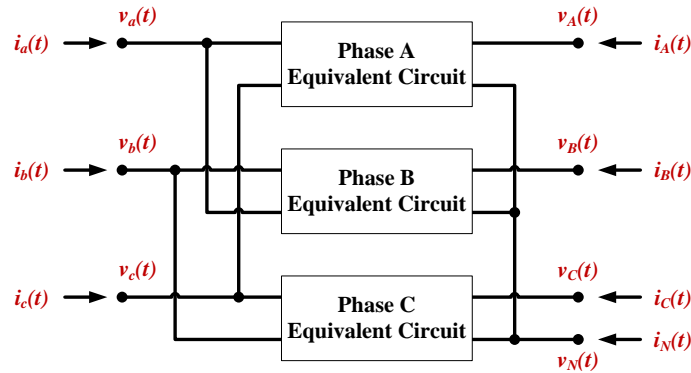


Figure 9.2 Three-Phase, Delta-Wye-Connected Transformer

The instrumentation of the transformer typically includes the terminal voltages and currents as well as other measurements such as neutral current. All the available measurements should be included in the analytics of the protection function for the three phase transformer. This section briefly describes the constituent parts of the setting-less protection for the transformer and then presents an example result, typical timing data and discussion of issues associated with transformer protection.

Mathematical Model: The mathematical model of the three phase transformer is expressed in the SCAQCF Model. The exact model and form is provided in Appendix 3.

System State: The system state is defined by the SCAQCF model. There are totally 68 state variables (when the transformer is delta-wye-connected, and when the exponent n is five). Note that the states are classified as external state and internal states. There are 14 external states and 54 internal states.

Measurements: For this example of a three phase transformer we have 13 actual measurements that consist of six across measurements (PTs that measure voltages across phase a-N, b-N, c-N, A-N, B-N, and C-N); and 7 through measurements from CTs that measure currents through phases a, b, c, A, B, C, and N. When two consecutive sampling points are imported, the first point becomes a measurement for the intermediate time t_m , and the second point becomes a measurement for the current time t . As a result, a total of 26 measurements can be formed from actual measurement channels. In addition to the actual measurements, 54 virtual measurements can be introduced from the transformer model, and 2 pseudo measurements for neutral voltages can be added. Therefore, a total of 82 measurements can be used for the dynamic state estimation, providing a redundancy of 20.6%.

Using the above model the following events were considered: (a) normal operating condition, (b) transformer energization (inrush current), (c) transformer over-excitation, (d) through fault condition, and (e) internal fault condition. For each event, the system was simulated and a COMTRADE file was generated with the time waveforms of the actual measurements. Subsequently the COMTRADE file was “played” back through the setting-less protection for the transformer. The results were recorded into another COMTRADE file. The output file includes the following data: (a) the actual measurements, (b) the estimated states of the transformer, (c) the estimated values of the actual measurements, (d) the normalized measurement residuals, i.e. difference between the actual measurements and the estimated values of the actual measurements divided by the meter accuracy (meter standard deviation of measurement error) and (e) the relay decision (trip/non-trip). Graphs of the input COMTRADE file data and the output COMTRADE file data are provided in the report "IR_SettingLessProtection_Transformers.docx" for each of the events listed above. Here we provide an example of these graphs. Specifically, Figure 9.3 illustrates the estimated values of across and through measurements and the trip/non-trip decision (i.e., the confidence level). Note that this event includes an internal fault for 0.05 seconds. Note the relay tripped for the internal fault.

Execution Time: For this event, the execution time of the state estimation at each set of data was measured and reported in Figure 9.3. Note that average execution time for each state estimation process is around 5ms. This value is to be compared with the sampling rate of the data acquisition system of the relay. For a sampling rate of 4 ks/s the state estimation is called 2,000 times per second. This means that the data for the state estimation are coming in one set per 0.5ms. Therefore the state estimation is performed in greater time that the period between two successive sets of data. The objective is to perform the analytics of the setting-less protection in less than 50% of the time between two successive sets of data. Therefore, we should reduce the processing time by upgrading hardware and by optimizing the codes. Furthermore, since the transformer model has quadratic nonlinear terms, the Jacobian matrix H is updated every iteration during dynamic state estimation and the inverse of the information matrix (i.e., H^TWH) is computed every iteration. The information matrix includes linear and quadratic terms; the linear terms should be computed only once and only the quadratic terms should be updated each iteration – this will speed up the algorithm considerable.

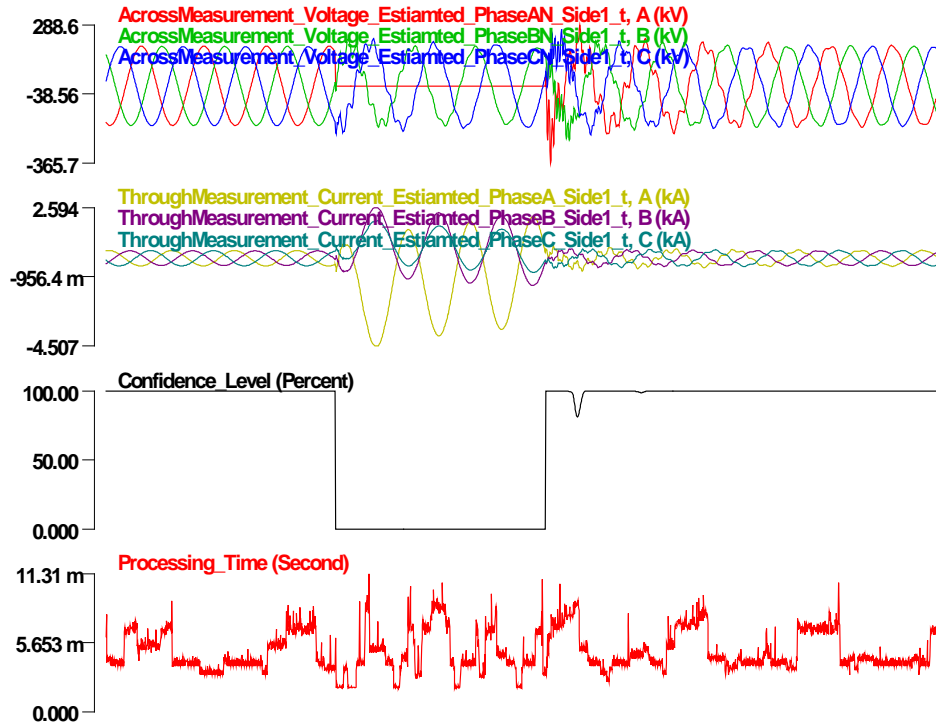


Figure 9.3 Result of an Example Test System with Internal Fault

9.2 Setting-less Relay Description

This section describes the overall implementation of the setting-less protective relay. The architecture of this relay is shown in Figure 6.1. Note that the relay requires the model of the zone to be protected and the actual (physical) measurements from the data acquisition system. The model must be provided in the SCAQCF syntax which is defined in this

document. Then the remaining analytics are automatically constructed and executed. These are: the pointers that provide the interrelationship of the actual measurements to the zone model, the creation of the measurement models for the actual, virtual, derived and pseudo measurements, the dynamic state estimation, the bad data detection and identification and the protection logic.

Note that the data acquisition system is continuously streaming measurement into the relay with a specific rate. Typical rates are 2,000 to 5,000 samples per second. As it will be seen later, the model of the component to be protected is derived in the SCAQCF by using the quadratic integration. The SCAQCF model is expressed in terms of the values of the various variables at two consecutive time instances (two consecutive samples) and past history samples. This means that the analytics of the setting-less relay operate on samples of two consecutive time instances. This is illustrated in Figure 9.4. The samples (measurements) at the two consecutive time instances t and $(t-t_s)$ are used. Note that t_s defines the sampling period. For the typical sampling rates referenced above the mining sampling period will be 200 microseconds (5,000 samples per second). This means that the analytics of the setting-less relay must be performed within the time interval of 400 microseconds (before the next set of data arrive). Obviously, there should be a margin. For this reason the goal for the setting-less relay is to perform the analytics in time less than 200 microseconds. Numerical experiments have been performed and the performance is documented in this report.

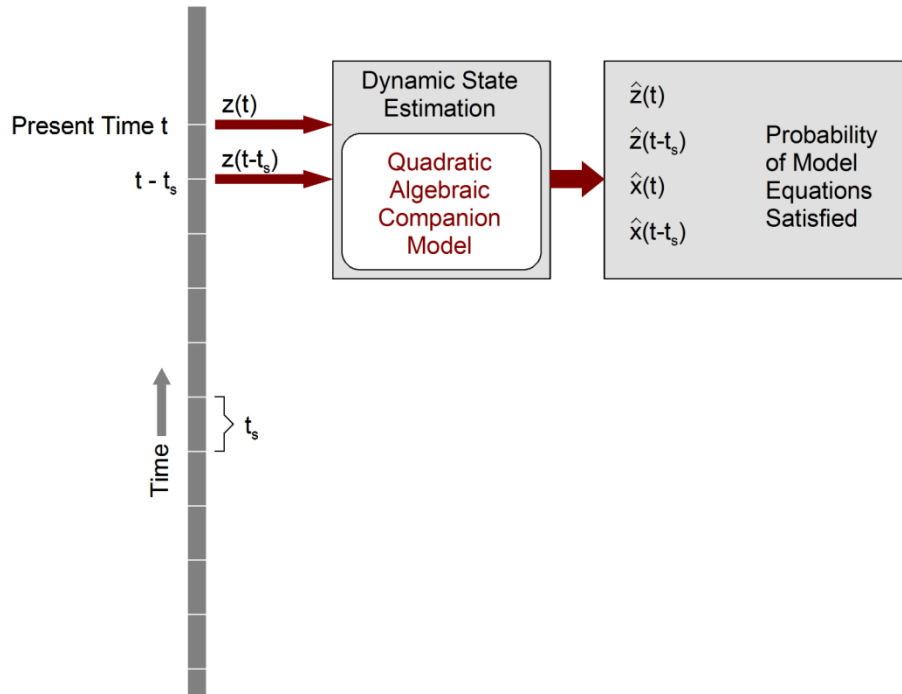


Figure 9.4 Illustration of Time Samples Utilized at each iteration of the Setting-less Relay Analytics

9.3 Three Phase Transformer Model

This section describes the transformer model. In this section, we present the final SCAQCF model of the three-phase, two-winding, variable-tap, and saturable-core transformer as follows:

$$\begin{bmatrix} i_{3\phi}(t) \\ 0 \\ i_{3\phi}(t_m) \\ 0 \end{bmatrix} = \begin{bmatrix} Y_{11} & Y_{12} & Y_{13} & Y_{14} \\ Y_{21} & Y_{22} & Y_{23} & Y_{24} \\ Y_{31} & Y_{32} & Y_{33} & Y_{34} \\ Y_{41} & Y_{42} & Y_{43} & Y_{44} \end{bmatrix} \cdot \begin{bmatrix} v_{3\phi}(t) \\ y_{3\phi}(t) \\ v_{3\phi}(t_m) \\ y_{3\phi}(t_m) \end{bmatrix} - \begin{bmatrix} N_{11} & N_{12} \\ N_{21} & N_{22} \\ N_{31} & N_{32} \\ N_{41} & N_{42} \end{bmatrix} \cdot \begin{bmatrix} v_{3\phi}(t-h) \\ y_{3\phi}(t-h) \end{bmatrix} + \begin{bmatrix} f_{3\phi,1}(t) \\ f_{3\phi,2}(t) \\ f_{3\phi,1}(t_m) \\ f_{3\phi,2}(t_m) \end{bmatrix}$$

where

$$i_{3\phi}(t) = [i_a(t), i_b(t), i_c(t), i_A(t), i_B(t), i_C(t), i_N(t)]^T$$

$$Y_{eq} = \begin{bmatrix} Y_{11} & Y_{12} & Y_{13} & Y_{14} \\ Y_{21} & Y_{22} & Y_{23} & Y_{24} \\ Y_{31} & Y_{32} & Y_{33} & Y_{34} \\ Y_{41} & Y_{42} & Y_{43} & Y_{44} \end{bmatrix}$$

$$v_{3\phi}(t) = [v_a(t), v_b(t), v_c(t), v_A(t), v_B(t), v_C(t), v_N(t)]^T$$

$$y_{3\phi}(t) = [i_{mA}(t), e_A(t), \lambda_A(t), i_{1LA}(t), i_{3LA}(t), y_{1A}(t), y_{2A}(t), y_{3A}(t), z_A(t), \\ i_{mB}(t), e_B(t), \lambda_B(t), i_{1LB}(t), i_{3LB}(t), y_{1B}(t), y_{2B}(t), y_{3B}(t), z_B(t), \\ i_{mC}(t), e_C(t), \lambda_C(t), i_{1LC}(t), i_{3LC}(t), y_{1C}(t), y_{2C}(t), y_{3C}(t), z_C(t)]^T$$

$$N_{eq} = \begin{bmatrix} N_{11} & N_{12} \\ N_{21} & N_{22} \\ N_{31} & N_{32} \\ N_{41} & N_{42} \end{bmatrix}$$

$$f_{3\phi,1}(t) = \begin{bmatrix} x_{1\phi}(t)^T \cdot Q_1 \cdot x_{1\phi}(t) \\ x_{1\phi}(t)^T \cdot Q_2 \cdot x_{1\phi}(t) \\ \vdots \\ x_{1\phi}(t)^T \cdot Q_7 \cdot x_{1\phi}(t) \end{bmatrix}$$

$$f_{3\phi,2}(t) = \begin{bmatrix} x_{1\phi}(t)^T \cdot Q_8 \cdot x_{1\phi}(t) \\ x_{1\phi}(t)^T \cdot Q_9 \cdot x_{1\phi}(t) \\ \vdots \\ x_{1\phi}(t)^T \cdot Q_{27} \cdot x_{1\phi}(t) \end{bmatrix}$$

The derivation of the transformer model is documented in Appendix 3.

For three-phase, delta-wye transformer ($n = 5$), there are 68 states (34 for time step t and 34 for intermediate time step t_m) as listed in Table 9.1.

Table 9.1 All State Variables of the Three-Phase Transformer ($n = 5$)

State	Type	Time	Description
$x_1 = v_a(t)$	External	t	Phase-a terminal voltage at the primary side
$x_2 = v_b(t)$	External	t	Phase-b terminal voltage at the primary side
$x_3 = v_c(t)$	External	t	Phase-c terminal voltage at the primary side
$x_4 = v_A(t)$	External	t	Phase-A terminal voltage at the secondary side
$x_5 = v_B(t)$	External	t	Phase-B terminal voltage at the secondary side
$x_6 = v_C(t)$	External	t	Phase-C terminal voltage at the secondary side
$x_7 = v_N(t)$	External	t	Neutral terminal voltage at the secondary side
$x_8 = i_{mA}(t)$	Internal	t	Magnetizing current at the primary-side, phase-a coil
$x_9 = e_A(t)$	Internal	t	Phase-a winding voltage at the primary side
$x_{10} = \lambda_A(t)$	Internal	t	Magnetic flux linkage at the phase-a core
$x_{11} = i_{1LA}(t)$	Internal	t	Phase-a terminal current at the primary side
$x_{12} = i_{3LA}(t)$	Internal	t	Phase-A terminal current at the secondary side
$x_{13} = y_{1A}(t)$	Internal	t	Additional state for the nonlinear term at phase a
$x_{14} = y_{2A}(t)$	Internal	t	Additional state for the nonlinear term at phase a
$x_{15} = y_{3A}(t)$	Internal	t	Additional state for the nonlinear term at phase a
$x_{16} = z_A(t)$	Internal	t	Additional state for the nonlinear term at phase a
$x_{17} = i_{mB}(t)$	Internal	t	Magnetizing current at the primary-side, phase-b coil
$x_{18} = e_B(t)$	Internal	t	Phase-b winding voltage at the primary side
$x_{19} = \lambda_B(t)$	Internal	t	Magnetic flux linkage at the phase-b core

State	Type	Time	Description
$x_{20} = i_{1LB}(t)$	Internal	t	Phase-b terminal current at the primary side
$x_{21} = i_{3LB}(t)$	Internal	t	Phase-B terminal current at the secondary side
$x_{22} = y_{1B}(t)$	Internal	t	Additional state for the nonlinear term at phase b
$x_{23} = y_{2B}(t)$	Internal	t	Additional state for the nonlinear term at phase b
$x_{24} = y_{3B}(t)$	Internal	t	Additional state for the nonlinear term at phase b
$x_{25} = z_B(t)$	Internal	t	Additional state for the nonlinear term at phase b
$x_{26} = i_{mC}(t)$	Internal	t	Magnetizing current at the primary-side, phase-c coil
$x_{27} = e_C(t)$	Internal	t	Phase-c winding voltage at the primary side
$x_{28} = \lambda_C(t)$	Internal	t	Magnetic flux linkage at the phase-c core
$x_{29} = i_{1LC}(t)$	Internal	t	Phase-c terminal current at the primary side
$x_{30} = i_{3LC}(t)$	Internal	t	Phase-C terminal current at the secondary side
$x_{31} = y_{1C}(t)$	Internal	t	Additional state for the nonlinear term at phase c
$x_{32} = y_{2C}(t)$	Internal	t	Additional state for the nonlinear term at phase c
$x_{33} = y_{3C}(t)$	Internal	t	Additional state for the nonlinear term at phase c
$x_{34} = z_C(t)$	Internal	t	Additional state for the nonlinear term at phase c
$x_{35} = v_a(t_m)$	External	t_m	Phase-a terminal voltage at the primary side
$x_{36} = v_b(t_m)$	External	t_m	Phase-b terminal voltage at the primary side
$x_{37} = v_c(t_m)$	External	t_m	Phase-c terminal voltage at the primary side
$x_{38} = v_A(t_m)$	External	t_m	Phase-A terminal voltage at the secondary side
$x_{39} = v_B(t_m)$	External	t_m	Phase-B terminal voltage at the secondary side
$x_{40} = v_C(t_m)$	External	t_m	Phase-C terminal voltage at the secondary side
$x_{41} = v_N(t_m)$	External	t_m	Neutral terminal voltage at the secondary side
$x_{42} = i_{mA}(t_m)$	Internal	t_m	Magnetizing current at the primary-side, phase-a coil
$x_{43} = e_A(t_m)$	Internal	t_m	Phase-a winding voltage at the primary side
$x_{44} = \lambda_A(t_m)$	Internal	t_m	Magnetic flux linkage at the phase-a core
$x_{45} = i_{1LA}(t_m)$	Internal	t_m	Phase-a terminal current at the primary side
$x_{46} = i_{3LA}(t_m)$	Internal	t_m	Phase-A terminal current at the secondary side

State	Type	Time	Description
$x_{47} = y_{1A}(t_m)$	Internal	t_m	Additional state for the nonlinear term at phase a
$x_{48} = y_{2A}(t_m)$	Internal	t_m	Additional state for the nonlinear term at phase a
$x_{49} = y_{3A}(t_m)$	Internal	t_m	Additional state for the nonlinear term at phase a
$x_{50} = z_A(t_m)$	Internal	t_m	Additional state for the nonlinear term at phase a
$x_{51} = i_{mB}(t_m)$	Internal	t_m	Magnetizing current at the primary-side, phase-b coil
$x_{52} = e_B(t_m)$	Internal	t_m	Phase-b winding voltage at the primary side
$x_{53} = \lambda_B(t_m)$	Internal	t_m	Magnetic flux linkage at the phase-b core
$x_{54} = i_{1LB}(t_m)$	Internal	t_m	Phase-b terminal current at the primary side
$x_{55} = i_{3LB}(t_m)$	Internal	t_m	Phase-B terminal current at the secondary side
$x_{56} = y_{1B}(t_m)$	Internal	t_m	Additional state for the nonlinear term at phase b
$x_{57} = y_{2B}(t_m)$	Internal	t_m	Additional state for the nonlinear term at phase b
$x_{58} = y_{3B}(t_m)$	Internal	t_m	Additional state for the nonlinear term at phase b
$x_{59} = z_B(t_m)$	Internal	t_m	Additional state for the nonlinear term at phase b
$x_{60} = i_{mC}(t_m)$	Internal	t_m	Magnetizing current at the primary-side, phase-c coil
$x_{61} = e_C(t_m)$	Internal	t_m	Phase-c winding voltage at the primary side
$x_{62} = \lambda_C(t_m)$	Internal	t_m	Magnetic flux linkage at the phase-c core
$x_{63} = i_{1LC}(t_m)$	Internal	t_m	Phase-c terminal current at the primary side
$x_{64} = i_{3LC}(t_m)$	Internal	t_m	Phase-C terminal current at the secondary side
$x_{65} = y_{1C}(t_m)$	Internal	t_m	Additional state for the nonlinear term at phase c
$x_{66} = y_{2C}(t_m)$	Internal	t_m	Additional state for the nonlinear term at phase c
$x_{67} = y_{3C}(t_m)$	Internal	t_m	Additional state for the nonlinear term at phase c
$x_{68} = z_C(t_m)$	Internal	t_m	Additional state for the nonlinear term at phase c

The state variables of the delta-wye-connected, three-phase transformer are defined as follows:

$$\begin{bmatrix} v_{3\phi}(t) \\ y_{3\phi}(t) \\ v_{3\phi}(t_m) \\ y_{3\phi}(t_m) \end{bmatrix}$$

9.4 Measurements Definition

To implement the setting-less transformer protection, the following measurements are required:

Actual measurements: six voltages at time t (phase a-N, phase b-N, phase c-N, phase A-N, phase B-N, and phase C-N); seven currents at time t (phase a, phase b, phase c, phase A, phase B, phase C, and phase N); six voltages at time t_m (phase a-N, phase b-N, phase c-N, phase A-N, phase B-N, and phase C-N); and seven currents at time t_m (phase phase a, phase b, phase c, phase A, phase B, phase C, and phase N). Typically, it is assumed that these measurements have a measurement error with standard deviation equal to 0.01pu.

Virtual measurements: measurements with a value equal to zero at time t [8th- to 34th-row in equation] and measurements with a value equal to zero at time t_m [42th- to 68th-row in equation]. These measurements represent the zero value on the left hand side of the 8th- to 34th-row and 42nd- to 68th-row in equation. Typically, it is assumed that these measurements have a measurement error with standard deviation equal to 0.01pu.

Pseudo measurements: one voltage at time t (phase N-g) and one voltage at time t_m (phase N-g). These measurements represent quantities that are normally not measured, such as ground voltage and current in the neutral. Typically, it is assumed that these measurements have a relatively large measurement error with standard deviation equal to 0.1pu.

Note that for this three-phase transformer, there are 26 actual measurements, 54 virtual measurements, and 2 pseudo measurements; there are a total of 82 measurements. It is noted that there are 68 states, and therefore, this provides a redundancy of 20.6% (i.e., $(82-68)/68$).

All across, through, virtual and pseudo measurements that are used for the dynamic state estimator are listed in Table 9.2, Table 9.3, Table 9.4, and Table 9.5, respectively. Note that the scales of standard deviations are as follows: $V_{scaleh} = 230$, $V_{scalel} = 115$, $I_{scaleh} = 0.4$, and $I_{scalel} = 0.8$.

It is important to point out that when two consecutive sampling points are imported, the first point becomes a measurement for the intermediate time t_m , and the second point becomes a measurement for the current time t .

Table 9.2 Actual Across Measurements for the Three-Phase Transformer

Type	Name	Measurement Model	Standard Deviation
Across	voltage_aN	$z_1 = v_a(t) - v_N(t)$	0.01 (p.u.) * Vscaleh
Across	voltage_bN	$z_2 = v_b(t) - v_N(t)$	0.01 (p.u.) * Vscaleh
Across	voltage_cN	$z_3 = v_c(t) - v_N(t)$	0.01 (p.u.) * Vscaleh
Across	voltage_AN	$z_4 = v_A(t) - v_N(t)$	0.01 (p.u.) * Vscalel
Across	voltage_BN	$z_5 = v_B(t) - v_N(t)$	0.01 (p.u.) * Vscalel
Across	voltage_CN	$z_6 = v_C(t) - v_N(t)$	0.01 (p.u.) * Vscalel
Across	voltage_aNm	$z_7 = v_a(t_m) - v_N(t_m)$	0.01 (p.u.) * Vscaleh
Across	voltage_bNm	$z_8 = v_b(t_m) - v_N(t_m)$	0.01 (p.u.) * Vscaleh
Across	voltage_cNm	$z_9 = v_c(t_m) - v_N(t_m)$	0.01 (p.u.) * Vscaleh
Across	voltage_ANm	$z_{10} = v_A(t_m) - v_N(t_m)$	0.01 (p.u.) * Vscalel
Across	voltage_BNm	$z_{11} = v_B(t_m) - v_N(t_m)$	0.01 (p.u.) * Vscalel
Across	voltage_CNm	$z_{12} = v_C(t_m) - v_N(t_m)$	0.01 (p.u.) * Vscalel

Table 9.3 Actual Through Measurements for the Three-Phase Transformer

Type	Name	Measurement Model	Standard Deviation
Through	current_a	$z_1 = i_a(t) = 1st\text{-row in equation}$	0.01 (p.u.) * Iscaleh
Through	current_b	$z_2 = i_b(t) = 2nd\text{-row in equation}$	0.01 (p.u.) * Iscaleh
Through	current_c	$z_3 = i_c(t) = 3rd\text{-row in equation}$	0.01 (p.u.) * Iscaleh
Through	current_A	$z_4 = i_A(t) = 4th\text{-row in equation}$	0.01 (p.u.) * Iscalel
Through	current_B	$z_5 = i_B(t) = 5th\text{-row in equation}$	0.01 (p.u.) * Iscalel
Through	current_C	$z_6 = i_C(t) = 6th\text{-row in equation}$	0.01 (p.u.) * Iscalel
Through	current_N	$z_7 = i_N(t) = 7th\text{-row in equation}$	0.01 (p.u.) * Iscalel
Through	current_am	$z_8 = i_a(t_m) = 35th\text{-row in equation}$	0.01 (p.u.) * Iscaleh
Through	current_bm	$z_9 = i_b(t_m) = 36th\text{-row in equation}$	0.01 (p.u.) * Iscaleh
Through	current_cm	$z_{10} = i_c(t_m) = 37th\text{-row in equation}$	0.01 (p.u.) * Iscaleh
Through	current_Am	$z_{11} = i_A(t_m) = 38th\text{-row in equation}$	0.01 (p.u.) * Iscalel
Through	current_Bm	$z_{12} = i_B(t_m) = 39th\text{-row in equation}$	0.01 (p.u.) * Iscalel
Through	current_Cm	$z_{13} = i_C(t_m) = 40th\text{-row in equation}$	0.01 (p.u.) * Iscalel
Through	current_Nm	$z_{14} = i_N(t_m) = 41st\text{-row in equation}$	0.01 (p.u.) * Iscalel

Table 9.4 Virtual Measurements for the Three-Phase Transformer

Type	Name	Measurement Model	Standard Deviation
Virtual	virtual_t_1	$z_1 = 0 = 8th\text{-row in equation}$	0.01 (p.u.)
Virtual	virtual_t_2	$z_2 = 0 = 9th\text{-row in equation}$	0.01 (p.u.)
Virtual	virtual_t_3	$z_3 = 0 = 10th\text{-row in equation}$	0.01 (p.u.)
Virtual	virtual_t_4	$z_4 = 0 = 11th\text{-row in equation}$	0.01 (p.u.)
Virtual	virtual_t_5	$z_5 = 0 = 12th\text{-row in equation}$	0.01 (p.u.)

Type	Name	Measurement Model	Standard Deviation
Virtual	virtual_t_6	$z_6 = 0 = 13th\text{-row in equation}$	0.01 (p.u.)
Virtual	virtual_t_7	$z_7 = 0 = 14th\text{-row in equation}$	0.01 (p.u.)
Virtual	virtual_t_8	$z_8 = 0 = 15th\text{-row in equation}$	0.01 (p.u.)
Virtual	virtual_t_9	$z_9 = 0 = 16th\text{-row in equation}$	0.01 (p.u.)
Virtual	virtual_t_10	$z_{10} = 0 = 17th\text{-row in equation}$	0.01 (p.u.)
Virtual	virtual_t_11	$z_{11} = 0 = 18th\text{-row in equation}$	0.01 (p.u.)
Virtual	virtual_t_12	$z_{12} = 0 = 19th\text{-row in equation}$	0.01 (p.u.)
Virtual	virtual_t_13	$z_{13} = 0 = 20th\text{-row in equation}$	0.01 (p.u.)
Virtual	virtual_t_14	$z_{14} = 0 = 21st\text{-row in equation}$	0.01 (p.u.)
Virtual	virtual_t_15	$z_{15} = 0 = 22nd\text{-row in equation}$	0.01 (p.u.)
Virtual	virtual_t_16	$z_{16} = 0 = 23rd\text{-row in equation}$	0.01 (p.u.)
Virtual	virtual_t_17	$z_{17} = 0 = 24th\text{-row in equation}$	0.01 (p.u.)
Virtual	virtual_t_18	$z_{18} = 0 = 25th\text{-row in equation}$	0.01 (p.u.)
Virtual	virtual_t_19	$z_{19} = 0 = 26st\text{-row in equation}$	0.01 (p.u.)
Virtual	virtual_t_20	$z_{20} = 0 = 27nd\text{-row in equation}$	0.01 (p.u.)
Virtual	virtual_t_21	$z_{21} = 0 = 28rd\text{-row in equation}$	0.01 (p.u.)
Virtual	virtual_t_22	$z_{22} = 0 = 29th\text{-row in equation}$	0.01 (p.u.)
Virtual	virtual_t_23	$z_{23} = 0 = 30th\text{-row in equation}$	0.01 (p.u.)
Virtual	virtual_t_24	$z_{24} = 0 = 31st\text{-row in equation}$	0.01 (p.u.)
Virtual	virtual_t_25	$z_{25} = 0 = 32nd\text{-row in equation}$	0.01 (p.u.)
Virtual	virtual_t_26	$z_{26} = 0 = 33rd\text{-row in equation}$	0.01 (p.u.)
Virtual	virtual_t_27	$z_{27} = 0 = 34th\text{-row in equation}$	0.01 (p.u.)

Type	Name	Measurement Model	Standard Deviation
Virtual	virtual_tm_1	$z_{28} = 0 = 42\text{nd-row in equation}$	0.01 (p.u.)
Virtual	virtual_tm_2	$z_{29} = 0 = 43\text{rd-row in equation}$	0.01 (p.u.)
Virtual	virtual_tm_3	$z_{30} = 0 = 44\text{th-row in equation}$	0.01 (p.u.)
Virtual	virtual_tm_4	$z_{31} = 0 = 45\text{th-row in equation}$	0.01 (p.u.)
Virtual	virtual_tm_5	$z_{32} = 0 = 46\text{th-row in equation}$	0.01 (p.u.)
Virtual	virtual_tm_6	$z_{33} = 0 = 47\text{th-row in equation}$	0.01 (p.u.)
Virtual	virtual_tm_7	$z_{34} = 0 = 48\text{th-row in equation}$	0.01 (p.u.)
Virtual	virtual_tm_8	$z_{35} = 0 = 49\text{th-row in equation}$	0.01 (p.u.)
Virtual	virtual_tm_9	$z_{36} = 0 = 50\text{th-row in equation}$	0.01 (p.u.)
Virtual	virtual_tm_10	$z_{37} = 0 = 51\text{st-row in equation}$	0.01 (p.u.)
Virtual	virtual_tm_11	$z_{38} = 0 = 52\text{nd-row in equation}$	0.01 (p.u.)
Virtual	virtual_tm_12	$z_{39} = 0 = 53\text{rd-row in equation}$	0.01 (p.u.)
Virtual	virtual_tm_13	$z_{40} = 0 = 54\text{th-row in equation}$	0.01 (p.u.)
Virtual	virtual_tm_14	$z_{41} = 0 = 55\text{th-row in equation}$	0.01 (p.u.)
Virtual	virtual_tm_15	$z_{42} = 0 = 56\text{th-row in equation}$	0.01 (p.u.)
Virtual	virtual_tm_16	$z_{43} = 0 = 57\text{th-row in equation}$	0.01 (p.u.)
Virtual	virtual_tm_17	$z_{44} = 0 = 58\text{th-row in equation}$	0.01 (p.u.)
Virtual	virtual_tm_18	$z_{45} = 0 = 59\text{th-row in equation}$	0.01 (p.u.)
Virtual	virtual_tm_19	$z_{46} = 0 = 60\text{th-row in equation}$	0.01 (p.u.)
Virtual	virtual_tm_20	$z_{47} = 0 = 61\text{st-row in equation}$	0.01 (p.u.)
Virtual	virtual_tm_21	$z_{48} = 0 = 62\text{nd-row in equation}$	0.01 (p.u.)
Virtual	virtual_tm_22	$z_{49} = 0 = 63\text{rd-row in equation}$	0.01 (p.u.)

Type	Name	Measurement Model	Standard Deviation
Virtual	virtual_tm_23	$z_{50} = 0 = 64th\text{-row in equation}$	0.01 (p.u.)
Virtual	virtual_tm_24	$z_{51} = 0 = 65th\text{-row in equation}$	0.01 (p.u.)
Virtual	virtual_tm_25	$z_{52} = 0 = 66th\text{-row in equation}$	0.01 (p.u.)
Virtual	virtual_tm_26	$z_{53} = 0 = 67th\text{-row in equation}$	0.01 (p.u.)
Virtual	virtual_tm_27	$z_{54} = 0 = 68th\text{-row in equation}$	0.01 (p.u.)

Table 9.5 Pseudo Measurements for the Three-Phase Transformer

Type	Name	Measurement Model	Standard Deviation
Pseudo	voltage_N	$z_I = 0 = v_N(t)$	0.1 (p.u.) * VscaleI
Pseudo	voltage_Nm	$z_2 = 0 = v_N(t_m)$	0.1 (p.u.) * VscaleI

Note that if there is no actual through measurement for the neutral phase (i.e., phase N), pseudo measurements for the phase-N current can be added with a standard deviation of 0.1 per unit.

9.5 Creation of Measurement Models

This section describes the creation of the mathematical models of the measurements. The proposed protection algorithm uses four types of measurements: across measurements, through measurements, virtual measurements, and pseudo measurements. It is important to point out that all measurements (e.g., z_1, z_2, \dots, z_m) can be expressed with the functions of state variables [e.g., $h_1(x), h_2(x), \dots, h_m(x)$] and measurement errors (e.g., $\eta_1, \eta_2, \dots, \eta_m$), forming the following the measurement model:

$$z = h(x) + \eta$$

where

$$z = \begin{bmatrix} z_1 \\ z_2 \\ \vdots \\ z_m \end{bmatrix}$$

$$h(x) = \begin{bmatrix} h_1(x) \\ h_2(x) \\ \vdots \\ h_m(x) \end{bmatrix}$$

$$\eta(x) = \begin{bmatrix} \eta_1(x) \\ \eta_2(x) \\ \vdots \\ \eta_m(x) \end{bmatrix}$$

To facilitate forming the measurement model, each measurement is expressed as the following standard form:

$$\mathbf{y}(\mathbf{x}, \mathbf{u}) = Y_{m,x} \mathbf{x} + \left\{ \begin{bmatrix} \vdots \\ \mathbf{x}^T F_{m,x}^i \mathbf{x} \\ \vdots \end{bmatrix} \right\} + Y_{m,u} \mathbf{u} + \left\{ \begin{bmatrix} \vdots \\ \mathbf{u}^T F_{m,u}^i \mathbf{u} \\ \vdots \end{bmatrix} \right\} + \left\{ \begin{bmatrix} \vdots \\ \mathbf{x}^T F_{m,xu}^i \mathbf{u} \\ \vdots \end{bmatrix} \right\} + C_m$$

The following sub-sections describe how to formulate measurement models according to the type of measurements.

9.5.1 Creation of Across Measurement Model

The voltage measurement, which is a typical type of across measurements, measures voltage values across two points, thus forming the following measurement model:

$$z_m = h_m(x) + \eta_m = x_i - x_j + \eta_m$$

where x_i and x_j refer to states corresponding to the measuring points.

9.5.2 Creation of Through Measurement Model

The current measurement, which is a typical type of through measurements, is the measured quantity of an electric current with directions. The measurement model of a current measurement can be derived from the device model, and therefore, the current measurement model at time t is one of rows of the following algebraic companion form:

$$i_{3\phi}(t) = Y_{11} v_{3\phi}(t) + Y_{12} y_{3\phi}(t) + Y_{13} v_{3\phi}(t_m) + Y_{14} y_{3\phi}(t_m) - N_{11} v_{3\phi}(t-h) - N_{12} y_{3\phi}(t-h) + f_{3\phi,1}(t)$$

In fact, the current measurement model is expressed as follows:

$$z_m = h_m(x) + \eta_m = i_{3\phi}^{(k)}(t) + \eta_m$$

where k indicates the k -th row of the vector, $i_{3\phi}(t)$.

Likewise, the current measurement model at the intermediate time (i.e., t_m) is based on one of rows of the following algebraic companion form:

$$i_{3\phi}(t_m) = Y_{31}v_{3\phi}(t) + Y_{32}y_{3\phi}(t) + Y_{33}v_{3\phi}(t_m) + Y_{34}y_{3\phi}(t_m) - N_{31}v_{3\phi}(t-h) - N_{32}y_{3\phi}(t-h) + f_{3\phi,1}(t_m)$$

In fact, the current measurement model is expressed as follows:

$$z_m = h_m(x) + \eta_m = i_{3\phi}^{(k)}(t_m) + \eta_m$$

where k indicates the k -th row of the vector, $i_{3\phi}(t_m)$.

9.5.3 Creation of Virtual Measurement Model

Virtual measurements are intrinsic characteristics of a specific device, so they can be used for state estimation. Indeed, similar to the case of current measurements, the virtual measurement model can be induced from the device model. In detail, the following algebraic companion forms, which are parts of the device model, can become the measurement model:

$$0 = Y_{21}v_{3\phi}(t) + Y_{22}y_{3\phi}(t) + Y_{23}v_{3\phi}(t_m) + Y_{24}y_{3\phi}(t_m) - N_{21}v_{3\phi}(t-h) - N_{22}y_{3\phi}(t-h) + f_{3\phi,2}(t)$$

$$0 = Y_{41}v_{3\phi}(t) + Y_{42}y_{3\phi}(t) + Y_{43}v_{3\phi}(t_m) + Y_{44}y_{3\phi}(t_m) - N_{41}v_{3\phi}(t-h) - N_{42}y_{3\phi}(t-h) + f_{3\phi,2}(t_m)$$

The virtual measurement model is the following format:

$$z_m = 0 = h_m(x) + \eta_m$$

9.5.4 Creation of Pseudo Measurement Model

The proposed protection scheme of the three-phase transformer has pseudo measurements related to the neutral voltage at time t and t_m . In this case, the pseudo measurement model has the following format:

$$z_m = 0 = h_m(x) + \eta_m = x_i + \eta_m$$

where x_i refer to a state that corresponds to the neutral voltage at time t or t_m .

9.6 State Estimation

The dynamic state estimation, which is used for the proposed protection method, is based on the weighted least squares method, which minimizes the sum of weighted residuals as follows:

$$\text{Min } J = [z - h(x)]^T W [z - h(x)]$$

where J is the objective function, and W is the weight matrix. The diagonal entries of the weight matrix consist of the inverse of the squared standard deviations of measurements.

$$W = \text{diag} \left\{ \frac{1}{\sigma_1^2}, \frac{1}{\sigma_2^2}, \dots, \frac{1}{\sigma_m^2} \right\}$$

where σ_m are the standard deviation of measurements. Eventually, the solution can be obtained by the Gauss-Newton iterative algorithm as follows:

$$x^{i+1} = x^i - (H^T W H)^{-1} H^T W (h(x^i) - z)$$

where H is Jacobian matrix of $h(x)$, i means the i -th iteration, and $H^T W H$ is the information matrix.

9.7 Protection Logic

The entire protection logic is based on measurements obtained from the hardware (e.g., PMU, relay, CT, and PT) and the dynamic state estimator. Once the microprocessor gets the measurements from both sides of a transformer under protection, the dynamic state estimation runs according to the transformer SCAQCF model. Then, the chi-square of all the measurements is calculated to check whether all the actual values for measurements correspond to simulated values from the model. Also, the confidence level of the measurements will be calculated to determine whether the transformer is in a healthy status. If the confidence level drops to a low value for several cycles, then the measurements do not fit the model, thus the internal transformer model is incorrect, indicating an internal fault. As a result, the relay would activate breakers and trip the transformer immediately. Meanwhile, during the state estimation process, the operating limit is being monitored so that the transformer will be tripped once it violates the operating limit.

The whole protection requires no setting for any protection equipment. Time synchronization is quite important for the protection scheme, otherwise the state

estimation cannot get the correct simulation results based on the incorrect measurements. In summary, fiber optics and GPS time alignment are two key technologies enabling this protection.

9.8 Numerical Experiments

The above described setting-less relay for transformers have been tested with simulated data. Specifically a test system was used to create a number of scenarios. For each scenario the system was simulated and the measurements of the relay were stored in a COMTRADE file. Figure 9.5 describes the overall approach for the feasibility test of the setting-less protection algorithm.

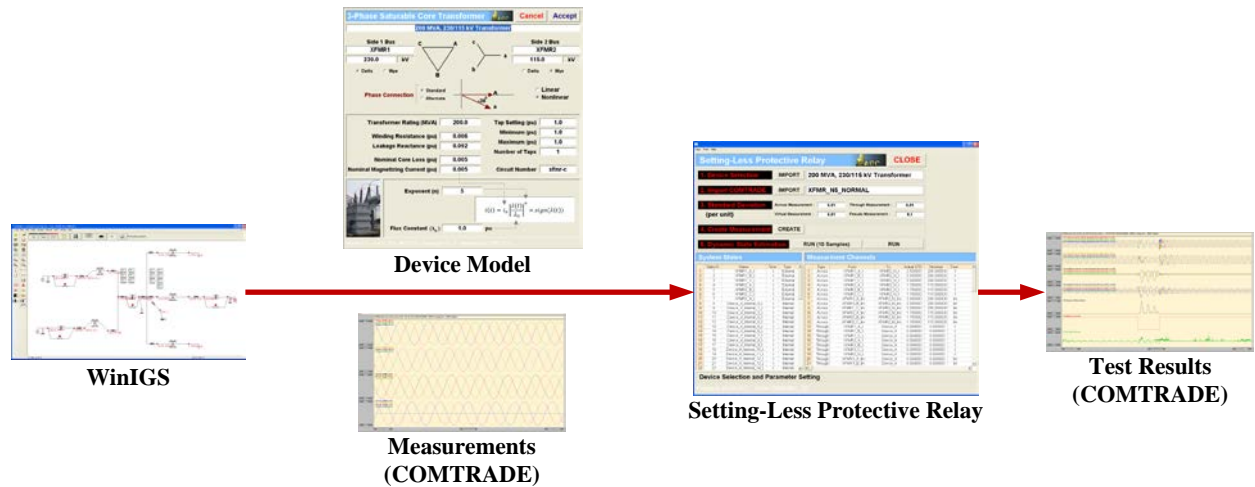


Figure 9.5 Test Scheme for verifying the Proposed Protection Method

To test the feasibility of the proposed protection method, a test system that includes a three-phase transformer under protection and an integrated system around the transformer is created as illustrated in Figure 9.6. The system consists of a 15kV-150MVA-rated generator, an 18kV-350MVA-rated generator, a 15kV-200MVA-rated generator, transformers, and transmission lines that connect load on each line. The three-phase transformer under protection is located at the middle of the entire system (see the red circle in Figure 9.6). Monitored are ten voltages and seven currents at both the terminals of the transformer.

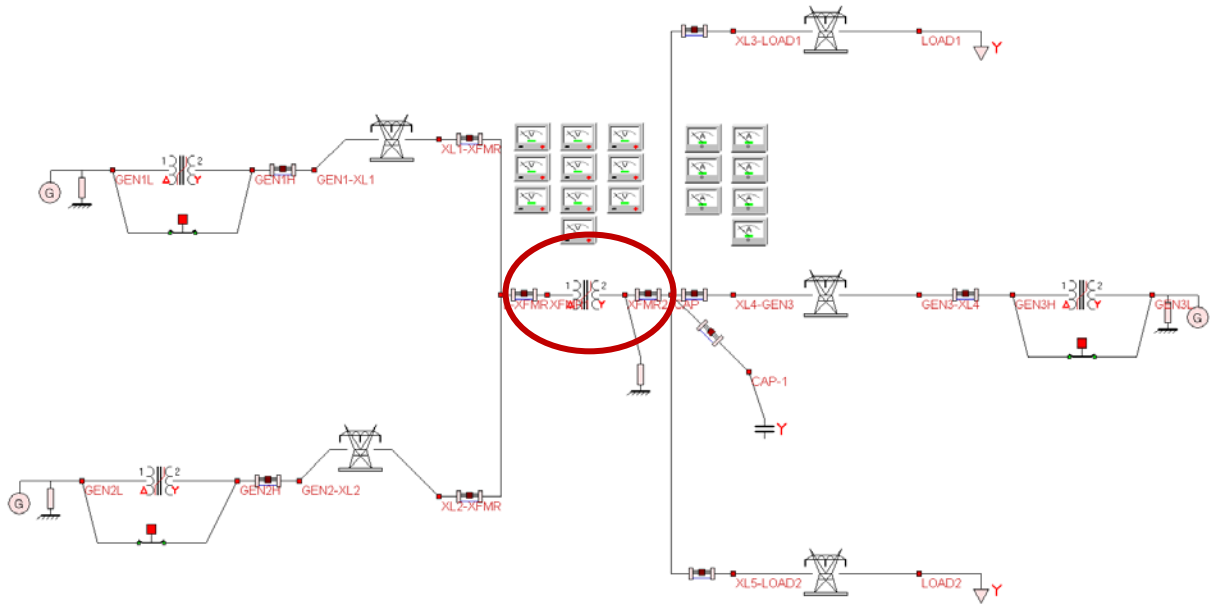


Figure 9.6 Test System for the Setting-Less Protection

The red area is the transformer zone being protected. As shown in the diagram, the measurements of voltages and currents on both sides are provided by PTs and CTs.

In this test, the exponent n , which expresses nonlinear characteristics between the magnetizing current and the flux linkage of the transformer core, is five, and the transformer is delta-wye-connected. The settings of the transformer under protection are shown in Figure 9.7.

3-Phase Saturable Core Transformer
Cancel
Accept

200 MVA, 230/115 kV Transformer

Side 1 Bus
XFMR1
230.0 kV
☒ Delta ☐ Wye

C A
B

Side 2 Bus
XFMR2
115.0 kV
☐ Delta ☒ Wye

c a
b

Phase Connection
☒ Standard ☐ Alternate

☐ Linear
☒ Nonlinear


Transformer Rating (MVA) 200.0
Winding Resistance (pu) 0.006
Leakage Reactance (pu) 0.092
Nominal Core Loss (pu) 0.005
Nominal Magnetizing Current (pu) 0.005

Tap Setting (pu) 1.0
Minimum (pu) 1.0
Maximum (pu) 1.0
Number of Taps 1
Circuit Number xfmr-c

Exponent (n) 5

Flux Constant (λ_0) 1.0 pu

$$i(t) = i_0 \left| \frac{\lambda(t)}{\lambda_0} \right|^n \times \text{sign}(\lambda(t))$$



WinIGS-T - Form: IGS_M173_N - Copyright © A. P. Meliopoulos 1998-2011

Figure 9.7 Settings of the Three-phase Transformer under Protection

The actual parameters of the single-phase transformer model are given in Table 9.6; the parameters are identical to all phases of the transformer.

Table 9.6 Transformer Parameters (Identical at All Phases)

Parameter	Value	Parameter	Value
r_l	2.3805 Ω	r_c	158700 Ω
L_l	0.096822 H	L_m	420.964824 H
r_2	0.198375 Ω	i_0	0.002050
L_2	0.008068 H	λ_0	0.862803
N	0.288675		

Five sets of different measurement signals are illustrated and tested using the setting-less protection scheme:

- Test Scenario 1: Normal operating condition
- Test Scenario 2: Transformer energization (inrush current)
- Test Scenario 3: Transformer overexcitation
- Test Scenario 4: Through fault condition
- Test Scenario 5: Internal fault condition

9.8.1 Test Scenario 1

For normal operating condition, the test system in Figure 9.6 is used. A set of measurement signals monitored during the normal operation condition is shown in the following figure:

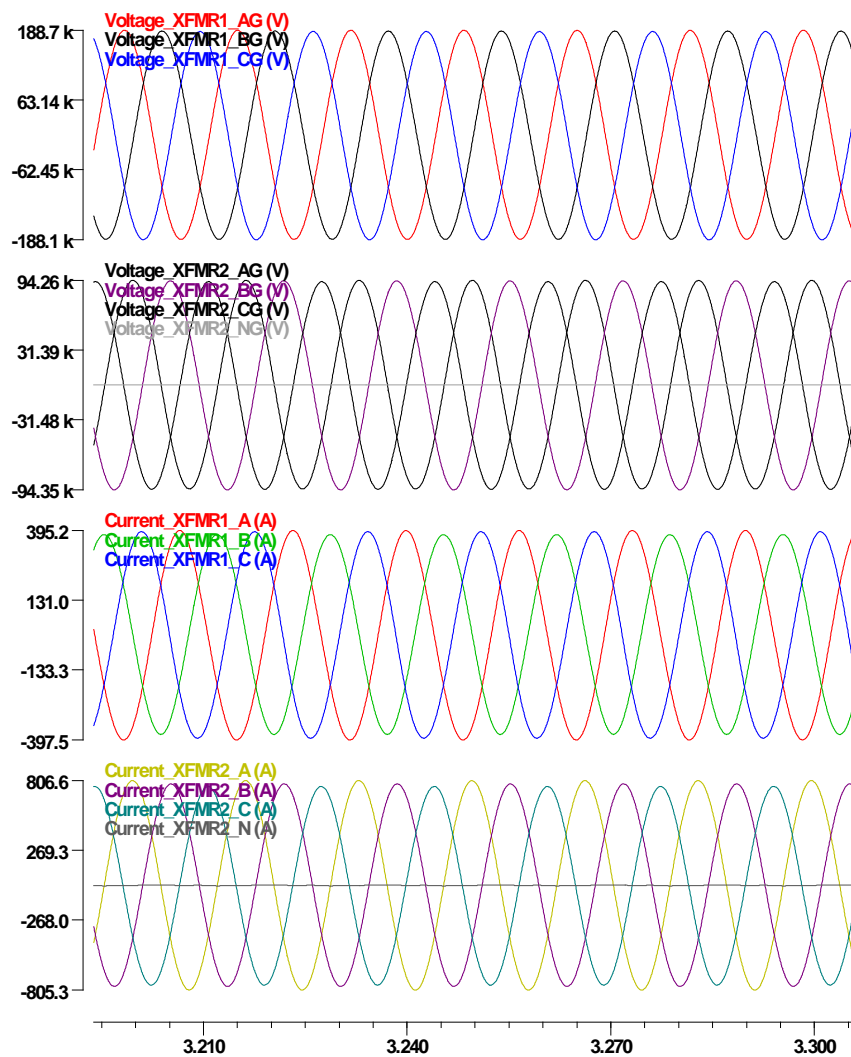


Figure 9.8 Measurement Signals of the Transformer (Normal Operating Condition)

9.8.2 Test Scenario 2

For transformer energization, the test system in Figure 9.6 is used. A set of measurement signals monitored during the energization is shown in the following figure:

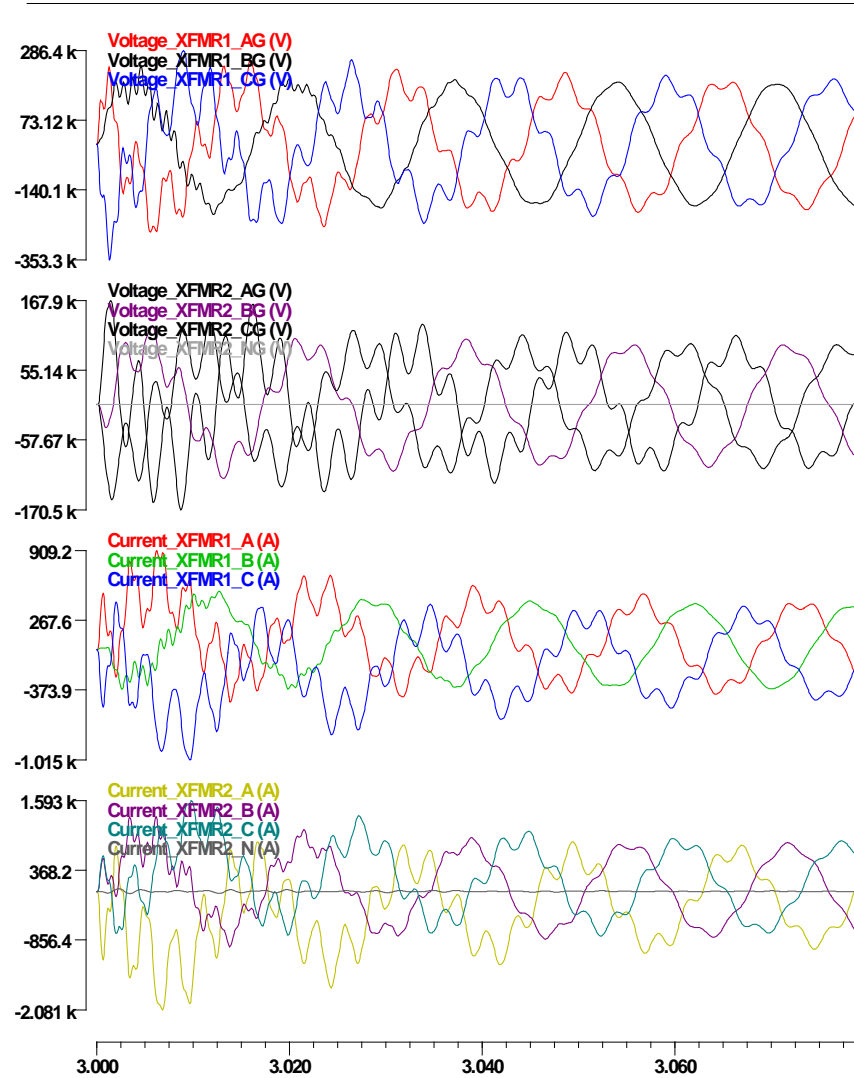


Figure 9.9 Measurement Signals of the Transformer (Transformer Energization)

9.8.3 Test Scenario 3

For transformer overexcitation, the test system in Figure 9.6 is used. A set of measurement signals monitored during the overexcitation is shown in the following figure:

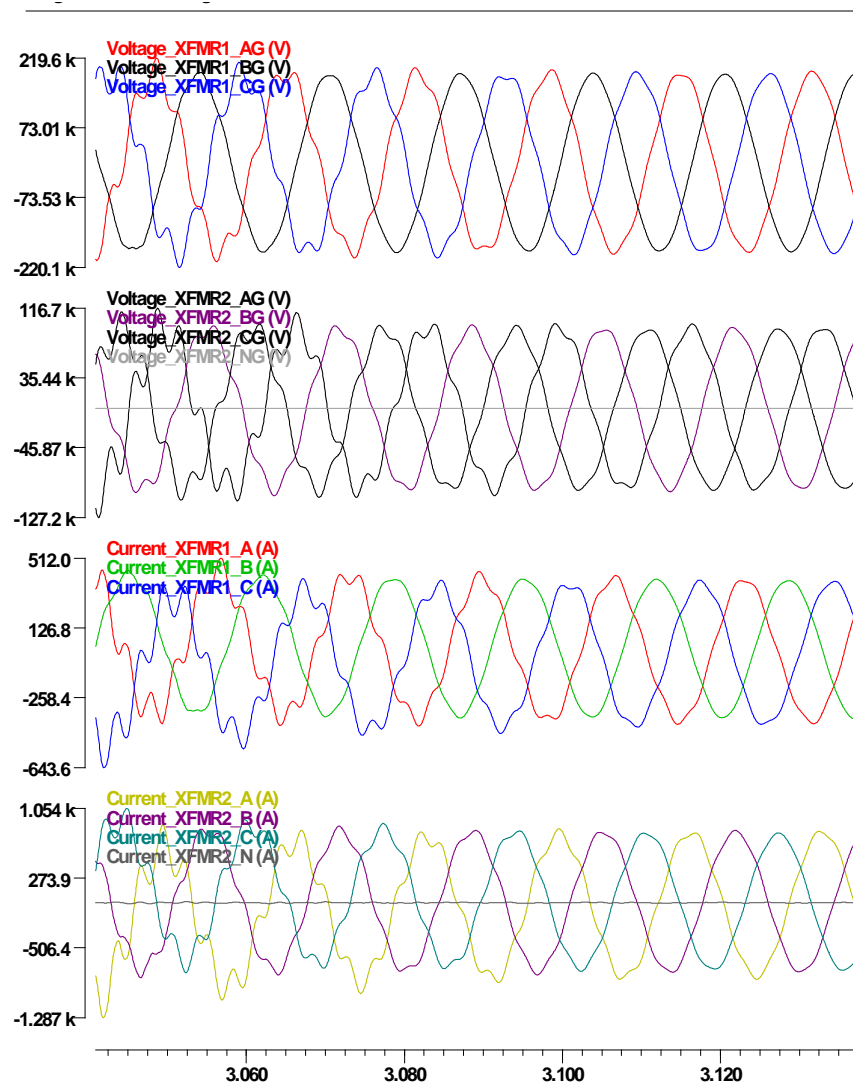


Figure 9.10 Measurement Signals of the Transformer (Transformer Overexcitation)

9.8.4 Test Scenario 4

For through fault condition, the test system in Figure 9.6 is used, but single-phase-to-ground fault is given at a certain bus outside the transformer under protection. The fault lasts for 0.05 seconds, and then it is cleared. In Figure 9.11, the faulted location is marked with the red circle.

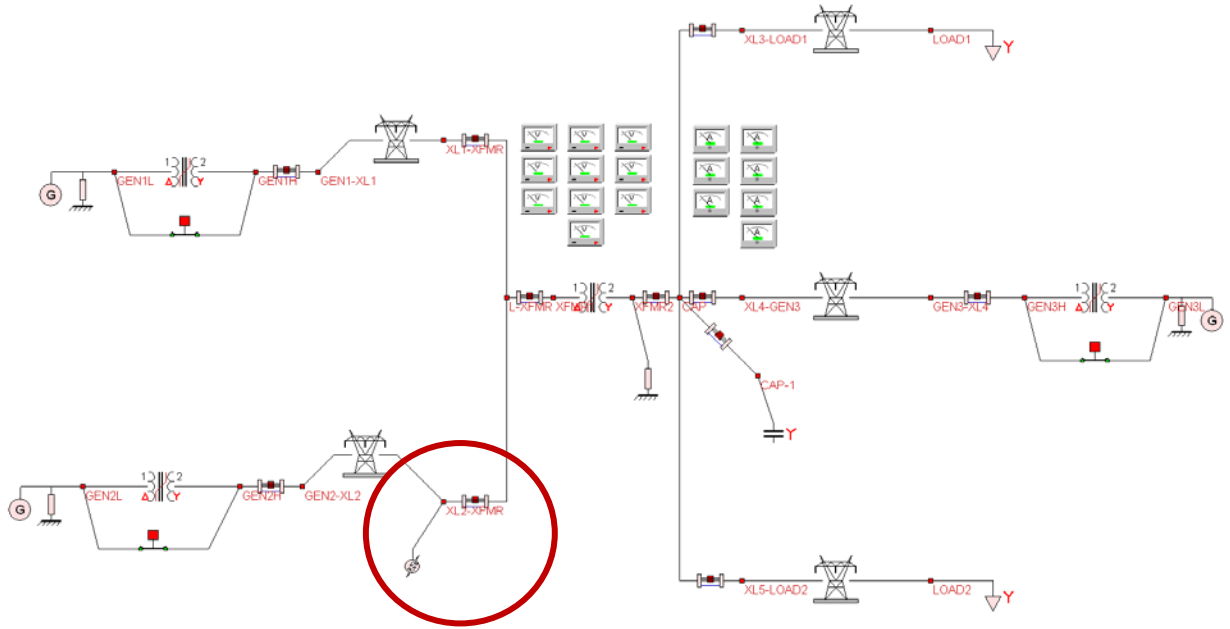


Figure 9.11 Fault Location in the Test System (Through Fault Condition)

A set of measurement signals monitored during the through fault condition is shown in the following figure. The single-phase-to-ground fault is given for 0.05 seconds, starting at 3.20 seconds.

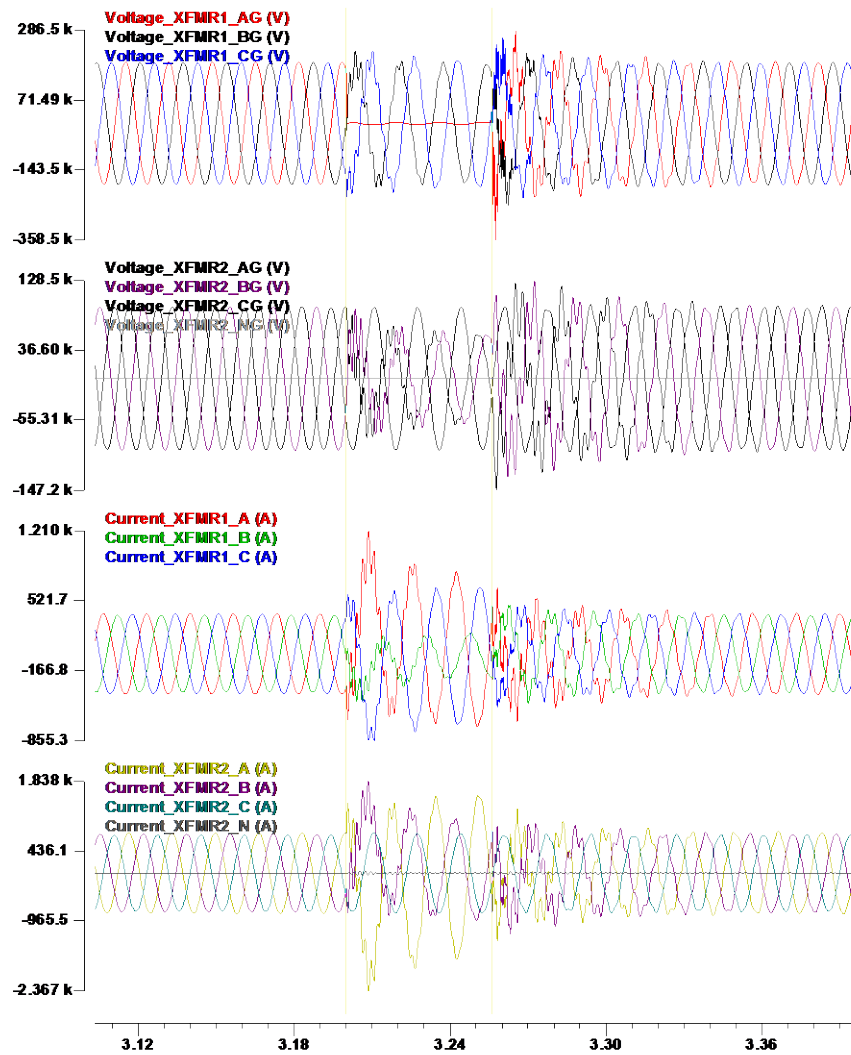


Figure 9.12 Measurement Signals of the Transformer (Through Fault Condition)

9.8.5 Test Scenario 5

For internal fault condition, the test system in Figure 9.6 is used. The single-phase-to-ground fault occurs at the phase-a terminal on the left side of the transformer for 0.05 seconds, and then the fault is cleared. In Figure 9.13 the faulted location is marked with the red circle.

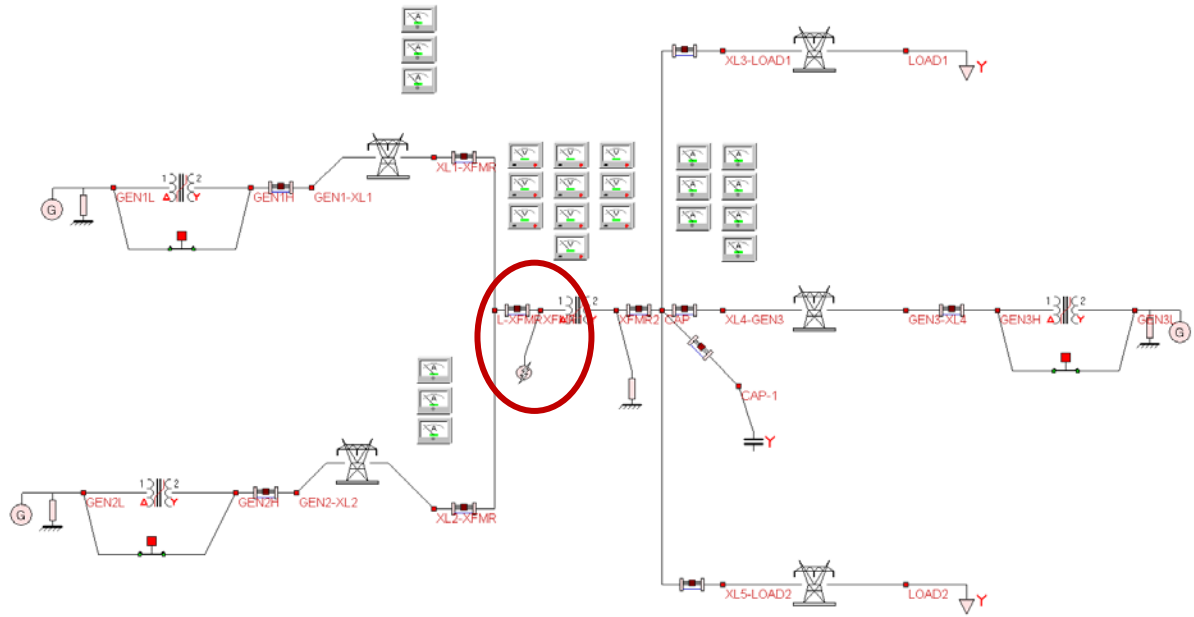


Figure 9.13 Fault Location in the Test System (Internal Fault Condition)

A set of measurement signals monitored during the internal fault condition is shown in the following figure. To simulate the internal fault condition, the single-phase-to-ground fault is given inside the transformer (phase a) for 0.05 seconds, starting at 3.20 seconds.

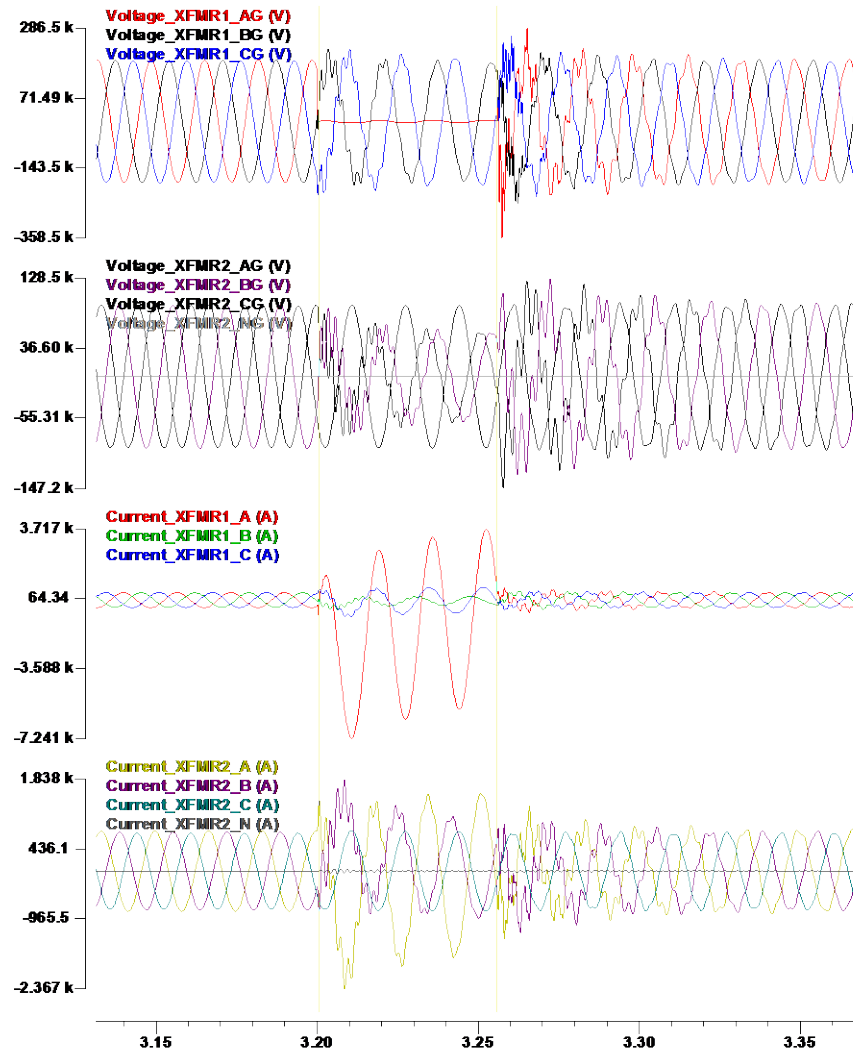


Figure 9.14 Measurement Signals of the Transformer (Internal Fault Condition)

Performance Results for Normal Operating Condition

For the normal operating condition, the confidence level obtained by the developed dynamic state estimator shows the following figures. The result graph shows 100% confidence level all the time, which means that measurements are consistent with the model and there is no fault condition during the simulation.

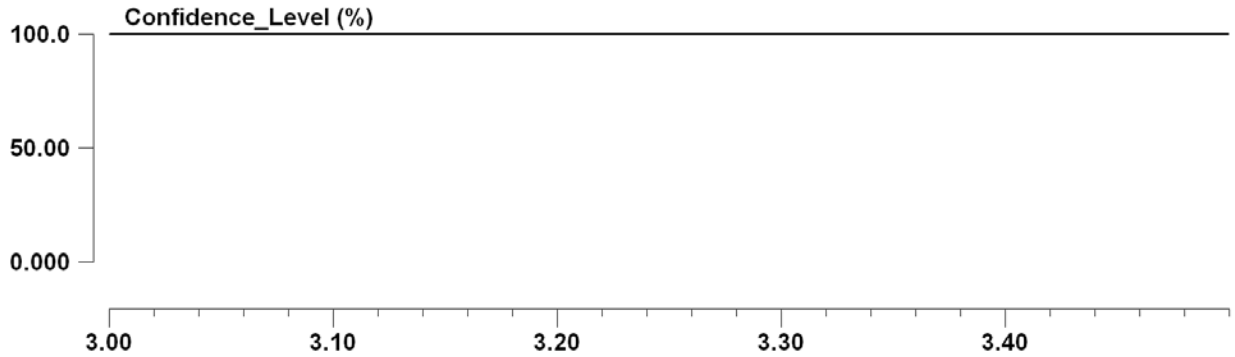


Figure 9.15 Confidence Level of the DSE (Normal Operating Condition)

Performance Results for Transformer Energization (Inrush Current)

For the transformer energization, the confidence level obtained by the developed dynamic state estimator shows the following figures. The result graph shows 100% confidence level all the time, which means that measurements are consistent with the model and there is no fault condition during the simulation.

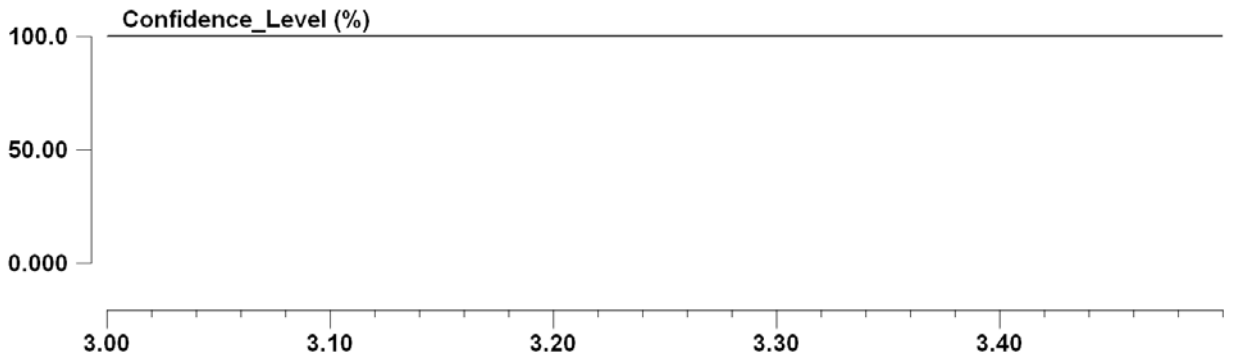


Figure 9.16 Confidence Level of the DSE (Transformer Energization)

Performance Results for Transformer Overexcitation

For the transformer overexcitation, the confidence level obtained by the developed dynamic state estimator shows the following figures. The result graph shows 100% confidence level all the time, which means that measurements are consistent with the model and there is no fault condition during the simulation.

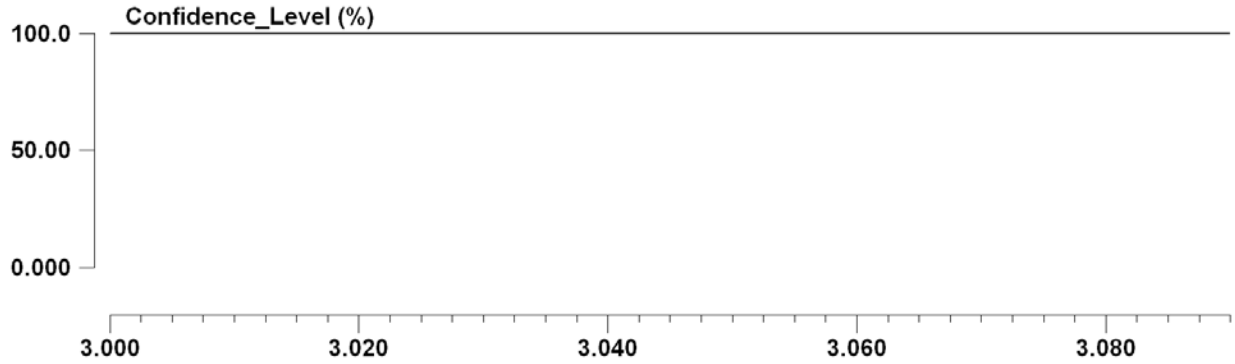


Figure 9.17 Confidence Level of the DSE (Transformer Overexcitation)

Performance Results for Through Fault Condition

For the through fault condition, the confidence level obtained by the developed dynamic state estimator shows the following figures. The result graph shows 100% confidence level all the time, which means that measurements are consistent with the model and there is no fault condition during the simulation.

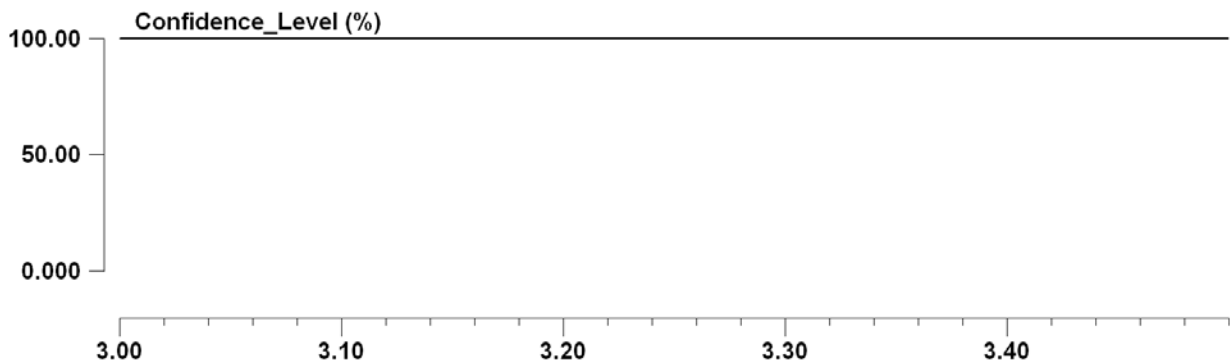


Figure 9.18 Confidence Level of the DSE (Through Fault Condition)

Performance Results for Internal Fault Condition

For the internal fault condition, the confidence level obtained by the developed dynamic state estimator shows the following figures. During most of the time, the confidence level is 100%, which means that measurements are consistent with the model. However, at time 0.2 second indicated by the red cycle, the confidence level drops to 0%, which means that an internal fault has occurred somewhere in the transformer. Then, the confidence level recovers 100% in 0.05s as the transformer returns to the normal operating condition.

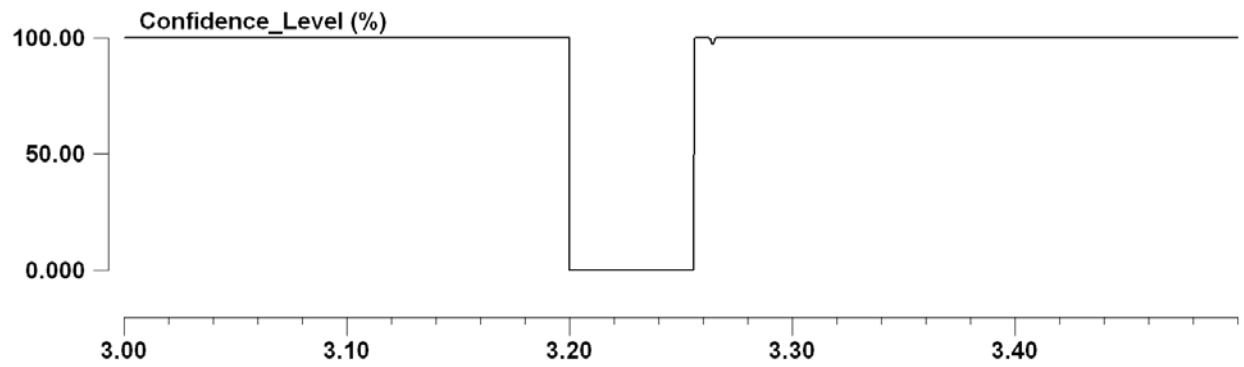


Figure 9.19 Confidence Level of the DSE (Internal Fault Condition)

Note that there is a specific duration in which the confidence level is zero, and therefore, it can be concluded that any internal faults have occurred in the transformer under protection during this period.

References

1. A. P. Sakis Meliopoulos, Anjan Bose, PSERC Publication 10-17, *Substation of the Future: A Feasibility Study*, October 2010.
2. A. P. Meliopoulos, G. Cokkinides, R. Huang, E. Farantatos, S. Choi, Y. Lee , “Wide Area Dynamic Monitoring and Stability Controls”, IREP Symposium 2010, Bulk Power System Dynamics and Control VIII, Buzios, Brazil, August 1-6, 2010.
3. A. P. Sakis Meliopoulos and George Cokkinides, *Power System Relaying: An Introduction, Book in Preparation*, 980 pages.
4. A. P. Sakis Meliopoulos, George Cokkinides, Renke Huang, Evangelos Farantatos, Sungyun Choi, Yonghee Lee and Xuebei Yu, "Smart Grid Technologies for Autonomous Operation and Control", *IEEE Transactions on Smart Grid*, Vol 2, No 1, March 2011.
5. Sungyun Choi, Yonghee Lee, George Cokkinides and A. P. Sakis Meliopoulos, "Transformer Dynamic State Estimation Using Quadratic Integration", *Proceedings of the 2011 Power Systems Conference & Exposition*, Phoenix, AZ, March 20-23, 2011.
6. Sungyun Choi, Yonghee Lee, George Cokkinides, and A. P. Meliopoulos, "Dynamically Adaptive Transformer Protection Using Dynamic State Estimation", *Proceedings of the PAC World Conference 2011*, Dublin, Ireland, June 27-30, 2011.
7. A. P. Sakis Meliopoulos, George Cokkinides, Sungyun Choi, Evangelos Farantatos, Renke Huang and Yonghee Lee, "Symbolic Integration and Autonomous State Estimation: Building Blocks for an Intelligent Power Grid", *Proceedings of the 2011 ISAP*, Xersonissos, Crete, Greece, September 25-28, 2011.
8. M. Kezunovic, “Translational Knowledge: From Collecting Data to Making Decisions in a Smart Grid,” *IEEE Proceedings*, April 2011
9. S. Vasilić, M. Kezunović, “Fuzzy ART Neural Network Algorithm for Classifying the Power System Faults,” *IEEE Transactions on Power Delivery*, Vol. 20, No. 2, pp 1306-1314, April 2005.
10. M. Kezunović, I. Rikalo, “Detect and Classify Faults Using Neural Nets,” *IEEE Computer Applications in Power*, Vol. 9, No. 4, pp 42-47, October 1996.
11. N. Zhang, M. Kezunović, “Transmission Line Boundary Protection Using Wavelet Transform and Neural Network,” *IEEE Transactions on Power Delivery*, Vol. 22, No. 2, pp 859-869, April 2007.
12. N. Zhang and M. Kezunović, “A Real Time Fault Analysis Tool for Monitoring Operation of Transmission Line Protective Relay,” *Electric Power Systems Research Journal*, Vol. 77, No. 3-4, pp 361-370, March 2007.
13. A. P. Sakis Meliopoulos, George Cokkinides, Zhenyu Tan, Sungyun Choi, Yonghee Lee, and Paul Myrda, "Setting-less Protection: Feasibility Study", *Proceedings of the of the 46st Annual Hawaii International Conference on System Sciences*, Maui, HI, January 7-10, 2013.

Appendix 1 Three Phase Capacitor Banks Model Derivation

This section describes the three-phase capacitor banks model for the state estimation based setting-less protection. The SCAQCF model is derived in three parts: (a) the capacitor bank compact model, (b) the capacitor bank quadratized model, (c) the capacitor bank algebraic quadratic companion form model.

A1.1 Compact Model Description

The three phase capacitor banks compact model is presented in this session.

The circuit model of the three phase capacitor bank is shown in Figure A1.1.

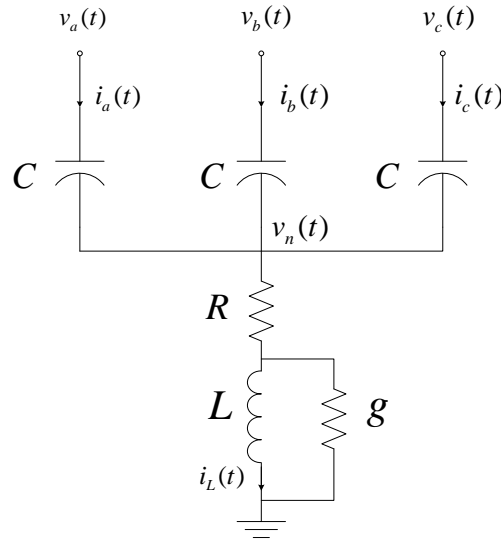


Figure A1.1 Three Phase Capacitor Banks Compact Model

The compact capacitor banks model is derived from this circuit and it is given with the following equations:

$$i_a(t) = C \cdot \frac{d}{dt}(v_a(t) - v_n(t))$$

$$i_b(t) = C \cdot \frac{d}{dt}(v_b(t) - v_n(t))$$

$$i_c(t) = C \cdot \frac{d}{dt}(v_c(t) - v_n(t))$$

$$0 = G \cdot v_n(t) - G \cdot L \cdot \frac{di_L(t)}{dt} - C \cdot \frac{d}{dt}(v_a(t) + v_b(t) + v_c(t) - 3 \cdot v_n(t))$$

$$0 = g \cdot L \cdot \frac{di_L(t)}{dt} - C \cdot \frac{d}{dt}(v_a(t) + v_b(t) + v_c(t) - 3 \cdot v_n(t)) + i_L(t)$$

In compact matrix form, the model is:

$$\begin{bmatrix} i(t) \\ 0 \end{bmatrix} = A \cdot \begin{bmatrix} v(t) \\ i_L(t) \end{bmatrix} + B \cdot \frac{d}{dt} \begin{bmatrix} v(t) \\ i_L(t) \end{bmatrix}$$

$$\text{where: } i(t) = \begin{bmatrix} i_a(t) \\ i_b(t) \\ i_c(t) \end{bmatrix}, \quad v(t) = \begin{bmatrix} v_a(t) \\ v_b(t) \\ v_c(t) \\ v_n(t) \end{bmatrix}$$

$$A = \begin{bmatrix} 0 & 0 & 0 & 0 & 0 \\ 0 & 0 & 0 & 0 & 0 \\ 0 & 0 & 0 & 0 & 0 \\ 0 & 0 & 0 & G & 0 \\ 0 & 0 & 0 & 0 & 1 \end{bmatrix}, \quad B = \begin{bmatrix} C & 0 & 0 & -C & 0 \\ 0 & C & 0 & -C & 0 \\ 0 & 0 & C & -C & 0 \\ -C & -C & -C & 3C & -GL \\ -C & -C & -C & 3C & gL \end{bmatrix}$$

A1.2 Quadratized Model Description

All the terms in the three phase capacitor bank model are linear and quadratic terms. Therefore the quadratized model is identical to the compact model. In compact matrix form, the model is:

$$\begin{bmatrix} i(t) \\ 0 \end{bmatrix} = A \cdot \begin{bmatrix} v(t) \\ i_L(t) \end{bmatrix} + B \cdot \frac{d}{dt} \begin{bmatrix} v(t) \\ i_L(t) \end{bmatrix}$$

$$\text{where: } i(t) = \begin{bmatrix} i_a(t) \\ i_b(t) \\ i_c(t) \end{bmatrix}, \quad v(t) = \begin{bmatrix} v_a(t) \\ v_b(t) \\ v_c(t) \\ v_n(t) \end{bmatrix}$$

$$A = \begin{bmatrix} 0 & 0 & 0 & 0 & 0 \\ 0 & 0 & 0 & 0 & 0 \\ 0 & 0 & 0 & 0 & 0 \\ 0 & 0 & 0 & G & 0 \\ 0 & 0 & 0 & 0 & 1 \end{bmatrix}, \quad B = \begin{bmatrix} C & 0 & 0 & -C & 0 \\ 0 & C & 0 & -C & 0 \\ 0 & 0 & C & -C & 0 \\ -C & -C & -C & 3C & -GL \\ -C & -C & -C & 3C & gL \end{bmatrix}$$

A1.3 SCAQCF Model Description

The state and control algebraic quadratic companion form model of the three phase capacitor bank model is derived after quadratic integration of the quadratized model with a time step h . The result is: (Note that there is no control variable in this model.)

At time t ,

$$\begin{aligned}
 i_a(t) &= -4 \cdot i_a(t_m) + \frac{6}{h} \cdot C \cdot (v_a(t) - v_n(t)) - (i_a(t-h) + \frac{6}{h} \cdot C \cdot (v_a(t-h) - v_n(t-h))) \\
 i_b(t) &= -4 \cdot i_b(t_m) + \frac{6}{h} \cdot C \cdot (v_b(t) - v_n(t)) - (i_b(t-h) + \frac{6}{h} \cdot C \cdot (v_b(t-h) - v_n(t-h))) \\
 i_c(t) &= -4 \cdot i_c(t_m) + \frac{6}{h} \cdot C \cdot (v_c(t) - v_n(t)) - (i_c(t-h) + \frac{6}{h} \cdot C \cdot (v_c(t-h) - v_n(t-h))) \\
 0 &= \frac{h}{6} \cdot G \cdot v_n(t) + \frac{2h}{3} \cdot G \cdot v_n(t_m) - (G \cdot L \cdot i_L(t) + C \cdot (v_a(t) + v_b(t) + v_c(t) - 3 \cdot v_n(t))) \\
 &\quad + (\frac{h}{6} \cdot G \cdot v_n(t-h) + G \cdot L \cdot i_L(t-h) + C \cdot (v_a(t-h) + v_b(t-h) + v_c(t-h) - 3 \cdot v_n(t-h))) \\
 0 &= \frac{h}{6} \cdot i_L(t) + \frac{2h}{3} \cdot i_L(t_m) - (C \cdot (v_a(t) + v_b(t) + v_c(t) - 3 \cdot v_n(t)) - g \cdot L \cdot i_L(t)) \\
 &\quad + (\frac{h}{6} \cdot i_L(t-h) + C \cdot (v_a(t-h) + v_b(t-h) + v_c(t-h) - 3 \cdot v_n(t-h)) - g \cdot L \cdot i_L(t-h))
 \end{aligned}$$

At time t_m ,

$$\begin{aligned}
 i_a(t_m) &= \frac{1}{8} \cdot i_a(t) + \frac{3}{h} \cdot C \cdot (v_a(t_m) - v_n(t_m)) - \frac{3}{h} \cdot (\frac{5h}{24} \cdot i_a(t-h) + C \cdot (v_a(t-h) - v_n(t-h))) \\
 i_b(t_m) &= \frac{1}{8} \cdot i_b(t) + \frac{3}{h} \cdot C \cdot (v_b(t_m) - v_n(t_m)) - \frac{3}{h} \cdot (\frac{5h}{24} \cdot i_b(t-h) + C \cdot (v_b(t-h) - v_n(t-h))) \\
 i_c(t_m) &= \frac{1}{8} \cdot i_c(t) + \frac{3}{h} \cdot C \cdot (v_c(t_m) - v_n(t_m)) - \frac{3}{h} \cdot (\frac{5h}{24} \cdot i_c(t-h) + C \cdot (v_c(t-h) - v_n(t-h))) \\
 0 &= -\frac{h}{24} \cdot G \cdot v_n(t) + \frac{h}{3} \cdot G \cdot v_n(t_m) - (G \cdot L \cdot i_L(t_m) + C \cdot (v_a(t_m) + v_b(t_m) + v_c(t_m) - 3 \cdot v_n(t_m))) \\
 &\quad + (\frac{5h}{24} \cdot G \cdot v_n(t-h) + G \cdot L \cdot i_L(t-h) + C \cdot (v_a(t-h) + v_b(t-h) + v_c(t-h) - 3 \cdot v_n(t-h))) \\
 0 &= -\frac{h}{24} \cdot i_L(t) + \frac{h}{3} \cdot i_L(t_m) - (C \cdot (v_a(t_m) + v_b(t_m) + v_c(t_m) - 3 \cdot v_n(t_m)) - g \cdot L \cdot i_L(t_m)) \\
 &\quad + (\frac{5h}{24} \cdot i_L(t-h) + C \cdot (v_a(t-h) + v_b(t-h) + v_c(t-h) - 3 \cdot v_n(t-h)) - g \cdot L \cdot i_L(t-h))
 \end{aligned}$$

Based on the above equations, it is very easy to write all equations into the following SCAQCF standard syntax:

$$\begin{bmatrix} i(t) \\ 0 \\ i(t_m) \\ 0 \end{bmatrix} = Y_{eq} \begin{bmatrix} v(t) \\ y(t) \\ v(t_m) \\ y(t_m) \end{bmatrix} + \begin{bmatrix} \begin{bmatrix} v(t) \\ y(t) \\ v(t_m) \\ y(t_m) \end{bmatrix}^T \\ \vdots \end{bmatrix} \cdot F_{eq,1} \cdot \begin{bmatrix} v(t) \\ y(t) \\ v(t_m) \\ y(t_m) \end{bmatrix} - b_{eq}$$

For three phase capacitor banks, there are 10 states (5 for time step t and 5 for intermediate time step t_m).

For time step t , the states are listed below.

The states are defined as follows:

External states:

1. $v_a(t)$: terminal voltage at phase A (kV);
2. $v_b(t)$: terminal voltage at phase B (kV);
3. $v_c(t)$: terminal voltage at phase C (kV)

Internal states:

1. $v_n(t)$: terminal voltage at neutral point (kV)
2. $i_L(t)$: current through the inductance (kA)

For time step t_m , the states are the same.

Appendix 2 Saturable Core Reactor Model Derivation

This section describes the single phase saturable reactor model for the state estimation based setting-less protection. The AQCF model is derived in 3 parts: (a) the reactor compact model, (b) the saturable core reactor quadratized model, (c) the SCAQCF Model

A2.1 Compact Model Description

The circuit model of the single phase reactor is shown in Figure A2.1. Note that in Figure A2-1, g_L is the conductance that models the core losses. In this section, “numerical stabilizers” have been included to eliminate possible numerical problems caused by the numerical integration rule. In Figure A2.1, g_c is the conductance of the “stabilizer”.

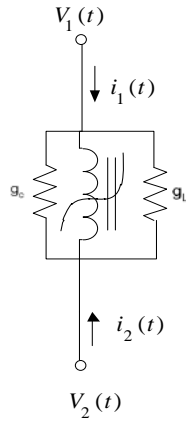


Figure A2.1 Single Phase Reactor Model

In compact form the model becomes:

$$\begin{aligned}
 i_1(t) &= i_0 \cdot \left| \frac{\lambda_1(t)}{\lambda_0} \right|^n \cdot \text{sign}(\lambda_1(t)) + (g_L + g_c) \cdot (v_1(t) - v_2(t)) \\
 i_2(t) &= -i_0 \cdot \left| \frac{\lambda_1(t)}{\lambda_0} \right|^n \cdot \text{sign}(\lambda_1(t)) - (g_L + g_c) \cdot (v_1(t) - v_2(t)) \\
 0 &= \frac{d\lambda_1(t)}{dt} - v_1(t) + v_2(t)
 \end{aligned}$$

where the i_0 is the current constant and λ_0 is the flux constant.

A2.2 Quadratized Model Description

In this proposed formulation there are no nonlinearities in the dynamic part of the model. That is, all nonlinearities can be moved to the algebraic part of the model by the introduction of additional appropriate state variables. Also note that the nonlinear equations are of degree no more than two (at most quadratic equations) which is also achieved by the introduction of additional appropriate state variables. Assumption (just for now): n is odd. (It will be removed in the future).

The model is quadratized by introducing additional internal state variables, so that the n -th exponent is replaced by equations of at most quadratic degree. Since the exact degree of nonlinearity is not known until the user specifies it, the model performs automatic quadratization of the equations. A special procedure is used, so that the model is quadratized using the minimum number of additional internal states. The methodology is based on expressing the exponent in binary form. The binary representation provides all the information about the number of new variables and equations that need to be introduced and about the form of the equations (products of new variables). As an example, the exponent n is defined to be 11 so that the $n+1$ -th exponent is even, which makes the term $\left[\text{sign}(\lambda_a(t)) \right]^{n+1}$ to be 1. Following this procedure the model is converted into the standard quadratized form:

$$\begin{aligned} i_1(t) &= \frac{i_0}{|\lambda_0|^{11}} \cdot y_5(t) + (g_L + g_C) \cdot (v_1(t) - v_2(t)) \\ i_2(t) &= -\frac{i_0}{|\lambda_0|^{11}} \cdot y_5(t) - (g_L + g_C) \cdot (v_1(t) - v_2(t)) \\ 0 &= \frac{d\lambda_1(t)}{dt} - v_1(t) + v_2(t) \\ 0 &= y_1(t) - \lambda_1(t)^2 \\ 0 &= y_2(t) - y_1(t)^2 \\ 0 &= y_3(t) - y_2(t)^2 \\ 0 &= y_4(t) - y_3(t) \cdot y_1(t) \\ 0 &= y_5(t) - y_4(t) \cdot \lambda_1(t) \end{aligned}$$

Above equations are written in compact matrix form as:

$$\begin{bmatrix} i(t) \\ 0 \end{bmatrix} = Y_{eq} \cdot \begin{bmatrix} v(t) \\ y(t) \end{bmatrix} + B \cdot \frac{d}{dt} \cdot \begin{bmatrix} v(t) \\ y(t) \end{bmatrix} + \begin{bmatrix} [v^T(t) \quad y^T(t)] \cdot F_{eq1(8 \times 8)} \cdot \begin{bmatrix} v(t) \\ y(t) \end{bmatrix} \\ \vdots \\ [v^T(t) \quad y^T(t)] \cdot F_{eq8(8 \times 8)} \cdot \begin{bmatrix} v(t) \\ y(t) \end{bmatrix} \end{bmatrix}$$

$$\text{where: } i(t) = \begin{bmatrix} i_1(t) \\ i_2(t) \end{bmatrix}, v(t) = \begin{bmatrix} v_1(t) \\ v_2(t) \end{bmatrix}, y(t) = \begin{bmatrix} \lambda_1(t) \\ y_1(t) \\ y_2(t) \\ y_3(t) \\ y_4(t) \\ y_5(t) \end{bmatrix}$$

$$Y_{eq} = \begin{bmatrix} g_L + g_C & -g_L - g_C & 0 & 0 & 0 & 0 & 0 & \frac{i_0}{|\lambda_0|^{11}} \\ -g_L - g_C & g_L + g_C & 0 & 0 & 0 & 0 & 0 & -\frac{i_0}{|\lambda_0|^{11}} \\ -1 & 1 & 0 & 0 & 0 & 0 & 0 & 0 \\ 0 & 0 & 0 & 1 & 0 & 0 & 0 & 0 \\ 0 & 0 & 0 & 0 & 1 & 0 & 0 & 0 \\ 0 & 0 & 0 & 0 & 0 & 1 & 0 & 0 \\ 0 & 0 & 0 & 0 & 0 & 0 & 1 & 0 \\ 0 & 0 & 0 & 0 & 0 & 0 & 0 & 1 \end{bmatrix}$$

$$B = \begin{bmatrix} 0 & 0 & 0 & 0 & 0 & 0 & 0 & 0 \\ 0 & 0 & 0 & 0 & 0 & 0 & 0 & 0 \\ 0 & 0 & 1 & 0 & 0 & 0 & 0 & 0 \\ 0 & 0 & 0 & 0 & 0 & 0 & 0 & 0 \\ 0 & 0 & 0 & 0 & 0 & 0 & 0 & 0 \\ 0 & 0 & 0 & 0 & 0 & 0 & 0 & 0 \\ 0 & 0 & 0 & 0 & 0 & 0 & 0 & 0 \\ 0 & 0 & 0 & 0 & 0 & 0 & 0 & 0 \end{bmatrix}$$

$$F_{eq1} = \dots = F_{eq3} = 0_{8 \times 8}$$

$$F_{eq4}: f_{eq[3 \times 3]} = -1, \quad \text{other elements are 0}$$

$$F_{eq5}: f_{eq[4 \times 4]} = -1, \quad \text{other elements are 0}$$

$$F_{eq6}: f_{eq[5 \times 5]} = -1, \quad \text{other elements are 0}$$

$$F_{eq7}: f_{eq[6 \times 4]} = -1, \quad \text{other elements are 0}$$

$$F_{eq8}: f_{eq[7 \times 3]} = -1, \quad \text{other elements are 0}$$

A2.3 SCAQCF Model Description

For the setting-less protection algorithm the equations for the saturable core reactor must be written in the algebraic quadratic companion form. By integrating the quadratized equation using the quadratic integration method with a time step h , the saturable core reactors model is obtained in the following form :

At time t ,

$$\begin{aligned}
 i_1(t) &= \frac{i_0}{|\lambda_0|^{11}} \cdot y_5(t) + g_L \cdot (v_1(t) - v_2(t)) \\
 i_2(t) &= -\frac{i_0}{|\lambda_0|^{11}} \cdot y_5(t) - g_L \cdot (v_1(t) - v_2(t)) \\
 0 &= \lambda_1(t) - \lambda_1(t-h) - \frac{h}{6}(v_1(t) - v_2(t)) - \frac{2h}{3}(v_1(t_m) - v_2(t_m)) \\
 &\quad - \frac{h}{6}(v_1(t-h) - v_2(t-h)) \\
 0 &= y_1(t) - \lambda_1(t)^2 \\
 0 &= y_2(t) - y_1(t)^2 \\
 0 &= y_3(t) - y_2(t)^2 \\
 0 &= y_4(t) - y_3(t) \cdot y_1(t) \\
 0 &= y_5(t) - y_4(t) \cdot \lambda_1(t)
 \end{aligned}$$

At time t_m ,

$$\begin{aligned}
 i_1(t_m) &= \frac{i_0}{|\lambda_0|^{11}} \cdot y_5(t_m) + g_L \cdot (v_1(t_m) - v_2(t_m)) \\
 i_2(t_m) &= -\frac{i_0}{|\lambda_0|^{11}} \cdot y_5(t_m) - g_L \cdot (v_1(t_m) - v_2(t_m)) \\
 0 &= \lambda_1(t_m) - \lambda_1(t-h) + \frac{h}{24}(v_1(t) - v_2(t)) - \frac{h}{3}(v_1(t_m) - v_2(t_m)) \\
 &\quad - \frac{5h}{24}(v_1(t-h) - v_2(t-h)) \\
 0 &= y_1(t_m) - \lambda_1(t_m)^2 \\
 0 &= y_2(t_m) - y_1(t_m)^2 \\
 0 &= y_3(t_m) - y_2(t_m)^2 \\
 0 &= y_4(t_m) - y_3(t_m) \cdot y_1(t_m) \\
 0 &= y_5(t_m) - y_4(t_m) \cdot \lambda_1(t_m)
 \end{aligned}$$

The algebraic quadratic companion form model of single phase reactor can be formulated as:

$$\begin{bmatrix} i(t) \\ 0 \\ i(t_m) \\ 0 \end{bmatrix} = Y_{eq} \cdot \begin{bmatrix} v(t) \\ y(t) \\ v(t_m) \\ y(t_m) \end{bmatrix} + \begin{bmatrix} [v^T(t) \quad y^T(t) \quad v^T(t_m) \quad y^T(t_m)] \cdot F_{eq1(16 \times 16)} \cdot \begin{bmatrix} v(t) \\ y(t) \\ v(t_m) \\ y(t_m) \end{bmatrix} \\ \vdots \\ [v^T(t) \quad y^T(t) \quad v^T(t_m) \quad y^T(t_m)] \cdot F_{eq16(16 \times 16)} \cdot \begin{bmatrix} v(t) \\ y(t) \\ v(t_m) \\ y(t_m) \end{bmatrix} \end{bmatrix} + B \cdot \begin{bmatrix} v(t-h) \\ y(t-h) \end{bmatrix}$$

where:

$$i(t) = \begin{bmatrix} i_1(t) \\ i_2(t) \end{bmatrix}, v(t) = \begin{bmatrix} v_1(t) \\ v_2(t) \end{bmatrix}, v(t-h) = \begin{bmatrix} v_1(t-h) \\ v_2(t-h) \end{bmatrix}, y(t) = \begin{bmatrix} \lambda_1(t) \\ y_1(t) \\ y_2(t) \\ y_3(t) \\ y_4(t) \\ y_5(t) \end{bmatrix}$$

$$y(t-h) = [\lambda_1(t-h)],$$

$$Y_{eq} = \begin{bmatrix} g_L & -g_L & 0 & 0 & 0 & 0 & 0 & \frac{i_0}{|\lambda_0|^{11}} & 0 & 0 & 0 & 0 & 0 & 0 & 0 \\ -g_L & g_L & 0 & 0 & 0 & 0 & 0 & -\frac{i_0}{|\lambda_0|^{11}} & 0 & 0 & 0 & 0 & 0 & 0 & 0 \\ -\frac{h}{6} & \frac{h}{6} & 1 & 0 & 0 & 0 & 0 & 0 & -\frac{2h}{3} & \frac{2h}{3} & 0 & 0 & 0 & 0 & 0 \\ 0 & 0 & 0 & 1 & 0 & 0 & 0 & 0 & 0 & 0 & 0 & 0 & 0 & 0 & 0 \\ 0 & 0 & 0 & 0 & 1 & 0 & 0 & 0 & 0 & 0 & 0 & 0 & 0 & 0 & 0 \\ 0 & 0 & 0 & 0 & 0 & 1 & 0 & 0 & 0 & 0 & 0 & 0 & 0 & 0 & 0 \\ 0 & 0 & 0 & 0 & 0 & 0 & 1 & 0 & 0 & 0 & 0 & 0 & 0 & 0 & 0 \\ 0 & 0 & 0 & 0 & 0 & 0 & 0 & 1 & 0 & 0 & 0 & 0 & 0 & 0 & 0 \\ 0 & 0 & 0 & 0 & 0 & 0 & 0 & 0 & g_L & -g_L & 0 & 0 & 0 & 0 & \frac{i_0}{|\lambda_0|^{11}} \\ 0 & 0 & 0 & 0 & 0 & 0 & 0 & 0 & -g_L & g_L & 0 & 0 & 0 & 0 & -\frac{i_0}{|\lambda_0|^{11}} \\ \frac{h}{24} & -\frac{h}{24} & 0 & 0 & 0 & 0 & 0 & 0 & -\frac{h}{3} & \frac{h}{3} & 1 & 0 & 0 & 0 & 0 \\ 0 & 0 & 0 & 0 & 0 & 0 & 0 & 0 & 0 & 0 & 0 & 1 & 0 & 0 & 0 \\ 0 & 0 & 0 & 0 & 0 & 0 & 0 & 0 & 0 & 0 & 0 & 0 & 1 & 0 & 0 \\ 0 & 0 & 0 & 0 & 0 & 0 & 0 & 0 & 0 & 0 & 0 & 0 & 0 & 1 & 0 \\ 0 & 0 & 0 & 0 & 0 & 0 & 0 & 0 & 0 & 0 & 0 & 0 & 0 & 0 & 1 \end{bmatrix}$$

$$B_{16 \times 3} = \begin{bmatrix} 0_{2 \times 3} \\ B_{1(1 \times 3)} \\ 0_{7 \times 3} \\ B_{2(1 \times 3)} \\ 0_{5 \times 3} \end{bmatrix}$$

$$B_1 = \begin{bmatrix} -\frac{h}{6} & \frac{h}{6} & -1 \end{bmatrix}$$

$$B_2 = \begin{bmatrix} -\frac{5h}{24} & \frac{5h}{24} & -1 \end{bmatrix}$$

$$\begin{aligned}
F_{eq1} &= \dots = F_{eq3} = 0_{16 \times 16} \\
F_{eq4}: f_{eq[3 \times 3]} &= -1, & \text{other elements are 0} \\
F_{eq5}: f_{eq[4 \times 4]} &= -1, & \text{other elements are 0} \\
F_{eq6}: f_{eq[5 \times 5]} &= -1, & \text{other elements are 0} \\
F_{eq7}: f_{eq[6 \times 4]} &= -1, & \text{other elements are 0} \\
F_{eq8}: f_{eq[7 \times 3]} &= -1, & \text{other elements are 0}
\end{aligned}$$

$$\begin{aligned}
F_{eq9} &= \dots = F_{eq11} = 0_{16 \times 16} \\
F_{eq12}: f_{eq[11 \times 11]} &= -1, & \text{other elements are 0} \\
F_{eq13}: f_{eq[12 \times 12]} &= -1, & \text{other elements are 0} \\
F_{eq14}: f_{eq[13 \times 13]} &= -1, & \text{other elements are 0} \\
F_{eq15}: f_{eq[14 \times 12]} &= -1, & \text{other elements are 0} \\
F_{eq16}: f_{eq[15 \times 11]} &= -1, & \text{other elements are 0}
\end{aligned}$$

Appendix 3 Transformer Model Derivation

This appendix describes the three-phase, two-winding, variable-tap, and saturable-core transformer. The development proceeds as follows: first, the basic mathematical model of the single-phase transformer model is presented as a compact model. Subsequently, the model is quadratized and then integrated with the quadratic integration method. The resulting model of the quadratic integration, referred to as the SCAQCF model, is cast into the standard syntax. Finally, three single-phase models are integrated into one SCAQCF model of the three-phase transformer.

The transformer under protection contains non-linear characteristics between the magnetizing current and the flux linkage of the transformer core, which is described by the following polynomial function with high degrees:

$$i_m(t) = i_0 \left| \frac{\lambda(t)}{\lambda_0} \right|^n \text{sign}(\lambda(t))$$

where $i_m(t)$ is the magnetizing current, $\lambda(t)$ the magnetic flux linkage, i_0 and λ_0 constants, $\text{sign}()$ a sign function, and n an exponent.

A3.1 Single-Phase Transformer Compact Model Description

To derive device model of the three-phase transformer, at first, we need to derive state space equations for the single-phase model. For this purpose, the equivalent circuit for the practical single-phase transformer is described in Figure A3.1. The loss in the primary winding occurs at the resistance r_1 in series with the primary winding. Similarly, the resistance r_2 accounts for the loss in the secondary winding. Two inductances, L_1 and L_2 , represent the magnetic flux leakage of the primary and secondary winding, respectively. The shunt core resistance r_c characterizes the core loss, and both the shunt inductance L_m and the magnetizing current $i_m(t)$ represent the reactive power loss in the magnetizing core.

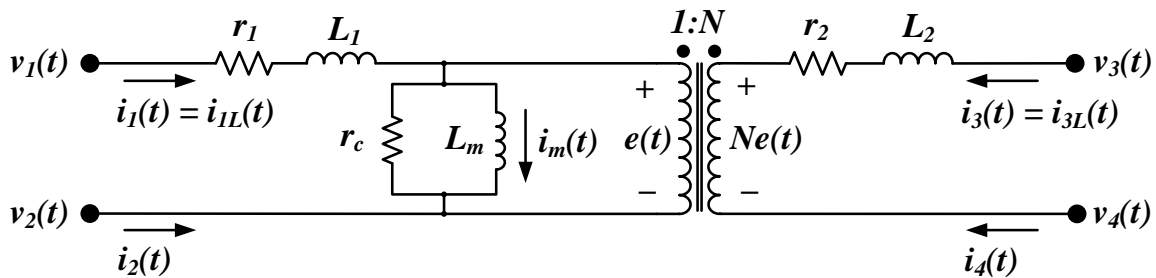


Figure A3.1 Single-phase Transformer Model under Protection

Circuit analysis can describe the single-phase transformer model, yielding the following equations:

$$i_1(t) = i_{1L}(t) \quad (\text{A3.1})$$

$$i_1(t) + i_2(t) = 0 \quad (\text{A3.2})$$

$$i_3(t) = i_{3L}(t) \quad (\text{A3.3})$$

$$i_3(t) + i_4(t) = 0 \quad (\text{A3.4})$$

$$r_c i_1(t) + r_c N i_3(t) = r_c i_m(t) + e(t) \quad (\text{A3.5})$$

$$i_m(t) = i_0 \left(\frac{\lambda(t)}{\lambda_0} \right)^5 \quad (\text{A3.6})$$

$$v_1(t) - v_2(t) = r_1 i_{1L}(t) + L_1 \frac{d}{dt} i_{1L}(t) + e(t) \quad (\text{A3.7})$$

$$v_3(t) - v_4(t) = r_2 i_{3L}(t) + L_2 \frac{d}{dt} i_{3L}(t) + Ne(t) \quad (\text{A3.8})$$

$$e(t) = \frac{d}{dt} \lambda(t) \quad (\text{A3.9})$$

Above equations can be rearranged as follows:

$$i_1(t) = i_{1L}(t) \quad (\text{A3.10})$$

$$i_1(t) + i_2(t) = 0 \quad (\text{A3.11})$$

$$i_3(t) = i_{3L}(t) \quad (\text{A3.12})$$

$$i_3(t) + i_4(t) = 0 \quad (\text{A3.13})$$

$$r_c i_1(t) + r_c N i_3(t) = r_c i_m(t) + e(t) \quad (\text{A3.14})$$

$$0 = i_m(t) - i_0 \left(\frac{\lambda(t)}{\lambda_0} \right)^5 \quad (\text{A3.15})$$

$$v_1(t) - v_2(t) = r_1 i_{1L}(t) + L_1 \frac{d}{dt} i_{1L}(t) + e(t) \quad (\text{A3.16})$$

$$v_3(t) - v_4(t) = r_2 i_{3L}(t) + L_2 \frac{d}{dt} i_{3L}(t) + Ne(t) \quad (\text{A3.17})$$

$$0 = e(t) - \frac{d}{dt} \lambda(t) \quad (\text{A3.18})$$

Based on the above equations, state variables can be determined as follows:

$$s_{1\phi}(t) = [v_1(t), v_2(t), v_3(t), v_4(t), i_m(t), e(t), \lambda(t), i_{1L}(t), i_{3L}(t)]^T \quad (\text{A3.19})$$

where $s_{1\phi}(t)$ is the vector of state variables without introducing additional state variables for nonlinear terms. However, the high-order nonlinear term in equation (A3.15) needs to be quadratized into several non-linear terms whose order is at most two, thereby introducing additional state variables and equations.

A3.2 Single-Phase Transformer Quadratized Model Description

The single-phase transformer model is non-linear. Therefore, the model should be quadratized by introducing additional state variables. The final quadratized model, for an exponent $n = 5$, is provided below. Note that only the 10th, 11th, and 12th equations are quadratic.

$$i_1(t) = i_{1L}(t) \quad (\text{A3.1})$$

$$i_1(t) + i_2(t) = 0 \quad (\text{A3.2})$$

$$i_3(t) = i_{3L}(t) \quad (\text{A3.3})$$

$$i_3(t) + i_4(t) = 0 \quad (\text{A3.4})$$

$$r_c i_1(t) + r_c N i_3(t) = r_c i_m(t) + e(t) \quad (\text{A3.5})$$

$$0 = i_m(t) - z(t) \quad (\text{A3.6})$$

$$0 = v_1(t) - v_2(t) - e(t) - r_1 i_{1L}(t) - L_1 \frac{d}{dt} i_{1L}(t) \quad (\text{A3.7})$$

$$0 = v_3(t) - v_4(t) - N \cdot e(t) - r_2 i_{3L}(t) - L_2 \frac{d}{dt} i_{3L}(t) \quad (\text{A3.8})$$

$$0 = e(t) - \frac{d}{dt} \lambda(t) \quad (\text{A3.9})$$

$$0 = y_1(t) - \left(\frac{\lambda(t)}{\lambda_0} \right)^2 \quad (\text{A3.10})$$

$$0 = y_2(t) - y_1(t)^2 \quad (\text{A3.11})$$

$$0 = y_3(t) - y_2(t) \cdot \frac{\lambda(t)}{\lambda_0} \quad (\text{A3.12})$$

$$0 = -i_0 y_3(t) + z(t) \quad (\text{A3.13})$$

The state of the single-phase transformer is defined as follows:

$$x_{1\phi}(t) = [v_1(t), v_2(t), v_3(t), v_4(t), i_m(t), e(t), \lambda(t), i_{1L}(t), i_{3L}(t), y_1(t), y_2(t), y_3(t), z(t)]^T \quad (\text{A3.14})$$

where $x_{1\phi}(t)$ is the vector of state variables with quadratized, sing-phase transformer model. The equations that describe the single-phase transformer can be written simply in the algebraic companion form (ACF) as follows:

$$X_1 \cdot i_{1\phi}(t) = X_2 \cdot x_{1\phi}(t) + X_3 \frac{d}{dt} x_{1\phi}(t) + f(t) \quad (\text{A3.15})$$

$$f(t) = \begin{bmatrix} x_{1\phi}(t)^T \cdot Q_1 \cdot x_{1\phi}(t) \\ x_{1\phi}(t)^T \cdot Q_2 \cdot x_{1\phi}(t) \\ \vdots \\ x_{1\phi}(t)^T \cdot Q_{13} \cdot x_{1\phi}(t) \end{bmatrix} \quad (\text{A3.16})$$

where

$$i_{1\phi}(t) = [i_1(t), i_2(t), i_3(t), i_4(t), 0, 0, 0, 0, 0, 0, 0, 0]^T \quad (\text{A3.17})$$

$$Q_{11} = \text{diag}([0, 0, 0, 0, 0, 0, 0, 0, 0, -1, 0, 0, 0]) \quad (\text{A3.23})$$

$$Q_{12} = \begin{bmatrix} 0 & 0 & 0 & 0 & 0 & 0 & 0 & 0 & 0 & 0 & 0 & 0 & 0 \\ 0 & 0 & 0 & 0 & 0 & 0 & 0 & 0 & 0 & 0 & 0 & 0 & 0 \\ 0 & 0 & 0 & 0 & 0 & 0 & 0 & 0 & 0 & 0 & 0 & 0 & 0 \\ 0 & 0 & 0 & 0 & 0 & 0 & 0 & 0 & 0 & 0 & 0 & 0 & 0 \\ 0 & 0 & 0 & 0 & 0 & 0 & 0 & 0 & 0 & 0 & 0 & 0 & 0 \\ 0 & 0 & 0 & 0 & 0 & 0 & 0 & 0 & 0 & 0 & 0 & 0 & 0 \\ 0 & 0 & 0 & 0 & 0 & 0 & 0 & 0 & 0 & 0 & -1/\lambda_0 & 0 & 0 \\ 0 & 0 & 0 & 0 & 0 & 0 & 0 & 0 & 0 & 0 & 0 & 0 & 0 \\ 0 & 0 & 0 & 0 & 0 & 0 & 0 & 0 & 0 & 0 & 0 & 0 & 0 \\ 0 & 0 & 0 & 0 & 0 & 0 & 0 & 0 & 0 & 0 & 0 & 0 & 0 \\ 0 & 0 & 0 & 0 & 0 & 0 & 0 & 0 & 0 & 0 & 0 & 0 & 0 \\ 0 & 0 & 0 & 0 & 0 & 0 & 0 & 0 & 0 & 0 & 0 & 0 & 0 \\ 0 & 0 & 0 & 0 & 0 & 0 & 0 & 0 & 0 & 0 & 0 & 0 & 0 \end{bmatrix} \quad (\text{A3.24})$$

Equation (A3.15) can be solved for $i_{1\phi}(t)$ using row operations, eventually being rearranged as follows:

$$i_{1\phi}(t) = A \cdot x_{1\phi}(t) + B \frac{d}{dt} x_{1\phi}(t) + f(t) \quad (\text{A3.25})$$

where

$$A = Y \cdot X_2 \quad (\text{A3.26})$$

$$B = Y \cdot X_3 \quad (\text{A3.27})$$

$$Y = \begin{bmatrix} 1 & 0 & 0 & 0 & 0 & 0 & 0 & 0 & 0 & 0 & 0 & 0 & 0 \\ -1 & 1 & 0 & 0 & 0 & 0 & 0 & 0 & 0 & 0 & 0 & 0 & 0 \\ 0 & 0 & 1 & 0 & 0 & 0 & 0 & 0 & 0 & 0 & 0 & 0 & 0 \\ 0 & 0 & -1 & 1 & 0 & 0 & 0 & 0 & 0 & 0 & 0 & 0 & 0 \\ -r_c & 0 & -r_c N & 0 & 1 & 0 & 0 & 0 & 0 & 0 & 0 & 0 & 0 \\ 0 & 0 & 0 & 0 & 0 & 1 & 0 & 0 & 0 & 0 & 0 & 0 & 0 \\ 0 & 0 & 0 & 0 & 0 & 0 & 1 & 0 & 0 & 0 & 0 & 0 & 0 \\ 0 & 0 & 0 & 0 & 0 & 0 & 0 & 1 & 0 & 0 & 0 & 0 & 0 \\ 0 & 0 & 0 & 0 & 0 & 0 & 0 & 0 & 1 & 0 & 0 & 0 & 0 \\ 0 & 0 & 0 & 0 & 0 & 0 & 0 & 0 & 0 & 1 & 0 & 0 & 0 \\ 0 & 0 & 0 & 0 & 0 & 0 & 0 & 0 & 0 & 0 & 1 & 0 & 0 \\ 0 & 0 & 0 & 0 & 0 & 0 & 0 & 0 & 0 & 0 & 0 & 1 & 0 \\ 0 & 0 & 0 & 0 & 0 & 0 & 0 & 0 & 0 & 0 & 0 & 0 & 1 \end{bmatrix} \quad (\text{A3.28})$$

A3.3 Single-Phase Transformer SCAQCF Model Description

To derive the SCAQCF of the single-phase transformer model, the differential equations in equation (A3.25) should be integrated using the quadratic integration method with the integration time step, h . Note that in equation (A3.25), only the seventh-, eighth-, and ninth-row equations, which are the differential equations, (A3.7), (A3.8), and (A3.9), have differential terms, so they should be integrated quadratically. As a result, the AQCF of the single-phase transformer is obtained as follows:

$$\begin{bmatrix} i_{1\phi}(t) \\ i_{1\phi}(t_m) \end{bmatrix} = L \begin{bmatrix} x_{1\phi}(t) \\ x_{1\phi}(t_m) \end{bmatrix} - N \cdot x_{1\phi}(t-h) + \begin{bmatrix} f(t) \\ f(t_m) \end{bmatrix} \quad (\text{A3.1})$$

where

$$L = \begin{bmatrix} A_1 & 0 \\ \frac{h}{6}A_2 + B_2 & \frac{2h}{3}A_2 \\ A_3 & 0 \\ 0 & A_1 \\ -\frac{h}{24}A_2 & \frac{h}{3}A_2 + B_2 \\ 0 & A_3 \end{bmatrix} \quad (\text{A3.2})$$

$$N = \begin{bmatrix} 0 \\ -\frac{h}{6}A_2 + B_2 \\ 0 \\ 0 \\ -\frac{5h}{24}A_2 + B_2 \\ 0 \end{bmatrix} \quad (\text{A3.3})$$

A_1 is the first six rows of the matrix A , A_2 is the 7th to 9th rows of the matrix A , A_3 is the 10th to 13th rows of the matrix A , and B_2 is the 7th to 9th rows of matrix B .

A3.4 Three-Phase Transformer SCAQCF Model Description

The AQCF of the three-phase, delta-wye-connected transformer can be derived by integrating three AQCFs of the single-phase transformer model as shown in Figure A3.2.

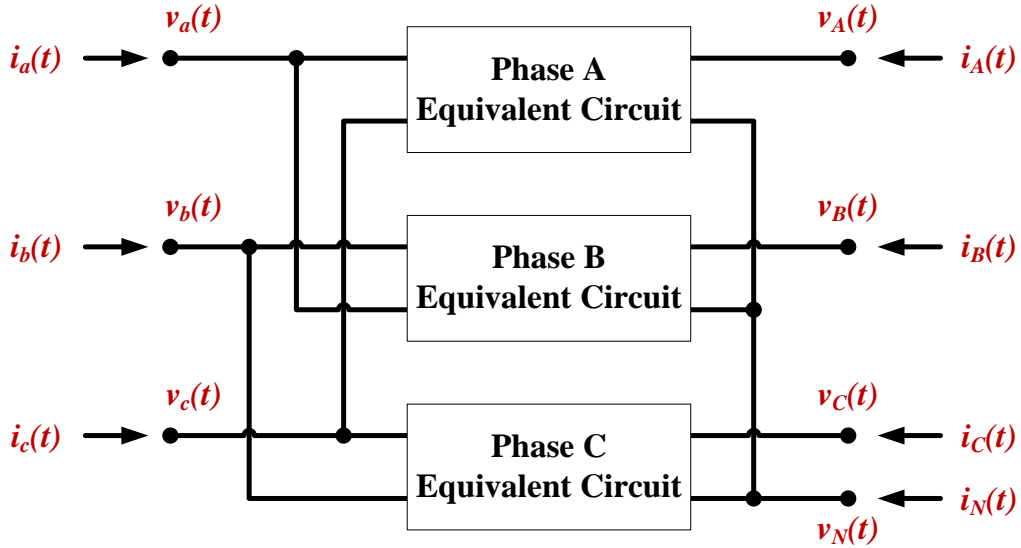


Figure A3.2 Delta-wye Connection of Three Single-phase Transformers

In order to integrate three SCAQCFs, the pointers of the single-phase SCAQCF need to be re-assigned to those of three-phase SCAQCF. Figure A3.3 shows the pointer mapping of external and internal states between single-phase SCAQCF and three-phase, delta-wye connected SCAQCF:

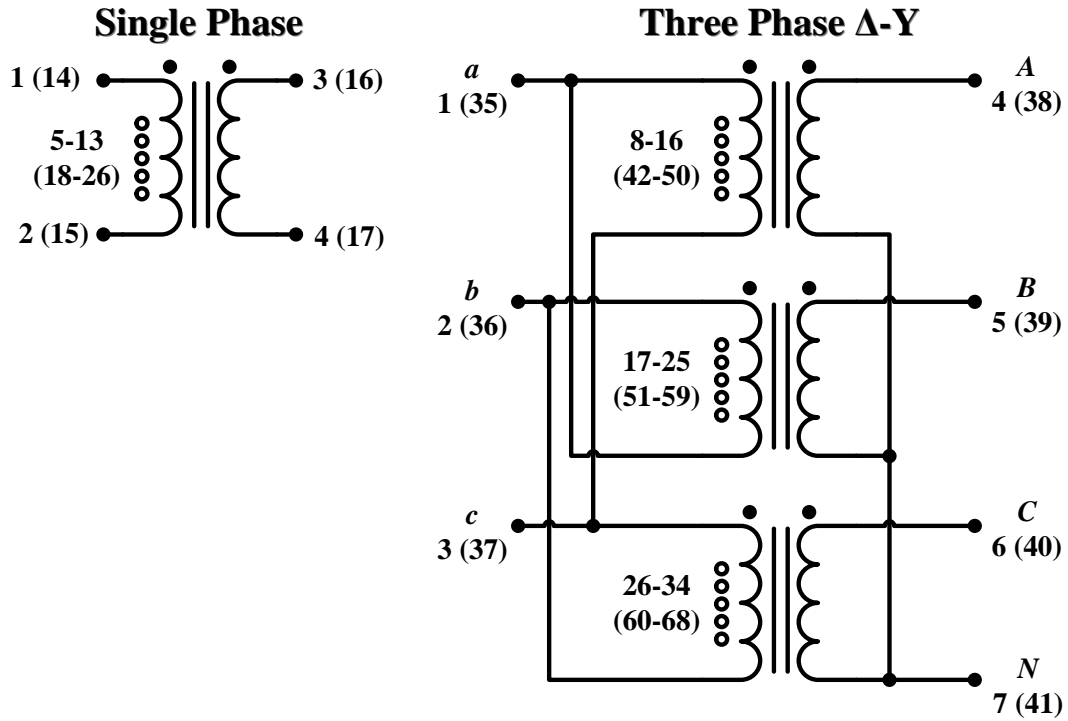


Figure A3.3 Delta-wye Connection Indices (Quadratic)

The device matrices L and N , which are described in the single-phase SCAQCF, (A3.1), are integrated based on the following algorithm, thereby providing the integrated matrices Y_{eq} and N_{eq} .

```

For   PHASE = 1:3
  For   I = 1:26
    K1 = POINTERPHASE (I)
    For   J = 1:26
      K2 = POINTERPHASE (J)
      Yeq(K1,K2) = Yeq(K1,K2) + L(I,J)
    End
    For   J = 1:13
      K2 = POINTERPHASE (J)
      Neq(K1,K2) = Neq(K1,K2) + N(I,J)
    End
  End
End
End

```

Here, PHASE is the index for each single-phase transformer. POINTER is changed according to the terminal to which each single-phase transformer is connected. They are shown in Table A3.1 or instance, POINTER₁(3) is 4.

Table A3.1 Pointer Elements for Delta-Wye Connection

Single-Phase Transformer	Pointer Elements (POINTER _{PHASE})
PHASE = 1	1, 3, 4, 7, 8, 9, 10, 11, 12, 13, 14, 15, 16, 35, 37, 38, 41, 42, 43, 44, 45, 46, 47, 48, 49, 50
PHASE = 2	2, 1, 5, 7, 17, 18, 19, 20, 21, 22, 23, 24, 25, 36, 35, 39, 41, 51, 52, 53, 54, 55, 56, 57, 58, 59
PHASE = 3	3, 2, 6, 7, 26, 27, 28, 29, 30, 31, 32, 33, 34, 37, 36, 40, 41, 60, 61, 62, 63, 64, 65, 66, 67, 68

As a result of integrating three SCAQCFs, three-phase transformer SCAQCF model can be obtained as follows:

$$\begin{bmatrix} i_{3\phi}(t) \\ 0 \\ i_{3\phi}(t_m) \\ 0 \end{bmatrix} = \begin{bmatrix} Y_{11} & Y_{12} & Y_{13} & Y_{14} \\ Y_{21} & Y_{22} & Y_{23} & Y_{24} \\ Y_{31} & Y_{32} & Y_{33} & Y_{34} \\ Y_{41} & Y_{42} & Y_{43} & Y_{44} \end{bmatrix} \cdot \begin{bmatrix} v_{3\phi}(t) \\ y_{3\phi}(t) \\ v_{3\phi}(t_m) \\ y_{3\phi}(t_m) \end{bmatrix} - \begin{bmatrix} N_{11} & N_{12} \\ N_{21} & N_{22} \\ N_{31} & N_{32} \\ N_{41} & N_{42} \end{bmatrix} \cdot \begin{bmatrix} v_{3\phi}(t-h) \\ y_{3\phi}(t-h) \end{bmatrix} + \begin{bmatrix} f_{3\phi,1}(t) \\ f_{3\phi,2}(t) \\ f_{3\phi,1}(t_m) \\ f_{3\phi,2}(t_m) \end{bmatrix} \quad (A3.1)$$

where

$$i_{3\phi}(t) = [i_a(t), i_b(t), i_c(t), i_A(t), i_B(t), i_C(t), i_N(t)]^T \quad (A3.2)$$

$$Y_{eq} = \begin{bmatrix} Y_{11} & Y_{12} & Y_{13} & Y_{14} \\ Y_{21} & Y_{22} & Y_{23} & Y_{24} \\ Y_{31} & Y_{32} & Y_{33} & Y_{34} \\ Y_{41} & Y_{42} & Y_{43} & Y_{44} \end{bmatrix} \quad (\text{A3.3})$$

$$v_{3\phi}(t) = [v_a(t), v_b(t), v_c(t), v_A(t), v_B(t), v_C(t), v_N(t)]^T \quad (\text{A3.4})$$

$$\begin{aligned} y_{3\phi}(t) = & [i_{mA}(t), e_A(t), \lambda_A(t), i_{1LA}(t), i_{3LA}(t), y_{1A}(t), y_{2A}(t), y_{3A}(t), z_A(t), \\ & i_{mB}(t), e_B(t), \lambda_B(t), i_{1LB}(t), i_{3LB}(t), y_{1B}(t), y_{2B}(t), y_{3B}(t), z_B(t), \\ & i_{mC}(t), e_C(t), \lambda_C(t), i_{1LC}(t), i_{3LC}(t), y_{1C}(t), y_{2C}(t), y_{3C}(t), z_C(t)]^T \end{aligned} \quad (\text{A3.5})$$

$$N_{eq} = \begin{bmatrix} N_{11} & N_{12} \\ N_{21} & N_{22} \\ N_{31} & N_{32} \\ N_{41} & N_{42} \end{bmatrix} \quad (\text{A3.6})$$

$$f_{3\phi,1}(t) = \begin{bmatrix} x_{1\phi}(t)^T \cdot Q_1 \cdot x_{1\phi}(t) \\ x_{1\phi}(t)^T \cdot Q_2 \cdot x_{1\phi}(t) \\ \vdots \\ x_{1\phi}(t)^T \cdot Q_7 \cdot x_{1\phi}(t) \end{bmatrix} \quad (\text{A3.7})$$

$$f_{3\phi,2}(t) = \begin{bmatrix} x_{1\phi}(t)^T \cdot Q_8 \cdot x_{1\phi}(t) \\ x_{1\phi}(t)^T \cdot Q_9 \cdot x_{1\phi}(t) \\ \vdots \\ x_{1\phi}(t)^T \cdot Q_{27} \cdot x_{1\phi}(t) \end{bmatrix} \quad (\text{A3.8})$$

Project Publications

1. A. P. Sakis Meliopoulos, George Cokkinides, Renke Huang, Evangelos Farantatos, Sungyun Choi, Yonghee Lee and Xuebei Yu, "Smart Grid Technologies for Autonomous Operation and Control", *IEEE Transactions on Smart Grid*, Vol 2, No 1, March 2011.
2. Sungyun Choi, Yonghee Lee, George Cokkinides and A. P. Sakis Meliopoulos, "Transformer Dynamic State Estimation Using Quadratic Integration", *Proceedings of the 2011 Power Systems Conference & Exposition*, Phoenix, AZ, March 20-23, 2011.
3. Sungyun Choi, Yonghee Lee, George Cokkinides, and A. P. Meliopoulos, "Dynamically Adaptive Transformer Protection Using Dynamic State Estimation", *Proceedings of the PAC World Conference 2011*, Dublin, Ireland, June 27-30, 2011.
4. A. P. Sakis Meliopoulos, George Cokkinides, Sungyun Choi, Evangelos Farantatos, Renke Huang and Yonghee Lee, "Symbolic Integration and Autonomous State Estimation: Building Blocks for an Intelligent Power Grid", *Proceedings of the 2011 ISAP*, Xersonissos, Crete, Greece, September 25-28, 2011.
5. A. P. Sakis Meliopoulos, George Cokkinides, Zhenyu Tan, Sungyun Choi, Yonghee Lee, and Paul Myrda, "Setting-less Protection: Feasibility Study", *Proceedings of the of the 46st Annual Hawaii International Conference on System Sciences (HICSS)*